Investigation of the P2Y$_{12}$ receptor in pulmonary arterial hypertension

Nur Nabilah Binti Abu Bakar

Registration number – 150140872

Thesis submitted for degree of Doctor of Philosophy

December 2019

Supervisors

1st Prof Allan Lawrie

2nd Prof Rob Storey

3rd Dr. Heather Judge

Infection, Immunity and Cardiovascular Department

Faculty of Medicine

University of Sheffield

Acknowledgments

First of all, I would like to express my sincere gratitude to my main supervisor Prof Allan Lawrie, who, particularly has been with me throughout the ups and downs of my doctoral journey. I would also like to thank both of my co- supervisors, Dr Heather Judge and Prof Rob Storey, for supporting me especially in the technical area related to $P2Y_{12}$. I would also like to thank the members of PVRG for their constant encouragement, valuable advice and in helping me out on the cell culture and animal work especially to Dr Josephine Pickworth who has been with me since the very first day of my laboratory work. I would like to acknowledge Prof Allan Lawrie, Ms. Nadine Arnold and, Dr. Laura West for helping me with the animal models used in this research, Dr Heather Judge for assisting me with platelet related work and radioligand binding assay. Also, Dr Josephine Pickworth who has helped me with the cell culture experiment.

Not to forget, my funding sources; the Government of Malaysia, the Ministry of Higher Education, University of Sains Islam Malaysia and my supervisor, Prof Allan Lawrie BHF fellowship. I am extremely thankful for their generosity. I would also like to express my sincere appreciation to my lovely family and friends who have helped me, physically and emotionally during the period I had bone trimalleolar fractures, plate insertion surgery to fix the bones, several months of immobilisation and physiotherapy sessions. It was a painful journey and without everyone's support, I would not have made it to the finish line. I would also like to express my gratitude to my family especially my parents, sisters, extended family and my fellow friends who have helped me financially and accommodated me in their home when I had financial issues.

My sincere thanks to Dr Josephine Pickworth and Dr Laura West for putting the effort and helping me out with the writing part and making this thesis submission a reality. I would also like to thank the Infection Immunity and Cardiovascular Disease department at the University of Sheffield Medical School. I have been in this group since 2013 when I first registered for my MSc and this entire journey has been a memorable time and a gift for myself. Finally, I would also like to thank everyone who has contributed directly or indirectly for their endless support and time.

Contents

List of Figures

List of Tables

List of Equations

Appendices

Abbreviations

®	Registered trademark
%	Percent
$\Delta\Delta C_T$	Delta delta Cycle Threshold
ΔC_T	Delta Cycle Threshold
µl	Microliter
α	Alpha
βγ	Beta gamma
α-SMA	α- Smooth muscle actin
$\alpha_{IIb}\beta_3$	Heterodimeric integrim
g	Gravity
ABEVG	Alcian Blue Van Gieson
ABC	Avidin-biotin complex
ACS	Acute coronary syndrome
ACVRL1	Activin receptor-like kinase 1
ADP	Adenosine diphosphate
AC	Adenylyl cyclase
ApoE	Apolipoprotein E
ATP	Adenosine triphosphate
BMT	Bone marrow transplant
BMP	Bone morphogenetic protein
BMPRII/BMPR2	Bone morphogenetic protein receptor type 2
BSA	Bovine serum albumin

cAMP	Cyclic adenosine monophosphate
cGMP	Cyclic guanosine monophosphate
CABG	Coronary artery bypass grafting
CAS	Chemical abstract service
CAT	Catalogue
CO	Cardiac output
COPD	Chronic obstructive pulmonary disease
CSA	Cross sectional area
CURE	Clopidogrel in Unstable Angina to Prevent Recurrent Events
CCL2	C-C motif chemokine ligand 2
CTEPH	Chronic thromboembolic pulmonary hypertension
CRP	C-reactive protein
Ctrl	Control
CWP	Capillary wedge pressure
DAB	3,3' -Diamino-benzidine
ECG	Electrogram
ENG	Endoglin
EGF	Epidermal growth factor
EndoMT	Endothelial to Mesenchymal to Transition
eNOS	Endothelial nitric oxide synthase
ERK	Extracellular signal-regulated kinase
ET-1	Endothelin 1
ET_A	Endothelin receptor A

ET$_B$	Endothelin receptor B
ePVRi	Estimated pulmonary vascular resistance
EtOH	Ethanol
FA	Final aggregation
FBS	Foetal bovine serum
FeCl$_3$	Ferric chloride
FGF	Fibroblast growth factor
FG	Full growth
GC	Guanylate cyclase
GPIIb IIIa	Integrin receptor
GPCR	G protein-coupled receptor
HAC	Histone acetylation
HDAC	Histone deacetylation
HCL	Hydrochloric acid
HIV	Human immunodeficiency virus
HIF-1α	Hypoxia-inducible factor -1 alpha
HPAH	Heritable PAH
HCAEC	Human coronary artery endothelial cells
HUVEC	Human umbilical vein endothelial cells
HTR2B	Serotonin receptor
HPAAF	Human pulmonary artery adventitial fibroblasts
IgG	Immunoglobulin G
IL-1	Interleukin 1

IL-1Ra	IL-1 receptor antagonist
IL-1β	Interleukin 1β
IL-6	Interleukin 6
IMS	Industrial methylated spirit
IPAH	Idiopathic pulmonary arterial hypertension
IQR	Interquartile range
ISWT	Incremental shuttle walking test
JNK	c-Jun NH2-terminal kinase
KCNK3	Voltage gated potassium channel
LV	Left ventricle
LVOT	Left ventricle outflow tract diameter
LTE$_4$	Leukotriene
LTB4	Leukotriene B4
LVeSP	Left ventricular end-systolic pressure
LVEH	Left ventricular ejection fraction
MA	Maximal aggregation
MAPK	Mitogen-activated protein kinase
MI	Myocardial infarction
MLCK	Myosin light chain kinase
MCP-1	Monocyte chemoattractant protein-1
MMP	Matrix metallopeptidase
mPAP	Mean pulmonary arterial pressure
Mct	Monocrotaline

M-PER	Mammalian Protein Extraction Reagent
NO	Nitric oxide
NRT	No reverse transcriptase control
NTC	No template control
P38 MAPK	P38 mitogen-activated protein kinase
PA	Pulmonary artery
PAAT	PA acceleration time
PAET	PA ejection time
PAEC	Pulmonary arterial endothelial cell
PAF	Platelet-activating factor
PAH	Pulmonary arterial hypertension
PAP	Pulmonary artery pressure
PASMC	Pulmonary arterial smooth muscle cell
PAR4	Protease-activated receptor
PBS	Phosphate-buffered saline
PCH	Pulmonary capillary haemangiomatosis
PCNA	Proliferating cell nuclear antigen
PCR	Polymerase chain reaction
PCWP	Pulmonary capillary wedge pressure
PDGF	Platelet derived growth factor
PET	Polyester
PGI_2	Prostacyclin
PGE_I	Prostaglandin E_I

PH	Pulmonary hypertension
PIP2	Phosphatidylinositol 4,5- biphosphate
PKA	Protein kinase A
PKG	cGMP dependent protein kinase
PLATO	PLATelet inhibition and patient Outcomes
PPH	Primary pulmonary hypertension
PPHN	Persistent pulmonary hypertension
PKC-ζ	Protein kinase C zeta
PDH	Pyruvate dehydrogenase
PDK1	Pyruvate dehydrogenase kinase 1
PRP	Platelet rich plasma
PPP	Platelet poor plasma
PIP2	Phosphatidylinositol 4,5 - biphosphate
PVR	Pulmonary vascular resistance
PVOD	Pulmonary veno-occlusive disease
RT-PCR	Real time polymerase chain reaction
RBC	Red blood cell
RHC	Right heart catheterisation
RNA	Ribonucleic acid
ROS	Reactive oxygen species
RQ	Relative quantitative
RV	Right ventricle
RVH	Right ventricular hypertrophy

RVSP	Right ventricular systolic pressure
RV FWTd	Right ventricular free wall thickness at diastole
s-VCAM1	Vascular cell adhesion molecule 1
siRNA	Small interference RNA
S	Septum
shRNA	Short hairpin RNA
SEM	Scanning electron microscopy
SERT	Serotonin transporter
SM	Serum starved media
SMCs	Smooth muscle cells
SMGM-2	Smooth muscle growth medium 2
SOD2	Superoxide dismutase-2
SMBM	Smooth muscle cell basal medium
SOP	Standard operating procedure
TA	Transplant atherosclerosis
TGF-β	Transforming growth factor beta
TBS	Tris buffered saline
TBST	Tris buffered saline with Tween 20
TCA	Tricarboxylic acid
TNF	Tumour necrosis
TNFα	Tumour necrosis factor- α
TRAP	Thrombin receptor activating peptide
TXB2	Thromboxane B2

VASP	Vasodilator-stimulated phosphoprotein
VASP-P	Vasodilator-stimulated phosphoprotein phosphorylation
VEGF	Vascular endothelial cell growth factor
VEGFR2	Vascular endothelial cell growth factor receptor 2
VSMC	Vascular smooth muscle cell
VTI	Velocity time interval
v/v	volume / volume
VWF	Von Willebrand factor
WP	Washed platelets
5HT	5 hydroxytryptomine
2MeSADP	2-methylthioadenosine diphosphate trisodium salt

Abstract

Rationale: Pulmonary arterial hypertension (PAH) is characterised by sustained vasoconstriction and narrowed pulmonary arteries due to vascular remodelling. The adenosine diphosphate receptor, P2Y$_{12}$ and its antagonist have been suggested to play a role in other diseases. Thus, I postulated that P2Y$_{12}$ receptor blockade may reduce disease progression of PAH.

Objective: I aimed in this thesis to study the effect of P2Y$_{12}$ receptor activation and its inhibition by P2Y$_{12}$ antagonist (cangrelor and clopidogrel) in PASMC and monocrotaline PAH rat model.

Methods and Results: qPCR analysis shows higher expression of *P2RY12* mRNA in patients with PAH, and pre-clinical disease models. Iloprost induced Vasodilator Stimulated Phosphoprotein phosphorylation showed by In-cell Western, 2MeSADP shows no effect of VASP phosphorylation inhibition in iloprost stimulated PASMC. However, 2MeSADP treated PASMC did display a migratory phenotype compared to unstimulated control cells; this migration was blocked by cangrelor. In monocrotaline-treated rats' therapeutic treatment with clopidogrel for 14 days reduced pulmonary vascular muscularisation, although there was no effect on haemodynamic indices of PAH.

Conclusion: Clopidogrel treatment of PAH reduced pulmonary vascular remodelling. I propose that this is mediated by a reduction in 2MeSADP induced migration in PASMC. Future work may determine if longer treatment with clopidogrel utilising the same or another P2Y$_{12}$ antagonist would have a therapeutic impact in PAH.

1   Introduction

1.1   Disease overview

1.1.1   Pulmonary circulation and the right heart

The mammalian circulation consists of pulmonary and systemic circulatory systems; the systemic circulation is responsible for delivering oxygenated blood from the heart to the rest of the body, whilst the function of the pulmonary circulation is to allow oxygen transfer (gaseous exchange) to the blood via the alveoli in the lungs. In the pulmonary circulation, deoxygenated blood (low oxygen blood) returns from the body into the right atria and then the right ventricle. From here, it is pumped through the lung via the pulmonary arteries (PA) for gas exchange in the alveolus. Oxygen rapidly diffuses across the thin airway and vessel walls into the blood where it is carried by haemoglobin molecules in red blood cells (RBC). This oxygen rich blood is then returned from the lung to the left side of the heart and pumped throughout the body (Naeije, 2013). These different functions of the pulmonary and systemic circulation require differing vasculature; i.e. right-sided pulmonary vasculature is a high flow but low-pressure system, whereas the left side systemic vasculature is a high-pressure system which determines its anatomical features: right heart (thin wall) and left heart (thick wall). In normal physiological conditions, the right ventricle has a thin wall that can adapt to elevations of pressure due to oxygen demand, but prolonged high pressure leads to chronic hypertension. To compensate for the sustained raised pressure and cardiac output, cardiomyocytes undergo cellular changes leading to pressure overload-induced hypertrophy. This right ventricular remodelling leads to heart failure and ultimately death (Pokreisz et al., 2007).

Interestingly, systemic and pulmonary pressures are independent and are unaffected by each other (Paulin et al., 2011). The two vascular beds are structured differently, demonstrated by the

fact that although a much smaller single organ vasculature, the pulmonary system is at least eight times bigger in size compared to the systemic system due to the large volume of small capillaries needed to obtain sufficient gas exchange (Yuan et al., 2011).

1.1.2 Pulmonary hypertension

Pulmonary hypertension (PH) is a life-limiting condition that comprises a spectrum of diseases, which are defined clinically as having a mean pulmonary artery pressure (mPAP) ≥20 mmHg at rest measured by right heart catheterisation (RHC) (Simonneau et al., 2019). RHC for the measurement of mPAP and cardiac output remains the gold standard to diagnose PH (Grignola, 2011; Humbert et al., 2006). A resting normal mPAP is between 8 and 20 mmHg (Simonneau et al., 2019). This increase in pressure leads to right ventricular hypertrophy which in turn eventually leads to patient death by right heart failure.

1.1.3 Pulmonary hypertension classification

Previously, the Dana Point 2008 Classification categorised PH into five subclasses according to the underlying cause of disease, idiopathic or due to secondary factors, such as genetics or other diseases. In 2018, PH classifications were updated, and some amendments were made during the 6th World Symposium held in Nice to improve the diagnosis of PH. The amendments involved haemodynamic and clinical classification of PH; they proposed to reduce the pulmonary artery pressure cut-off (less 20 mmHg), as 20 – 25 mmHg have been described to also result in poor outcomes. Pulmonary vascular resistance (PVR) was also included in the diagnosis criteria, which ≥3 wood units of PVR is used to define all forms of pre-capillary PH and also, >15 mmHg of pulmonary capillary wedge pressure was included as the criteria to determine the patients who

have combined pre- and post-capillary pressure. Exercise PH was abandoned because of the challenges to obtain diagnostic accuracy as exercise can increase cardiac output and pulmonary artery pressure. Other changes are presented in detail as reported by Simonneau and colleagues (Simonneau et al*., 2019).

Generally, PH classifications are pulmonary arterial hypertension (PAH, Group 1) which can be grouped as idiopathic, heritable, caused by other diseases, drug and toxin induced and persistent pulmonary hypertension (PPHN) of the new-born. Other groups of PH are pulmonary hypertension due to left heart disease (Group 2), pulmonary hypertension due to lung diseases and/or hypoxia (Group 3), chronic thromboembolic pulmonary hypertension (CTEPH) (Group 4), and PH with unclear multifactorial mechanisms (Group 5) (Simonneau et al*., 2013; Simonneau et al*., 2019).

1.1.4 Pulmonary arterial hypertension

Pulmonary arterial hypertension (group 1 PH) is defined as mean pulmonary artery pressure (mPAP) ≥20 mmHg at rest, pulmonary capillary wedge pressure (PCWP) ≤15 mmHg and a pulmonary vascular resistance (PVR) of more than 3 Wood units (Simonneau et al., 2019). Pulmonary arterial hypertension is caused by the progressive narrowing of blood vessels in the lung due to sustained vasoconstriction and vascular remodelling. Consequent to sustained vasoconstriction, PAH pathogenesis involves dysregulated cell proliferation, apoptosis, abnormal inflammatory response, thrombosis, and in rare occasions, can be initiated by a genetic mutation.

In the 1980s, the median survival time was less than 2.8 years, but it has since improved. Observation of qualified 2,635 patients from 55 sites in the United States, during the REVEAL registry study (Registry to Evaluate Early and Long-term Pulmonary Arterial Hypertension Disease Management) showed that patients survival was improved up to 7 years according to the patient's clinical diagnosis (Benza et al., 2012). Improved survival was due to the availability of specific vasodilator treatment, increased awareness and improved diagnosis (Gomberg-Maitland et al., 2011). In addition, prevalence of PAH is four-fold higher in women than men, although men have worse prognosis (Humbert et al., 2006).

The prevalence of PAH has been identified as 2 to 7.6 cases/million adults per year and the incidence of PAH as 11 to 26 cases/million adults (Humbert et al., 2006; Thenappan et al., 2007; Thenappan et al., 2018). The symptoms of PAH are non-specific such as fatigue and shortness of breath which make the disease difficult to diagnose, and patients frequently experience a delay in diagnosis of 2-3 years, and present with advanced disease (Strange et al., 2013). Currently,

there is no medical cure for PAH and despite the improved survival with current treatments, the disease is still fatal (Gomberg-Maitland et al., 2011).

1.2   Pathogenesis of PAH

The pathogenesis of PAH is driven by many factors; sustained pulmonary vasoconstriction, abnormal proliferation and apoptosis of vascular cells, inflammation, in-situ microthrombi and genetic factors. These are discussed below.

1.2.1 Sustained pulmonary vasoconstriction

Several pathways are known to be involved in the generation of pulmonary vasoconstriction. However, there are three main pathways targeted by current approved PAH therapies which are endothelin, nitric oxide, and prostacyclin.

1.2.1.1 Endothelin-1

High levels of endothelin-1 (ET-1) have been identified in the blood and lungs of PAH patients. Endothelin is responsible for regulating vasoconstriction through two endothelin receptors, ET_A and ET_B. In addition to regulating vasoconstriction, they also regulate cell proliferation. Stimulation of ET-1 leads to the phosphorylation of extracellular signal-regulated kinase (ERK) and mitogen-activated protein kinase (MAPK) signalling. These signalling pathways will further activate transcription factors such as c-jun, c-myc, c-fos, to regulate cell growth and proliferation (Bouallegue et al., 2007).

1.2.2.2 Nitric oxide

Activation of the nitric oxide (NO) pathway plays an important role as a vasodilator in regulating vascular tone. NO is produced endogenously in the endothelium by the enzyme endothelial nitric oxide synthase (eNOS). NO is diffused into smooth muscle cells (SMCs) where it stimulates the guanylate cyclase (GC) cascade. This initiates the production of cyclic guanosine monophosphate (cGMP) and decrease of myosin light chain phosphorylation, leading to vasodilation. The dephosphorylation of myosin light chain also causes the inhibition of cell growth and proliferation. Besides cGMP, NO also activates the ERK pathway promoting cell proliferation. Low levels of NO causes vasoconstriction and promotes cellular proliferation (Ghofrani et al., 2004; Wang et al., 2007).

1.2.2.3 Prostacyclin

Prostacyclin released by endothelial cells acts via the G protein-coupled receptor, IP receptor. Prostacyclin/IP binding regulates vessel relaxation via activation of the cyclic AMP (cAMP) pathway, which further activates protein kinase A (PKA). This activation regulates vessel relaxation. Beyond vessel relaxation, it also functions as an inhibitor of cell proliferation. Low levels/impairment of IP receptor expression causes vasoconstriction (Clapp et al., 2001). Akagi and colleagues showed that it also stimulates apoptosis and was inhibited by prostacyclin antagonist (Akagi et al., 2013).

1.2.2 Pulmonary vascular remodelling

The initial factor causing PAH remains to be fully elucidated but at the early stage of disease pathogenesis, endothelial dysfunction is thought to be an important factor.

1.2.2.1 Endothelial cell dysfunction and resistance to apoptosis

Endothelial dysfunction is an early trigger of PAH. Pulmonary arterial endothelial cell (PAEC) dysfunction, apoptosis and proliferation have been associated with accumulation of plexiform lesions in disease (Abe et al., 2010; Jonigk et al., 2011). BMPR2 mutations are a known causative agent in disease, and studies have shown that loss of function in the bone morphogenetic protein (BMP) signalling increases endothelial apoptosis (Teichert-Kuliszewska et al., 2006). This evidence further supports the hypothesis that endothelial apoptosis plays a role in initiating PAH pathogenesis.

There is also other evidence showing that endothelial dysfunction leads to the emergence of apoptosis resistant endothelial cells. Vascular endothelial cell growth factor (VEGF) and its receptor 2 (VEGFR2) expression are responsible for maintaining endothelial cell proliferation, migration and survival (Al-Husseini et al., 2015). Blocking of this receptor has been shown, in a normoxic animal model, lead to smooth muscle cell proliferation and a combination of chronic hypoxia and VEGFR2 receptor inhibition lead to apoptosis-resistant endothelial cell proliferation (Taraseviciene-Stewart et al., 2001). This evidence also shows that endothelial dysfunction plays a crucial role in the emergence of apoptosis resistant endothelial cells and smooth muscle cell proliferation in PAH.

1.2.2.2 Endothelial cell proliferation

Mechanisms regulating endothelial cell proliferation are still unclear. The proliferation of endothelial cells contributes to the development of concentric as well as plexiform lesions (Jonigk et al., 2011; Tuder & Graham, 2010). When the endothelial lining is damaged, the intimal layer of smooth muscle cells is exposed to circulating signalling molecules and growth factors which can stimulate intimal proliferation. Plexiform lesions are thought to be a hallmark of late stage/severe PAH. They are complex vascular formations made up of accumulations of hyperproliferative endothelial cells, smooth muscle cells and apoptosis resistant cells. Subsequently, these occlude the vessel and form a remodelled pulmonary artery in severe PAH. This has been demonstrated by the histological findings of Abe et al., (2010) in rats and human by Tuder's group (Abe et al., 2010; Stacher et al., 2012; Tuder & Graham, 2010).

1.2.2.3 Pulmonary arterial smooth muscle cell proliferation and apoptosis.

In PAH, pulmonary vascular remodelling and thickening of the vessel wall are largely caused by the accumulation and migration of alpha smooth muscle actin positive cells. It is thought that these cells are primarily derived from pulmonary artery smooth muscle cell (PASMC). Some of these cells may also derive from the endothelium and become more "smooth muscle like" through the process of Endothelial-to-Mesenchymal Transition (EndoMT) (Ranchoux et al., 2015). These events result in the thickening of media, intima, and adventitia, especially in the distal pulmonary artery (Chazova et al., 1995). Progressive PASMC proliferation is one of the cofactors for PAH pathogenesis, predominantly affecting the medial layer of the pulmonary artery. The exact molecular mechanism of PASMC proliferation and apoptosis remains unclear as normal PASMCs maintain low proliferative activity and a contractile phenotype (Fernandez et al., 2015).

Changes to cellular proliferation in pulmonary vessels after the onset of endothelial dysfunction bring about an increase in exposure of the smooth muscle cell layer to circulating factors. There are different factors that contribute to PASMC proliferation; BMPR2 signalling, growth factors, vasoactive compounds (nitric oxide, endothelin-1, and prostacyclin), transcription factors, and serotonin (5-hydroxytryptomine, 5-HT) (Rabinovitch, 2008; Wilkins, 2012). These are described in more detail later in section 1.3.

1.2.2.4 Fibroblast proliferation

It is important to mention that fibroblasts are increased in the area of pulmonary vascular adventitia in PAH patients and PH animal models (El Kasmi et al., 2014; Li et al., 2012). Fibroblasts are important cells in the vascular injury response and the most abundant cells in the adventitial compartment. When activated, fibroblasts increase the secretion of growth factors, cytokines and chemokines, inflammatory markers, and this can lead to the proliferative phenotype and extracellular matrix remodelling (Stenmark et al., 2012). Hypoxia and inflammation can cause fibroblasts to migrate, differentiate and proliferate.

There are various pathways that have been associated with hyper-proliferative fibroblast phenotype which contribute to vascular remodelling and PAH, such as leukotriene B4 (LTB4) in the leukotriene pathway. The adventitial layer has been found to have an abundance of LTB4. A recent study demonstrated LTB4 found in human pulmonary artery adventitial fibroblasts (HPAAF) induced differentiation, proliferation, and migration of the adventitial fibroblast. Inhibition of LTB4 signalling via its receptor, (BLT-1) caused inhibition of proliferation and migration. These effects were also observed when p38 mitogen-activated protein kinase (p38 MAPK) and Nox4 were blocked, demonstrating linkage in the signalling pathway (Qian et al.,

2015). Other pathways have also been associated with fibroblast proliferation. For instance, active form of protein kinase C zeta (PKC-ζ) was found on proliferative fibroblast retrieved from hypoxic calf which suggest that PKC-ζ functions as DNA replication repressor. Inhibition or loss of function of PKC-ζ leads to fibroblast proliferation (Das et al., 2008). Exploring the fibroblast proliferation pathway in relation to PAH might also contribute to identifying pathway specific alternative treatments in PAH.

1.2.3 In-situ thrombosis

The complex network of signalling pathways causing thrombus formation is initiated by platelet activation, shape change and aggregation, and involves granule secretion, receptor activation, calcium mobilisation and G-coupled receptor signalling (Daniel et al., 1998; Storey, 2006).

Besides thrombosis, activated platelets are also involved in the vasoconstriction and abnormal vascular remodelling by secreting mediators such as platelet-activating factor (PAF) and growth factors including platelet-derived growth factor (PDGF) through different pathways. For instance, platelets produce angiotensin and PDGF which promotes angiogenesis and proliferation of PASMCs (Niu et al., 2009; Schermuly et al., 2005).
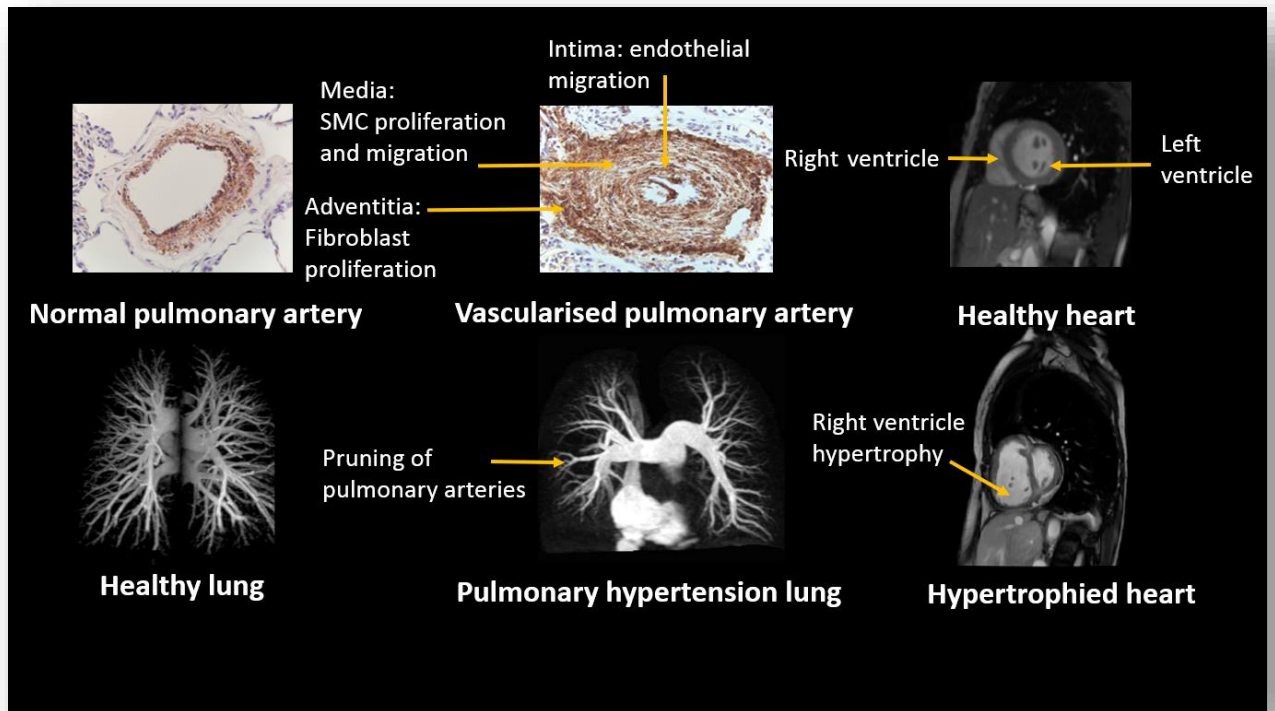
Figure 1-1: Healthy to diseased lung and artery in PAH

Figure above shows the progression of the disease from a healthy vessel to a diseased vessel (top left to middle left) and a healthy lung to a diseased lung (bottom left to bottom middle) and then on the right it shows the healthy heart (top right) and a diseased heart with right ventricular hypertrophy (bottom right). Micrographs were obtained from Prof Allan Lawrie and MRI pictures are courtesy of Prof Jim Wild and Prof David Kiely.

Pathogenesis of PAH affects all layers of pulmonary arteries; intima, media, and adventitia. In a normal pulmonary artery, there is a monolayer of endothelial cells lining the intima, smooth muscle cells in the media and the outer layer which is the adventitia consists of collagen fibres and fibroblasts. During disease development, changes in the morphological pattern of the pulmonary artery leads to vascular lesion formation (plexiform and concentric lesions) which causes narrowing of the pulmonary artery as shown in Figure 1-1. Narrowed pulmonary artery leads to increased vascular resistance causing the increase in pressure (Humbert et al., 2004; Rabinovitch, 2008).

1.3 Molecular mechanism of PAH

The molecular mechanisms involved in PAH are very complex. Below are some of the aspects which contribute to PAH pathogenesis, including mutation, epigenetics, cell metabolism, growth factors and inflammation amongst others.

1.3.1 Genetic mutation

The most common genetic driver involved in PAH pathogenesis is bone morphogenetic protein receptor Type II (BMPRII) gene mutation. Approximately 80% of cases have heterozygous BMPRII mutation, and 20% are classified as idiopathic PAH cases (Gräf et al., 2018; Thomson et al., 2000). Mutation of the BMPRII gene leads to altered cell growth and proliferation involving transforming growth factor beta (TGF-β) signalling associated with dysfunctional SMAD pathway in PASMCs (Hollopeter et al., 2001; Yang et al., 2005) leading to PASMC proliferation and apoptosis (Toshner et al., 2009).

Other than BMPRII, genes that have been shown to influence PAH development are SMAD genes (Pfarr et al., 2013), Serotonin Transporter (SERT) (Qin et al., 2013), voltage gated potassium channel (KCNK3) (Ma et al., 2013), Activin receptor-like kinase 1 (ACVRL1) and other genes involved in TGF-β signalling (Montani et al., 2013; Thomson et al., 2000). To unveil the additional sequence variation contributing to the genetic mutation in PAH, recently whole genome sequencing has revealed SOX17, ATP13A3, AQP1, GDF2 genes as having rare causal variants (Graf et al., 2018). In addition, patients diagnosed with PAH are advised to undergo genetic mutation screening, which include BMPRII (Toshner et al., 2009), activin A receptor-like kinase type 1 (ACVR1), endoglin (ENG) (Pfarr et al., 2013), and SMAD8 genes (Montani et al., 2013).

1.3.2 Epigenetics

The field of epigenetics covers the alterations of gene expression that are not due to physical mutation of the DNA code but are modifications of the method used for the expression of that gene, as detailed below.

1.3.2.1. DNA methylation in PAH

DNA methylation is the addition of methyl groups to the DNA molecule (C-5 position of the cytosine ring) in a promoter region. This causes gene transcription to be suppressed and affects gene expression. One of the examples of DNA methylation is the suppression of mitochondrial superoxide dismutase-2 (SOD2) in PAH. Since the SOD2 gene shows no mutation in PAH, this led to the hypothesis by Archer et al., (2010) that decreased SOD2 expression is related to epigenetic dysregulation. They have shown that SOD-mimetic therapy leads to a less developed PAH phenotype, such as SOD knockdown, which is associated with a proliferative phenotype, as well as apoptosis resistance in PASMC (Archer et al., 2010).

1.3.2.2 Histone acetylation in PAH

Histone acetylation (HAC) is involved in gene silencing in PAH. HAC occurs when acetyl groups are added to lysine residues of histone property, which changes the property of DNA transcription. Histone deacetylation (HDAC) is the opposite of HAC. There is robust evidence showing that HDAC inhibitors play a role in other diseases such as cancer and can act as anti-tumour agent. Nozik-Grayck et al., (2016) found that SOD3 suppression was not because of DNA methylation as 5-aza-2'-deoxycytidine (DNA methylation inhibitor) treated human PASMC failed

to increase SOD3 mRNA. However, HDAC inhibitor increased SOD3 mRNA (Nozik-Grayck et al., 2016).

1.3.2.3. Non-coding RNA in PAH

Non-coding RNA can be described as a transcribed gene that will not be translated into a functional protein. Non-coding RNA can be categorised as short RNAs such as microRNA, that are less than 200 nucleotides in size, or long non-coding RNAs that range more than 200 nucleotides in length.

MicroRNA has been shown to be robustly involved in PAH and a review on the effects of epigenetic mechanisms in PAH has been published recently (Luna et al., 2018). They have summarised several microRNAs linked to PAH. There are several microRNAs that are dysregulated in PAH; i.e. increased levels of miR-21 causes proliferation in PASMC (Sarkar et al., 2019) and MiR-140-5p increases smooth muscle cell proliferation via the SMURF1 pathway (Rothman et al., 2016). Previous findings have shown that manipulating the expression of microRNA in experimental models in other diseases such as pulmonary hypertension (Rothman et al., 2016) and Alzheimer's disease (Sarkar et al., 2019) may become a potential therapeutic target.

1.3.3 Growth factors

Growth factors are known to contribute to the cell growth, migration, proliferation, and survival. High levels of growth factors such as platelet derived growth factor (PDGF), epidermal growth factor (EGF), and fibroblast growth factor (FGF) have been strongly implicated in causing PASMC

proliferation and migration via the extracellular signal-regulated kinase (ERK) pathway (Perros et al., 2008; Li et al., 2011; Ren et al., 2011).

PDGF is synthesised by different cell types such as endothelial cells, smooth muscle cells, macrophages and can be released by platelets (Ross, 1989). *In vitro* and human studies show that PDGF is a major contributor to cell proliferation in PAH (Ren et al., 2011). Elevated levels of PDGF receptor mRNA and PDGFR-β protein expression observed in lung transplanted PAH patients compared to control groups show that growth factors like PDGF play a role in PAH pathogenesis. In addition, in PASMCs, the phosphorylation of PDGFR-β, cell proliferation and migration are inhibited by the presence of imatinib (a tyrosine kinase inhibitor (TKI)) (Perros et al., 2008). This study shows that inhibition of receptor expression and investigation of molecular pathways involved can contribute to the invention of therapeutic strategies.

Since PDGF has been shown to induce cell proliferation and migration, utilising PDGF as a positive control to study PASMC phenotype changes due to activation or inhibition of P2Y$_{12}$ receptor in this present study would be beneficial.

1.3.4 Inflammation

Inflammation is now being acknowledged as a factor contributing to the pathogenesis of PAH. It may act as an "initial hit"; i.e. inflammatory response from infections or other diseases, or a genetic mutation involving an inflammatory response related to the BMP pathway; or, it also may act as a "secondary hit" in the progression of pathogenesis promoting vascular remodelling by stimulating growth factors causing further disease progression. However, the exact mechanism of inflammation contributing to the pathogenesis of PAH, especially in vascular remodelling, is

still unclear. Recent studies have shown that inflammatory cells contribute to the pathogenesis of PAH. Build-up of perivascular inflammatory cells have been documented in the adventitia of idiopathic pulmonary arterial hypertension (IPAH) arteries including macrophages, dendritic cells, monocytes, mast cells, T-cells, helper T-cells, cytotoxic T-cells, and B cells (Savai et al., 2012). Cytokines and chemokines play an important role in inflammation. Soon et al., (2009) showed that levels of serum cytokines including tumour necrosis factor-α (TNF-α), interleukin-6 (IL-6) and interleukin-1β (IL-1β) are elevated in PAH patients compared to healthy controls (Itoh et al., 2006; Soon et al., 2010). Cytokines can influence contractility and vascular remodelling. For instance, IL-1 and IL-6 can induce expression of fibroblast growth factor-2 and mediate smooth muscle cell proliferative responses respectively (Izikki et al., 2009; Savale et al., 2009; Steiner et al., 2009).

Much evidence shows inflammation is identified as causal for vascular proliferation rather than consequential. Below is an explanation describing the common inflammatory mediators involved in PAH based on experimental and clinical evidence. As mentioned before, IL-1 is elevated in PAH patients (Soon et al., 2010) and promotes vascular remodelling in PAH. Studies by Lawrie et al., (2011) showed that treating with IL-1 receptor antagonist *(Anakinra) (*IL-1Ra) in mice reduced PAH progression (Lawrie et al., 2011).

Steiner et al., (2009) showed that IL-6 induced inflammation can lead to the development of PAH. In their study, lung specific IL-6 overexpressing transgenic mice developed vascular hypertrophy and increased pulmonary arterial pressure, and this was worsened in hypoxic compared to normoxic conditions. The histological appearance showed that IL-6 overexpression induced PAEC cellular proliferation, as plexogenic and thick concentric lesions stained positively with an endothelial cell marker similar to human PAH lung. The authors also suggest that IL-6

overexpression contributes to vasculopathy within the PA wall via a pro-proliferative, apoptosis resistant mechanism (Steiner et al., 2009). Moreover, genetic mutation also seems to influence alterations in inflammatory response and adverse remodelling which may be part of the mechanism that predisposes to PAH pathogenesis. This can be seen in PAH where defects in the BMPRII signalling pathway results in increased production of IL-6 (Hagen et al., 2007) and there is also evidence showing where IL-1ß signalling interacts with dysfunctional BMPRII to increase inflammatory responses (Pickworth et al., 2017).

Plasma monocyte chemoattractant protein-1 (MCP-1, also known as C-C motif chemokine ligand 2 (CCL2)) is produced by monocyte/macrophages, endothelial and smooth muscle vascular cells, and fibroblasts. MCP-1 is a key modulator of monocyte and macrophage activation, recruitment, and migratory response to cells, or a site of injury. In addition, Sanchez et al., (2007) showed that MCP-1 stimulates increased endothelial cell migration compared to non-stimulated conditions and monocyte migration was reduced in the presence of CCL2-blocking antibodies. They also showed that patient PASMCs show higher proliferation and migration activity compared to normal controls (Sanchez et al., 2007). Itoh et al., (2006) showed that MCP-1 was elevated in IPAH patient's plasma compared to healthy controls. However, they found no significant correlation between MCP-1 level and haemodynamic variables. Interestingly, an increased level of MCP-1 was observed in a sample group at an early stage of the disease, which could be a useful tool for early diagnosis in pulmonary hypertension development (Itoh et al., 2006).

Mitogen-activated protein kinase (MAPK) signalling consists of three major downstream signalling pathways; ERK, JNK and p38. MAPK signalling is activated when there is an increased level of cytosolic calcium, which is stimulated by growth factors such as PDGF, TGF-β, VEGF or

cytokines. It is also an important part of the inflammatory and vascular remodelling pathways (Wilkins, 2012; Yu et al., 2015).

1.3.5 Cell metabolism dysfunction

Metabolic dysfunction relates to switching from mitochondrial oxidative phosphorylation to glycolysis (Warburg effect). The Warburg effect was discovered in the 1920s by Otto Warburg. This metabolic switch increases glucose, lipid, and insulin production. Cells predominantly produce energy with increased glycolysis followed by lactic acid fermentation in the cytosol region rather than the oxidation of pyruvate in mitochondria, as in most normal cells. In the presence of oxygen, however, the mitochondrial tricarboxylic acid (TCA) cycle, metabolises glucose to carbon dioxide, and this occurs by the oxidation of glycolytic pyruvate. This phenomenon has been associated with tumour growth and the wound healing process, where cell proliferation activity is high. In oncology, the Warburg effect produces a large amount of lactate and this provides a suitable environment for cancer progression. Mitochondrial abnormalities in vascular cells could cause the hyperproliferation in PAH. The exact involvement of the Warburg effect in PAH remains unknown but there are certain pathways that have been reportedly involved in PASMC; PI3K/AKT/mTOR/HIF-1α (Xiao et al., 2017) and PAEC; Rho-kinase α (ROCK2) (Qiao et al., 2016), BMPR (Takahashi et al., 2007), Caveolin-1 (Nickel et al., 2015), and HIF-1α (Fijalkowska et al., 2010). There is evidence in human and preclinical PAH of the increase of lactate synthesis, increased glucose and low tricarboxylic acid (TCA) activity (Fessel et al., 2012). As the Warburg effect is related to PASMC and PAEC proliferation and involved in the vascular remodelling in PAH, exploring the pathway may contribute to therapeutic benefits.

Hypoxia is one of the factors involved in PAH pathogenesis and studies have shown that it can activate hypoxia-inducible factor 1-alpha (HIF-1α) (Bonnet et al., 2006). In PAH, via the PDGF pathway, HIF-1α activates cell proliferation (Xiao et al., 2017) and activates glycolic genes including pyruvate dehydrogenase kinase 1 (PDK1) (Archer et al., 2008; Kim et al., 2006). PDK1 inactivates TCA cycle enzymes known as pyruvate dehydrogenase (PDH), which converts pyruvate to acetyl-CoA. Due to increased level of PDK1 expression, adenosine triphosphate (ATP) levels and hypoxic reactive oxygen species (ROS) are increased and decreased respectively (Kim et al., 2006).
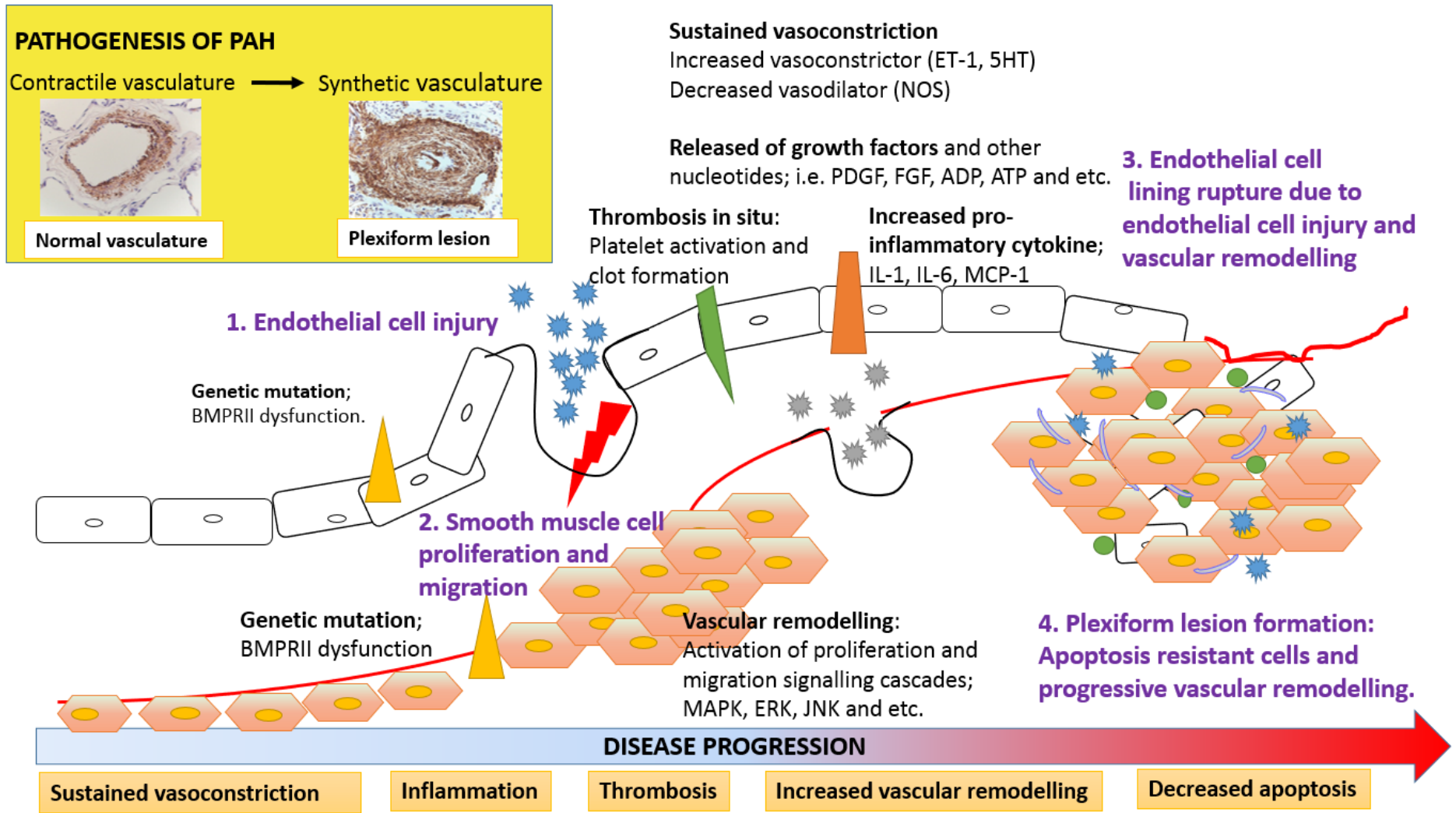
Figure 1-2: Diagrammatic representation of PAH pathogenesis.

Figure 1-2 shows the diagrammatic representation of PAH pathogenesis. PAH can be caused by multifactorial factors; progressive vascular remodelling, sustained vasoconstriction, in-situ thrombosis, inflammation, genetic mutation, and environmental factors such as hypoxia. It starts with endothelial cell injury or dysfunction. In normal conditions, the thin single layered endothelium forms an interior surface for blood flow and is responsible for providing a compatible interface for maintaining homeostasis, cell to cell interaction and complex signalling pathway such as BMPR signalling, prostacyclin pathway, nitric oxide pathway and endothelin pathway. During endothelial cell injury **(1 and 3)**, damaged vascular lining will cause platelet activation, activation of molecular signalling and release of certain mediators such as vasoconstrictor molecules and pro-inflammatory cytokines. The muscularisation process is followed by smooth muscle cell proliferation and migration due to the activation or deactivation of certain pathways **(2)**. The most common pathway is MAPK, ERK, and c-Jun NH2-terminal kinase (JNK). This can be stimulated by upregulation by certain nucleotides or growth factors such as PDGF, FGF, ADP, ATP, and downregulation of certain pathways such as cAMP signalling pathway and BMP signalling. Smooth muscle cell phenotypic changes (proliferation and migration) is observed and at this stage it is still reversible. Over time, cellular composition and signalling pathways triggered by the microenvironment contribute to plexiform lesion phenotype, which is the hallmark for PAH **(4).** At this stage, it is irreversible and will cause fatality if left untreated. Other factors such as cell metabolism dysfunction and epigenetics also contribute to PAH pathogenesis (Rabinovitch, 2008; Wilkins, 2012).

1.4 PAH therapies

Currently, pharmacological treatments are given to alleviate symptoms via vasodilation rather than to prevent disease progression. Identifying a key pathway in reversing disease pathogenesis would be of therapeutic value in PAH. The treatment of PAH focuses on these three important pathways; endothelin pathway, nitric oxide pathway and prostacyclin pathway, as shown in Table 1-1.

To date, there is no medical cure for PAH. Lung transplant may improve survival but there is a shortage of donor lungs and it does not restore life expectancy to normal. Endothelin receptor antagonists (bosentan and macitentan) target the vasoconstriction pathway via blockade of ET_A and ET_B which leads to vasodilation. In the nitric oxide pathway, PDE-5 inhibitors (sildenafil, tadalafil) inhibit cyclic guanosine monophosphate (cGMP) degradation regulating relaxation of the vascular smooth muscle leading to vasodilation. In addition, decreased prostacyclin production in patients leads to decreased vasodilation. Prostacyclin is responsible for the inhibition of platelet aggregation via cAMP signalling. Epoprostanol, trepostinil and iloprost are prostacyclin analogues that bind to IP receptors increasing cAMP level leading to increased levels of protein kinase A (PKA) enzyme and initiate vasodilation. Selexipag, a selective IP receptor agonist which is orally available has been shown to have affinity binding to IP receptor and can overcome limitations associated with other IP receptor agonists (Asaki et al., 2015). Most research focuses on exploring the underlying molecular mechanism of PAH pathogenesis. By increasing the understanding of the disease's molecular mechanism, new potent therapeutic targets can be identified (Clapp et al., 2001; Ghofrani et al., 2004; Humbert et al., 2004; Asaki et al., 2015; Fan et al., 2015)

Table 1-1: PAH treatment.

Adapted from Humbert et al., 2004

PAH treatment
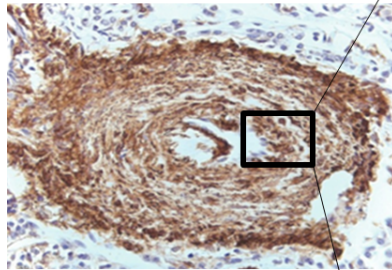
Pulmonary artery

Actions	Pathway	Drug name	Function	Side effects	Reference
Prostacyclin and its analogues	Prostacyclin	Epoprostenol, Treprostinil, Beraprost, Iloprost	Vasodilator and anti-proliferation	Jaw pain, diarrhea, headache and nausea	Asaki et al., 2015; Clapp et al., 2001; Humbert, Sitbon, & Simonneau, 2004
Non prostanoid IP receptor agonist	Prostacyclin	Oral drug selexipag			
Guanylate cyclase stimulator	Nitric oxide	Riociguat		Constipation, nausea, anaemia, headache	Jing et al., 2013
Phosphodiesterase – 5 – inhibitor	Nitric oxide	Sildenafil and tadalafil		Visual disturbance, headache and insomnia	Ghofrani et al., 2004
Endothelin receptor antagonist	Endothelin	Bosentan, macitentan and ambrisentan	Inhibits vasoconstriction and proliferation	Headache, fatigue and tiredness	Humbert, Sitbon, et al., 2004
Calcium channel blockers	-	Nifedipine and diltiazem	Inhibits intracellular Ca^{2+} influx and vasoconstriction	Constipation, headache and rash	Fan et al., 2015
Anticoagulants	Coagulation	Heparin, warfarin	Decrease hypercoagulability	Abdominal pain, bleeding, flatulence	Said 2014

1.5   P2Y$_{12}$ receptor

In this project, I aimed to investigate the role of the P2Y$_{12}$ receptor in PAH disease. Purinergic receptors are membrane receptors involved in mediating a diverse range of cellular functions, including cell proliferation and apoptosis, platelet activation and aggregation, inflammation, and vessel tone. There are three different groups of purinergic receptors; P1, P2Y and P2X, each with multiple subtypes (Wang et al., 2003). These groups are distinguished by their reactivity to purinergic nucleotides; P1 (adenosine), P2Y receptors (ATP, ADP, UTP and UDP) as shown in Table 1-2 and P2X receptors (ATP).

Table 1-2: P2Y receptors

The type of P2Y receptor, its activation nucleotide, and its function, respectively:

P2Y	Function	Mechanism	Activation nucleotide	Reference
$P2Y_1$	Haemostasis and thrombosis	Triggers platelet change through Gq signalling pathway	ADP	(Léon et al., 1999)
$P2Y_2$	Proinflammatory	Interacts with α_v integrin to stimulate cell migration to promote chemotaxis and inflammatory cell (monocyte) recruitment.	UTP	(Bagchi et al., 2005; Liao et al., 2007)
$P2Y_4$	Visual and auditory	Regulates K^+ secretion in the apical membrane by the strial marginal epithelial cell. Involve in the inter retinal signalling and auditory transmission	UTP	(Marcus et al., 2005; Ward et al., 2008)
$P2Y_6$	Proinflammatory, bone resorption	Stimulates inflammatory cell secretion such as macrophage. Stimulates bone resorption and the formation of osteoclasts.	UDP	(Bar et al., 2008; Orriss et al., 2011)
$P2Y_{11}$	Cell activity and inflammatory response	Involved in stimulating dendritic cells maturation for the immune response, involve in the neutrophil apoptosis inhibition, regulate negative inhibition for TLR signalling	ATP	(Kaufmann et al., 2005; Vaughan et al., 2007; Wilkin et al., 2001)
$P2Y_{12}$	Platelet aggregation	Involved in Gi signalling activation, GPIIb/IIIa receptor activation, platelet degranulation and sustained platelet aggregation	ADP	(Angiolillo & Capranzano, 2008)
$P2Y_{13}$	Bone formation HDL uptake	Involved in the process of osteoblasts cell formation, involve in the mechanism of High-Density Lipoproteins (HDLs) uptake by the liver.	ADP	(Biver et al., 2013; Lichtenstein et al., 2015)
$P2Y_{14}$	Gastric function, Immune function Insulin secretion	Stimulates stomach contractility, and modulate insulin secretion by the pancreatic islet cells, stimulate IL-8 release in the endometrial epithelium cell.	Nucleotide sugar (UDP sugar and UDP glucose, UDP galactose)	(Arase et al., 2009; Bassil et al., 2009; Meister et al., 2014)

1.5.1 P2Y$_{12}$ Structure and function

The P2Y$_{12}$ receptor is a 7-transmembrane G protein-coupled receptor (GPCR). P2Y$_{12}$ is mainly expressed, though not exclusively, in platelets where it plays an important role in platelet aggregation. Adenosine diphosphate (ADP) binds to the P2Y$_1$ receptor and induces calcium mobilisation, platelet shape change and platelet aggregation. Whilst P2Y$_1$ activation is rapid but reversible, P2Y$_{12}$ is particularly important as it sustains activation by ADP and other agonists, through its activation of PI3K. This leads to irreversible platelet aggregation making it a key target for acute coronary syndrome treatment.

Although P2Y$_{12}$ was not identified until 2001 (Foster et al., 2001; Hollopeter et al., 2001), a congenital abnormality in a protein later discovered to be P2Y$_{12}$ receptor, was first described in 1992 (Cattaneo et al., 1992). The P2Y$_{12}$ receptor was identified by Hollopeter and colleagues in 2001 using genetically engineered *Xenopus* oocytes which allowed the identification of G$_i$-linked responses. In their study, they managed to identify and isolate the P2Y$_{12}$ gene from the platelet cDNA library and expressed it in the *Xenopus* oocytes. They proved that a frameshift mutation caused by a 2-base pair deletion in the P2Y$_{12}$ gene led to prolonged bleeding (Hollopeter et al., 2001).

One of the core functions of the P2Y$_{12}$ receptor is the inhibition of adenylyl cyclase via the G$_i$ signalling pathway resulting in low levels of cAMP (Hardy et al., 2004). In addition to adenylyl cyclase inhibition, the P2Y$_{12}$ receptor also plays a role in calcium signalling by prolonging the elevated levels of calcium in the cell, leading to platelet activation (shape change and granule release) (Daniel et al., 1998; Hardy et al., 2004).

Activation of heterodimeric integrin $\alpha_{IIb}\beta_3$, which has also been recognised as the fibrinogen receptor, is influenced by ADP/P2Y$_{12}$ activation as well. This activation causes cross linking of platelets as fibrinogen binds to activated fibrinogen receptors on other platelets to form a platelet plug. Gi signalling activation originating from P2Y$_{12}$ and ADP binding can also trigger the stimulation of other signalling pathways, release of microparticles, increased response to other platelet agonists, fibrin formation, and sustained platelet aggregation (Trumel et al., 1999).

1.5.2 P2Y$_{12}$ expression

P2Y$_{12}$ receptor is found mostly on the platelets. However, expression has also been demonstrated on different cell types including vascular smooth muscle cells (Wihlborg et al., 2004; Rauch et al., 2010), amongst other cells, detailed in Table 1-3. All these findings show that, even though P2Y$_{12}$ receptor plays a role in ADP-induced platelet activation, it may have multiple functions and important roles in different cells and tissues.

Table 1-3: P2Y$_{12}$ expression in other cells or tissues, technique(s) of identification and its function respectively

Cells	Site of origin	Function	Techniques	Reference
Endothelial cells	Cell lines	Not stated	Immunoblotting was performed for P2Y$_{12}$ identification in cell lines; Human coronary artery endothelial cells (HCAEC), human umbilical vein endothelial cells (HUVEC)	(Shanker et al., 2006)
Smooth muscle cells	Internal mammary artery and distal internal mammary vein	Stimulate vasoconstriction, increased IL-6 expression, and SMC mitogenesis after pre-stimulation with thrombin.	mRNA quantification by real-time polymerase chain reaction (RT-PCR), DNA synthesis and cell proliferation assay	(Wihlborg et al., 2004; Rauch et al., 2010)
Microglia	Brain tissue	Stimulates the integrin-β1 by the action of ATP mediated by P2Y$_{12}$	Quantification of antibody of activated integrin-β1 by Immunoprecipitation	(Ohsawa et al., 2010)
Cholangiocytes	Liver tissue	Ciliary P2Y$_{12}$ receptor acts as a chemosensory organelle to detect biliary nucleotides by transducing signals into a cAMP signalling cascade.	P2Y$_{12}$ expression is quantified by RT-PCR and localisation of P2Y$_{12}$ attached to cholangiocyte cilia was observed by Immunogold scanning electron microscopy (SEM)	(Masyuk et al., 2008)
Dendritic cells	Blood	Enhance specific T-cells activation	Mice lacking P2Y$_{12}$ were generated	(Ben et al., 2010)
Osteoclasts	Bone tissue	Bone-resorbing osteoclast (OC) activity	Observation of decrease OC activity in mice lacking P2Y$_{12}$ receptor analysed by μCT scanning.	(Su et al., 2012)
Spleen endothelial cells	Rat spleen	Unknown	Observed by the immunofluorescence microscopy and the localisation of the receptors were observed by Immunogold Electron Microscopy	(Uehara & Uehara, 2014)
Leukocytes	Blood	Stimulates the release cytokines for inflammatory response	Leukapheresis (for blood sample) and RT-PCR for mRNA quantification	(Diehl et al., 2010)

1.5.3 Platelet P2Y$_{12}$ activation

During endothelial cell injury, the medial layer, collagen and disrupted sub-endothelial matrix are exposed to circulating platelets leading to increased leukocyte adhesion. Due to high shear stress, endothelial von Willebrand Factor (vWF) is translocated from the Weibel-Palade bodies to the cell surface to allow platelet adhesion. Platelets are activated and release their granule contents such as growth factors, ADP, ATP and other inflammatory molecules, facilitating further platelet activation and aggregation (Rendu & Brohard-Bohn, 2001).

Besides ADP, thrombin can also cause platelet activation and release of granule contents. Even though ADP is recognised as a weak agonist compared to thrombin, only ADP activation of P2Y$_{12}$ sustains and amplifies activation responses leading to irreversible aggregation (Hollopeter et al., 2001).

Transmembrane ectonucleotide CD39 and ecto-5'-nucleotidase CD73 are responsible for the conversion of ATP to ADP by the action of extracellular dephosphorylation (Visovatti et al., 2012). Both co-mediators are involved in the inflammatory response, cell proliferation and thrombosis. Evidence of altered nucleotides and ectonucleotides in PAH have been shown by Visovatti et al., (2012). They showed by comparing 20 participants (10 healthy control subjects and 10 advanced IPAH patients) using thin layer chromatography and flow cytometry that CD39, ATPase and ADPase expression are increased in IPAH patients (Visovatti et al., 2012).
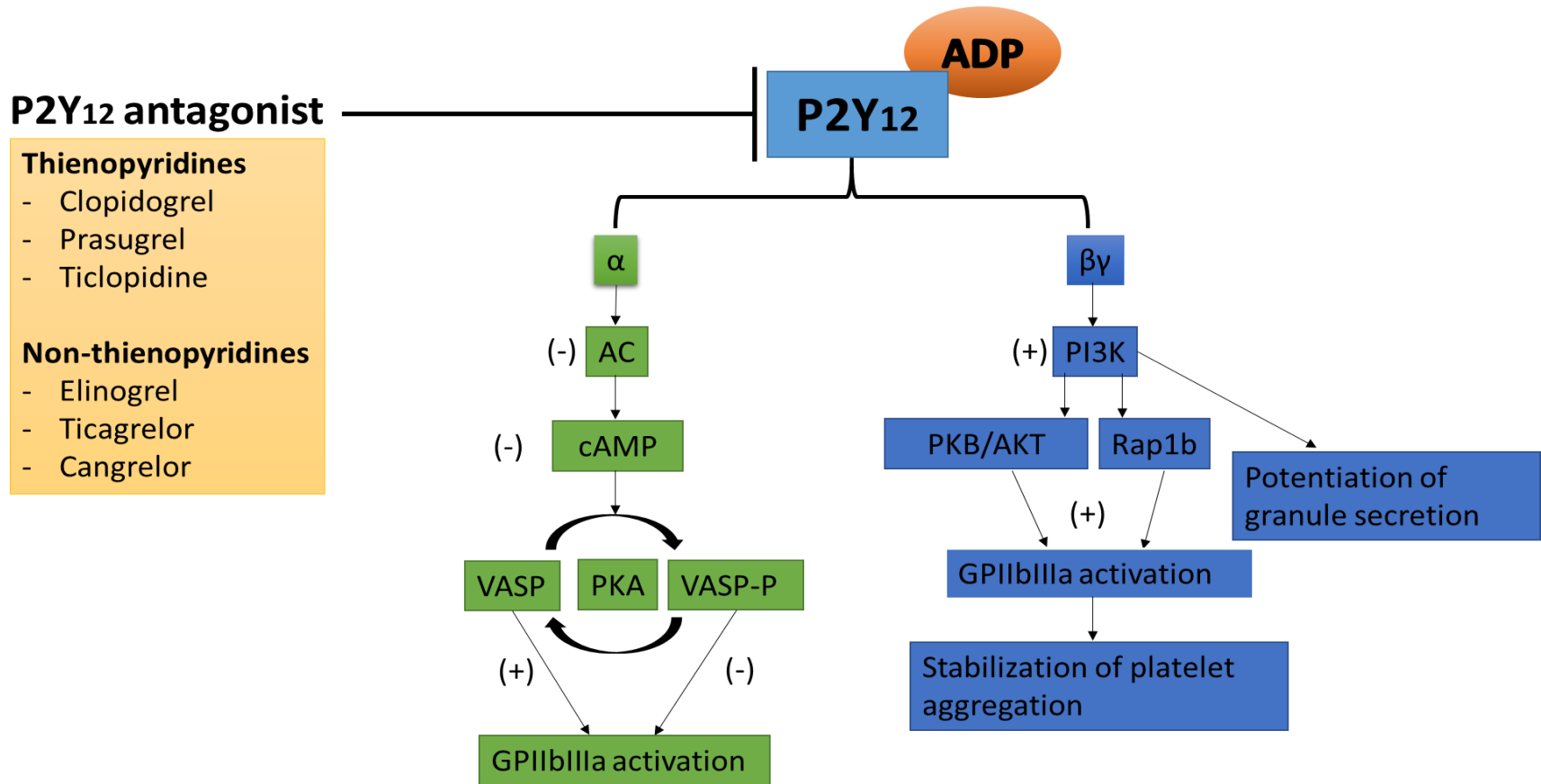
Figure 1-3: P2Y$_{12}$ signalling pathway in platelets

Figure 1-3 shows the P2Y$_{12}$ signalling pathway in platelets. Adenosine diphosphate (ADP) binds to P2Y$_{12}$, a G-protein coupled receptor, which liberates its Gi protein subunits, alpha (α) and beta gamma ($\beta\gamma$). Alpha subunits will attach to the adenylate cyclase subunits which is an enzyme responsible for catalysing the transformation of ATP to cyclic AMP (cAMP), a second messenger. This binding results in inhibition of adenylate cyclase activity. In the absence of Gi inhibition, ATP will then be converted to cyclic AMP. cAMP will bind to protein kinase (PKA) which phosphorylates Vasodilator-stimulated phosphoprotein (VASP). Therefore, there will be lower levels of phosphorylated VASP in the presence of ADP. On the other hand, P2Y$_{12}$ antagonists block the inhibitory effect of P2Y$_{12}$ on adenylyl cyclase (AC), therefore enabling cAMP synthesis and VASP phosphorylation, which then promotes vasodilation/resting platelet. The information above in Figure 1-3 was adapted with permission from Angiolillo et al., (2008). (Angiolillo et al., 2008).

1.5.4 P2Y$_{12}$ intracellular signalling

In addition to platelet aggregation, ADP-P2Y$_{12}$ activation is required for multiple functions; co-factor for thromboxane A$_2$ signalling (Paul et al., 1999), α-granule secretion (Quinton et al., 2004) and fibrinogen receptor activation, which is critical for the formation of a platelet plug (Daniel et al., 1998; Quinton et al., 2002).

ADP-P2Y$_{12}$ binding will activate intracellular coupled Gi protein which consists of different subunits; α, β, and γ where β and γ form a complex. P2Y$_{12}$-ADP binding liberates the Gi protein subunits and the α unit attaches to adenylyl cyclase leading to its inhibition and reduction in the conversion of ATP to cyclic AMP (cAMP), a second messenger. This inhibition of adenylyl cyclase (or adenylate cyclase) leads to a reduction in vasodilator-stimulated phosphoprotein (VASP) phosphorylation. In the absence of Gi inhibition, ATP will be converted to cyclic AMP and binds to protein kinase A (PKA). PKA, a cAMP- dependent enzyme, will only be activated in the presence of cAMP. Cyclic AMP will bind to PKA to promote VASP phosphorylation. Therefore, in the presence of ADP, there will be lower levels of phosphorylated VASP and sustained platelet aggregation. VASP phosphorylation and dephosphorylation levels are dependent on the level of cyclic nucleotides (Geiger et al., 1999; Glenn et al., 2013).

Upon P2Y$_{12}$-ADP binding, the β and γ complex formed will activate PI3-K signalling resulting in the activation of Akt and small GTPase Rap1b (Woulfe et al., 2002). PI3-K signalling will mediate granule secretion and platelet activation, amplifying platelet aggregation. This is thought to be brought about by the generation of PI3K product called phosphatidylinositol 4,5- biphosphate (PIP2). PI3-K signalling can be stimulated by thrombin but without the addition of P2Y$_{12}$ activation

only results in reversible aggregation (Dangelmaier et al., 2001; Kauffenstein et al., 2001; Trumel et al., 1999).

Furthermore, blocking P2Y$_{12}$ signalling shows the reduction in the release of platelet activation marker P-selectin (Quinton et al., 2004). P2Y$_{12}$ is also involved in GPIIbIIIa integrin (also known as αIIbβ3) activation which is responsible for platelet spreading on fibrinogen via PI3-K/Akt signalling (O'Brien et al., 2012). Absence of P2Y$_{12}$ activation leads to reversible platelet aggregation and cause GPIIbIIIa inactivation due to PI3K/Akt signalling inactivation. In addition, study by O' Brien et al., (2012) showed that P2Y$_{12}$ $^{-/-}$ platelets resulted in partial inhibition of platelet spreading compared to the control. Akt phosphorylation was significantly reduced in platelets from P2Y$_{12}$ knockout mice. This addressed the importance of P2Y$_{12}$ receptor activation and downstream signalling activation; i.e. PI3K and Akt signalling in platelets spreading (O'Brien et al., 2012). This study proved that lack of P2Y$_{12}$ receptor activation causes reduced platelet spreading.

In addition, the activation of P2Y$_{12}$ and Gi signalling activation leads to other intracellular signalling pathways such as the extracellular-signal-regulated kinase (ERK), myosin light chain kinase (MLCK), and Src family kinases (Kolen & Slegers, 2006; Van Kolen et al., 2006). Recently, it was also discovered that P2Y$_{12}$ activation by ADP results in cofilin dephosphorylation in brain cells (Niu et al., 2017).

1.5.5 P2Y$_{12}$ receptor promotes thrombosis

ADP and P2Y$_{12}$ receptor play a vital role in thrombosis by promoting sustained platelet aggregation and P2Y$_{12}$ was cloned from rat and human cDNA libraries in *Xenopus* oocytes, which was designed to identify the functional P2Y$_{12}$ receptor in human and animal platelets (Foster et al., 2001; Hollopeter et al., 2001). Since this time, Remjin and colleagues performed an investigation to elucidate the role of P2Y$_{12}$ in thrombus formation using healthy and P2Y$_{12}$ deficient blood samples, either with or without P2Y$_{12}$ antagonist treatment, cangrelor. They showed that platelet adhesion to fibrinogen is reduced and the thrombi formed are smaller in both the P2Y$_{12}$ deficient and cangrelor-treated groups (Remjin et al., 2002). This shows that P2Y$_{12}$ contributes to platelet plug formation and cangrelor is effectively blocking the P2Y$_{12}$/ADP platelet plug formation mediated pathway. In addition, to determine whether deficiency of P2Y$_{12}$ in platelets or vessel wall contribute to the response to injury and thrombosis, Evans et al., (2009) used a murine ferric chloride (FeCl$_3$) injury model and a bone marrow transplant (BMT) mouse model. In their FeCl$_3$ injury model, they observed thrombus formation in the carotid artery of P2Y$_{12}^{+/+}$ (wild type) mice, 30 minutes after injury. However, thrombus formation was significantly reduced in P2Y$_{12}^{-/-}$ deficient mice. They also showed in their BMT model using chimeric mice that a significant reduction in neointima formation was observed in mice with P2Y$_{12}$ deficient platelets, compared to those mice which expressed platelet P2Y$_{12}$. However, vessel wall P2Y$_{12}$ expression had no effect on neointima formation. This shows that in response to injury, P2Y$_{12}$-mediated platelet activation plays a significant role in thrombus and neointima formation (Evans et al., 2009).

1.5.6 P2Y$_{12}$ receptor and vasoconstriction

Besides promoting thrombosis, it has been shown that the P2Y$_{12}$ receptor stimulates vasoconstriction (Wihlborg et al., 2004). Kylhammar and colleagues investigated on the effects of P2Y$_{12}$ and P2Y$_1$ receptors in the acute hypoxic-pulmonary hypertension pig model and they looked whether ADP promotes vasoconstriction. They found that infusion of ADP caused an increase in the mean of pulmonary arterial pressure and pulmonary vascular resistance, which were fully reversible after stopping the infusion of ADP. They also showed that ADP promotes *in vivo* pulmonary vasoconstriction via the activation of P2Y$_1$ and P2Y$_{12}$ receptors. This was shown by introducing P2Y$_1$ and P2Y$_{12}$ antagonists pre-treatment, MRS2500 and cangrelor targeting P2Y$_1$ and P2Y$_{12}$ respectively (Mitchell et al., 2012; Kylhammar et al., 2014). However, Mitchell et al., (2012) argued that P2Y$_{12}$ antagonism inhibits contraction evoked by ATP. This suggests that vasoconstriction is mediated by ATP converted to ADP by the ecto-nucleotidase, which binds to P2Y$_{12}$ receptor promoting a contractile response (Mitchell et al., 2012).

1.5.7 P2Y$_{12}$ receptor and inflammatory response

P2Y$_{12}$ receptor has also been documented to be involved in the inflammatory response via platelet activation (Liu et al., 2011). Research by Liu et al., (2011) showed that P2Y$_{12}$ antagonists are an effective anti-inflammatory agent as an inflammatory response was suppressed following P2Y$_{12}$ antagonist treatment in a mouse myocardial infarction (MI) model. P2Y$_{12}$ antagonist reduced platelet mediated leukocyte conjugation in peripheral blood, suppressed inflammatory response and inflammatory mediators like matrix

metallopeptidase (MMP)-13, MMP-9, IL-1β and tumour necrosis factor-α (TNF-α) (Liu et al., 2011).

In addition, the NF- kB transcription factor consensus binding sites are found in the promotor region of P2Y$_{12}$, suggesting the P2Y$_{12}$ receptor may be inflammation responsive (Rauch et al., 2010). Interestingly, treatment with clopidogrel, a P2Y$_{12}$ antagonist, shows reduction in inflammatory markers such as C-reactive protein (CRP), CD40L, P-selectin and platelet-leukocyte interaction. This would suggest that the P2Y$_{12}$ receptor contributes to the inflammatory response, and that P2Y$_{12}$ antagonism may demonstrate anti-inflammatory effects (Steinhubl et al., 2007).

1.5.8 P2Y$_{12}$ receptor plays a role in vascular remodelling, cellular proliferation, and migration

Less is known about the contribution of P2Y$_{12}$ in other cells; i.e. vascular cells and brain cells. MAP kinase (Grobben et al., 2001), PI3-K (Pozios et al., 2001), and ERK (Shatos et al., 2008) are involved in signalling cascades regulating cell proliferation. Czajkowski et al., (2004) demonstrated the involvement and influence of P2Y$_{12}$ receptors in PI3-K/Akt and ERK1/2 signalling pathways suggesting that the P2Y$_{12}$ receptor can evoke cell proliferation via ERK1/2. This was demonstrated by blocking P2Y$_{12}$ with a potent antagonist, AR-C69931MX in cultured C6 glioma cells. They observed p44/42 MAPK phosphorylation in dose dependant manner was inhibited with the addition of P2Y$_{12}$ antagonist. Also, from western blot analysis, 2 minutes pre-treatment with P2Y$_{12}$ antagonist and 5 minutes with agonist (ADP), ERK was phosphorylated and this action was inhibited with AR-C69931 treatment. Other findings include ADP induced C6 glioma cell proliferation and ERK1/2 signalling were involved (Czajkowski et al., 2004). Rauch et al., (2010) demonstrated that pre-incubation with

thrombin together with 2-methylthioadenosine diphosphate trisodium salt (2MeSADP) in smooth muscle cells resulted in increased $P2Y_{12}$ receptor expression. Pre-exposure of thrombin (to activate NF-kB) significantly increases smooth muscle cell number and promotes a mitogenic response to 2MeSADP via $P2Y_{12}$ suggesting that besides a pro-inflammatory role, $P2Y_{12}$ also has pro-mitogenic properties (Rauch et al., 2010). $P2Y_{12}$ has also been shown to regulate proliferation in cancer cells (Haynes et al., 2006).

Niu et al., (2017) showed that $P2Y_{12}$ promotes migration in VSMCs in a model of atherogenesis via cofilin protein dephosphorylation, which was confirmed in a mouse model of lentivirus-mediated $P2Y_{12}$ specific short hairpin RNA (shRNA), where $P2Y_{12}$ receptor expression was reduced in vascular smooth muscle cell (VSMC) (Niu et al., 2017). There is also evidence showing the involvement of $P2Y_{12}$ in migration via different pathways such as MCP1 (Harada et al., 2011).

$P2Y_{12}$ inhibitors (clopidogrel, prasugrel and ticagrelor) have been shown to affect proliferation of endothelial cells (Korybalska et al., 2018). Harada et al., (2011) have shown that using $P2Y_{12}$ knockout mice, $P2Y_{12}$ plays a role in transplant atherosclerosis (TA). They also showed that the specific cells involved in luminal occlusion reduction which were identified using histological analysis; bone marrow derived smooth muscle like cells and CD45+ leukocytes (Harada et al., 2011). There have been studies reporting a role for $P2Y_{12}$ in atherosclerosis as well (Abele et al., 2009; West et al., 2014). Clopidogrel has been shown to reduce atherosclerotic lesion size in a murine $ApoE^{-/-}$ (Apoliprotein E) knockout model of atherosclerosis (Abele et al., 2009). West et al., (2014) also showed the contribution of $P2Y_{12}$ in attenuating atherogenesis (West et al., 2014). Finally, Giachini et al., (2014) demonstrated

that clopidogrel treatment inhibits vascular remodelling in hypertensive rats (Giachini et al., 2014).

1.5.9 P2Y$_{12}$ antagonists

Clopidogrel (a P2Y$_{12}$ antagonist) has been used for more than 20 years in patients with acute coronary syndromes (ACS) (Cattaneo, 2015; Cattaneo, 2011). Clopidogrel (and **Prasugrel**) is a thienopyridine P2Y$_{12}$ antagonist. Following oral administration, it is rapidly absorbed in the intestine and activated in the liver. This conversion needs two sequential oxidation steps for clopidogrel to achieve its active metabolite. Clopidogrel irreversibly binds (with a di-sulphide bridge) to the P2Y$_{12}$ receptor inhibiting platelet aggregation by preventing the direct binding of ADP to P2Y$_{12}$. Dual antiplatelet treatment combined with aspirin helps in reducing major CV events; coronary stent thrombosis and ischemic heart disease. Several studies have documented the effectiveness of clopidogrel in reducing cardiovascular disease events; Clopidogrel in Unstable Angina to Prevent Recurrent Events (CURE) by the CURE investigators (Yusuf et al., 2000), Reduction of Myocardial Damage during Angioplasty study (Patti et al., 2005), CLARITY trial study (Zambahari et al., 2007) and others. In the CURE study, they showed that clopidogrel is safe for long term usage. CURE reported on a meta-analysis of thienopyridines treatment (i.e. clopidogrel and ticlopidine) in vascular diseases. From the large meta-analysis of a randomised clinical trial involving 508 centres located in 28 countries, the researchers showed that superior effects were observed for acute and long termed dual treatment of clopidogrel combined with aspirin, compared to aspirin treatment alone in cardiovascular patients. Patients treated with clopidogrel maintained full anti platelet action several hours after administration, which makes clopidogrel useful in acute and chronically ill

patients such as stroke, myocardial infarction and those undergoing stent implantation or non-elective percutaneous coronary intervention (Yusuf et al., 2000).

In addition to cardiovascular disease, clinical trials of clopidogrel has been conducted in several diseases, including cancer (Denslow et al., 2017) and systemic sclerosis (Ntelis et al., 2016). At the moment, clinical research of $P2Y_{12}$ inhibitor in PH or diseases related to PH is limited. However, there are a few reports that have been published in recent years that might suggest the role of $P2Y_{12}$ receptor in disease related to PH (Campo et al., 2017; Ntelis et al., 2016; Robbins et al., 2006).

A clinical trial on the effect of $P2Y_{12}$ inhibitor, clopidogrel has been done on systemic sclerosis patients. Platelet activation causes increase in levels of serotonin and leads to fibroblast activation. Increased serotonin levels were observed in pulmonary hypertension patients. Study by Ntelis et al., (2016) showed that clopidogrel effectively inhibits ADP induced platelet activation in SSC patients. Also, they showed that clopidogrel reduced platelet aggregation but causes endothelial dysfunction. This was shown by the increased levels of vascular cell adhesion molecule 1 (s-VCAM1) which increase of s-VCAM1 represents worst endothelial function (Ntelis et al., 2016).

As previously mentioned, in-situ thrombosis is one of the mechanism involved in PAH pathogenesis and platelet aggregation favours the formation of in-situ thrombosis. A pilot study conducted by Robins et al., (2006) investigated the effect of clopidogrel and aspirin on platelet function and eicosanoid metabolism. Low levels of eicosanoid metabolism such as prostaglandin, a potent vasodilator was observed in PH. Robbins et al., (2006) showed that clopidogrel and aspirin reduced platelet activation. Aspirin inhibited the formation of Thromboxane B2 (TXB2) in idiopathic PH patients suggesting that the majority of TXB2 in blood is generated by platelets. There was no effect on PGI-M levels. This study may suggest

that clopidogrel and aspirin would be a suitable treatments for PH as they produce a favourable balance between TXB2 levels (vasoconstrictor) and PGI-M levels (vasodilator) (Robbins et al., 2006). More clinical trials are needed to draw this conclusion.

There are a small number of animal studies that have shown the important role of clopidogrel in PH (Wihlborg et al., 2004; Kylhammar et al., 2014). However, a common genetic mutation of cytochrome p450-1A in the hepatic metabolism pathway causes some patients to be unable to generate the active metabolite of clopidogrel, therefore, rendering it ineffective. This has led to the necessity for the development of other $P2Y_{12}$ targeted anti-platelet therapies that do not require any metabolite conversion.

Ticagrelor was the first oral reversible $P2Y_{12}$ antagonist. In the PLATO (PLATelet Inhibition and Patient Outcomes) PLATELET sub-study by Robert Storey et al., (2010), they showed that ticagrelor therapy has superior efficacy compared to clopidogrel. Ticagrelor achieves high efficacy of platelet activation inhibition in acute coronary syndrome patients (Storey et al., 2010). Ticagrelor has been also documented to reduce contractility of smooth muscle cells from rat tail artery (Grzesk et al., 2013). Ticagrelor has more potential than clopidogrel as ticagrelor can be used with the CYP2C19 gene defect, since no biotransformation in the liver is needed for ticagrelor to be in active form (Tantry et al., 2010). As mentioned in the literature, endothelial dysfunction is one of the major players in PAH pathogenesis and associated with COPD. Recently, Campo et al., (2017) showed the effect of ticagrelor and clopidogrel on endothelial cell function. In their clinical trial (The comparison between ticagrelor and clopidogrel effect on endothelial, platelet And iNflammation parameters in patiEnts with stable coronary artery disease and chronic obstructive pulmonary disease undergoing percutaneous coronary intervention) (NATHAN-NEVER), they showed that with 1

month of ticagrelor treatment, lower levels of endothelial apoptosis and a better platelet inhibition were identified in COPD patients. Study by Campo et al., (2017) suggests that ticagrelor maybe superior to clopidogrel in moderating endothelial function (Campo et al., 2017). This may suggest that by inhibiting platelet activation and endothelial dysfunction, ticagrelor may be a potential treatment for PH.

Cangrelor is an intravenously administered and a reversible $P2Y_{12}$ inhibitor with high affinity binding which does not rely on any metabolic conversion, unlike clopidogrel. It also causes fast onset and offset of activation and has been said to reduce thrombotic complications. The pharmacokinetic criteria for cangrelor allows it to be rapidly cleared from plasma with a half-life of 2.6 to 3.3 minutes after administration and platelet function is stabilised within an hour (Angiolillo & Capranzano, 2008). Studies have shown that cangrelor is safe to be used as it reduces ischemic events (Angiolillo et al., 2012) and stent thrombosis without causing bleeding problems (Bhatt et al., 2013). The BRIDGE study showed that cangrelor reduces bleeding complications by maintaining platelet inhibition for those undergoing coronary artery bypass grafting (CABG) surgery (Angiolillo et al., 2012).

1.6 $P2Y_{12}$ in Pulmonary Hypertension

As highlighted above, $P2Y_{12}$, has been shown to play a role in cell proliferation (Rauch et al., 2010), migration and, vasoconstriction (Wihlborg et al., 2004; Kylhammar et al., 2014) and it can modulate various vascular pathologies (Syberg et al., 2012; West et al., 2014). As such, there is a plausible role for $P2Y_{12}$ and its inhibition in PAH. Kylhammar and colleagues found that the $P2Y_{12}$ antagonist, cangrelor reduced ADP-mediated vasoconstriction in an acute hypoxic pig model (Kylhammar et al., 2014). However, the specific role of $P2Y_{12}$ in PASMC and pulmonary vascular remodelling remains unclear.

1.7 Hypothesis and aims

My hypothesis is the $P2Y_{12}$ receptor plays a significant role in PAH pathogenesis, and treatment with a $P2Y_{12}$ antagonist will modulate disease progression.

Therefore, I aim to explore, through *in vitro* and *in vivo* methods, the role of $P2Y_{12}$ in PAH. To achieve this aim, I have outlined four project objectives:

1. To determine the expression level of $P2Y_{12}$ receptor at an mRNA level in healthy and diseased PASMCs of human patients.

2. To investigate $P2Y_{12}$ receptor activation on vasodilator stimulated phosphoprotein pathway.

3. To investigate $P2Y_{12}$ receptor blockade and its effect on signalling mechanisms involved in PASMC phenotypes; proliferation and migration.

4. To determine the effect of therapeutic treatment with a $P2Y_{12}$ antagonist in an *in vivo* model of PH.
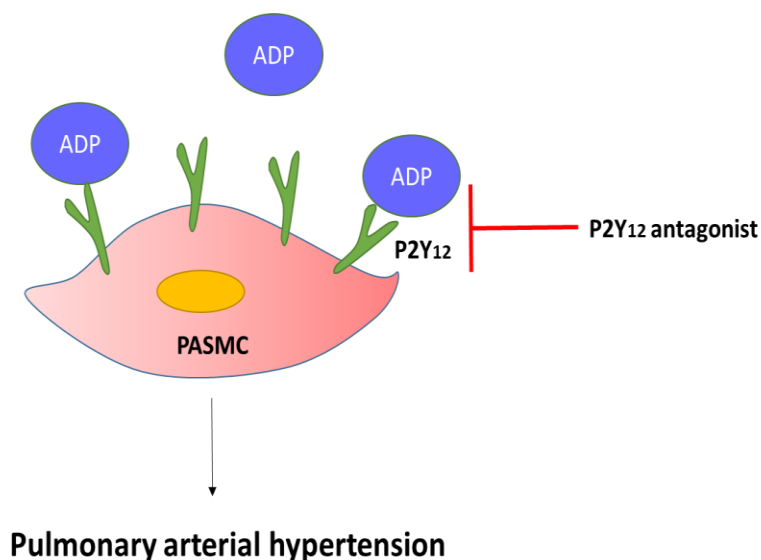
Figure 1-4: Schematic representation of PASMC expressed $P2Y_{12}$ receptor and $P2Y_{12}$ antagonist inhibited ADP/$P2Y_{12}$ binding on PASMC.

2 Methodology

2.1 Human Pulmonary Artery Smooth Muscle Cells (PASMCs) Culture

2.1.1 General procedure for cell culture

Experiments were performed in a class II safety cabinet, observing standard sterile techniques used for tissue culture. Cells were maintained in T75 flasks in a 37 ˚C incubator with 5% of CO_2. Detailed description on materials and reagents used in cell culture work can be referred to appendices; Appendix 1 and Appendix 4.

2.1.2 LONZA Pulmonary Artery Smooth Muscle Cells (PASMCs) passage

Commercially available human PASMCs were purchased from LONZA (Basel, Switzerland). Pulmonary Arterial Smooth Muscle Cells (PASMCs) (CC-2581) were cultured in smooth muscle growth medium 2 (SmGM-2) Bullet kit (Lonza CC_3182) which includes; 5% v/v foetal bovine serum (FBS), 0.2% v/v hFGF-β, 0.1% v/v insulin, gentamicin (30μg/ml) and amphotericin (15 ng/ml).

After the cultured T75 cm^2 flasks were 80% confluent, the cells were passaged into three different flasks coated with fibronectin (30 minutes preincubation with 13.5 ng/ml fibronectin (Sigma F0895)). For experimental procedures, cells were plated in 96-well plates or T25 cm^2 flasks according to the experimental requirements. Twice weekly passaging of PBS washed cells in T75 flasks was performed using 1.5 ml Trypsin EDTA (Gibco TE 1x), incubated for 1 minute at 37 ˚C before addition of trypsin neutraliser and dilution with 36 ml full growth media for return to three T75 flasks for further incubation.

2.1.3 Patient derived pulmonary vascular cell and LONZA human PASMCs culture

Patient cells previously isolated from a pulmonary artery obtained from a lung transplant were used in my experiments under the standard ethical approval (REC reference 18/YH/0441, Local approval: STH15222). These cells were cultured as previously detailed for LONZA smooth muscle cells. Cells obtained from lung transplant were processed by Prof Allan Lawrie. Patients' demographic data profiles are as shown in Table 2.1.

The healthy human control cell of PASMCs that were used in this study consist of different ages (Appendix 14), and both genders. PASMCs were purchased from LONZA and details on human PASMCs; i.e. lot numbers are as described in Appendix 14.

2.1.4 HPASMCs seeding

For experimental procedures, cells were seeded on 96-well plates at a density of 5×10^4 cells/ml (determined by haemocytometer) according to the experimental design and plate layout.

2.1.5 HPASMCs cell cycle synchronisation

To synchronise the cells to the same phase of the cell cycle prior to stimulation, ensuring a stable baseline, cells were quiesced for 48 hours using quiescent media (1:20 dilution of full growth media in smooth muscle cell basal medium (SmBM) (LONZA CC-3181)). For this study, involved different set-up of plate and flask for stimulations; 96-well plates requiring 200 µl of quiescent media per well, 10 ml in T75 cm² flask, and 4ml in T25 cm² flask.

Table 2-1: Demographic data of patients

Table shows the demographic data for two lung transplant donors used in this study, documenting the age, sex, ethnicity, diagnosis, treatment given, incremental shuttle walking test (ISTW), right heart catheterisation (RHC) and other diseases that may be involved.

Patients	Age	Sex	Ethnicity	Diagnosis	Treatment given	ISWT Distance	RHC (mPAP)	Other diseases
Donor 1	40	Female	White British	IPAH	Frusemide, Omeprazole, Spironolactone, Bosentan, Sildenafil, Frusemide, Omeprazole, Spironolactone, Sando-K, Paracetamol, Fragmin, Zopiclone, Ventavis	240	61	No
Donor 2	39	Female	White British	IPAH	Spironolactone, Frusemide, Paracetamol, Nefopam, Bosentan, Sildenafil, Ventavis	350	60	No

2.2 Taqman® Real Time Polymerase Chain Reaction (RT-PCR) Assay

RT-PCR is a variant of polymerase chain reaction (PCR) which allows specific, sensitive detection of RNA expression quantification through the creation of cDNA transcript from RNA. Details on materials and reagents used in this section are as described in Appendix 5.

2.2.1 Pulmonary Artery Smooth Muscle cells RT-PCR sample preparation

PASMCs were cultured (between passage 5 to passage 7) in T25 cm^2 flasks to approximately 80% confluence. The media was removed and 500 μl of TRI reagent® (Zymo Research) was added to the cells. This step was done to lyse the cells and protect the mRNA. Flasks were stored at -80 ˚C to preserve RNA integrity and aid lysis of cells.

2.2.2 PASMCs RNA extraction by using DirectZol MiniPrep

The Direct-zol RNA MiniPrep by Zymo was used for RNA purification according to manufacturer's instructions, as detailed below.

2.2.2.1 Preparation of DNAse I mix

DNAse I mix was prepared by reconstituting 250 units (lyophilised) in 250 μl DNAse/RNAse free water. For each reaction, a mixture was made of:

5 μl of the prepared DNA I mix

64 μl of RNA wash buffer,

8 μl 10X DNAse I reaction buffer, and

3 μl of DNAse/RNAse free water

2.2.2.2 RNA extraction

Samples were defrosted on ice, and Tri-reagent was transferred to a 1.5 ml RNAse free tube. 500 μl of ethanol was then added and mixed. The sample was then transferred into a Zymo-spin™ IIC column which was placed in a collection tube. The tubes were centrifuged for 10, 000 x g for 1 minute. After centrifugation, the flow through (waste) in the collection tube was discarded and the column was transferred into a new collection tube. Next, 400 μl of RNA wash buffer was added to the column which was placed in a new collection tube. The tubes were centrifuged for 10,000 x g for 1 minute. After centrifugation, the waste from the flow through in the collection tube was discarded and replaced with new collection tube. 80 μl of DNAse I mix was then added to the column. This was then incubated for 15 minutes at 37°C for 15 minutes and centrifuged for 30 seconds at 10,000 x g. Then, 400 μl of Direct-zol™ RNA pre-wash was added to the column and centrifuged for 1 minute at 10, 000 x g. The flow through obtained after the centrifugation was discarded and 700 μl of RNA wash buffer was added to the column. Then, the column was centrifuged at 10,000 x g for 1 minute and the flow through was discarded. To ensure complete removal of the wash buffer, the empty column was centrifuged again at 10,000 x g for 2 minutes. Then, the column was transferred into an RNAse-free tube. Next, 50 μl of DNAse/RNAse free water was added to the column matrix and centrifuged at 10,000 x g for 1 minute (final centrifugation). After the final centrifugation, concentration of obtained RNA was measured by Nanodrop 1000 before being stored at -80°C.

2.2.3 cDNA synthesis via RNA Reverse transcription

Reverse transcription was used for transcribing the RNA template and reverse transcriptase enzyme to generate cDNA using Applied Biosystems High Capacity RNA to cDNA™ kit (Thermo

fisher, cat number 4368814). In this method, 2000 ng of cDNA concentration was generated. To make 2000 ng of cDNA, 1000 ng (RNA input) of RNA concentration was used.

20 µl of reaction volume was required

9 µl template (containing 1 µg RNA) made up in RNAse free water

1 µl of 20X enzyme

10 µl of 2X RT buffer

To detect cross contamination, a no template control (NTC) which contain no RNA was used. Besides NTC, a no enzyme control which referred as no reverse transcriptase control (NRT), was also used to assess contamination. All the RNA sample mixtures prepared for cDNA synthesis were placed in an Applied Biosystems Veriti 96 well thermocycler and the cDNA synthesis process was set at 37°C for 60 minutes, 95°C for 5 minutes and 4°C on hold. cDNA was stored at -20°C until required for Taqman RT-PCR amplification.

2.2.4 Taqman RT-PCR

384-well clear bottom plates were used for Taqman RT-PCR assay. All samples were loaded in triplicate.

All samples were diluted 1/10 using 20 µl of prepared cDNA into 180 µl of RNAse-free water to give a 20 ng/µl cDNA input.

Wells were loaded as below:

5 µl of diluted cDNA

0.5 µl of 20x probe, (*18S* or *P2RY12*)

4.5 µl of Taqman Universal Master mix II (Thermofisher, 4440038)

Quantification was run using the 7900HT Fast Real-Time PCR system (Life Technologies). 45 cycles and 9600 Emulation mode setting was set-up. To get optimal amplification and maximal yield, thermal profile was set-up as follows: one cycle at 50 °C for 2 minutes and 95 °C for 10 minutes, and then, 45 cycles of 95 °C for 15 seconds and 60 °C for 1 minute.

2.2.4.1 Taqman RT-PCR data analysis

In RT-PCR, Ct (cycle threshold) is the number of cycles it takes to perform an exponential increase of the target gene. Positive reaction is identified by the accumulation of fluorescence signal. This was obtained from the Ct (cycle threshold) to cross a certain defined threshold. Raw data obtained was calculated by normalising against *18S* RNA by describing the difference between the averaged delta C_T (ΔC_T) of gene of interest. The averaged ΔC_T of reference gene which gives the value of delta delta C_T ($\Delta\Delta C_T$). The calculation is best described as follows:

Calculation for delta C_T (ΔC_T):

$\Delta C_T = C_T$ (target gene) – C_T (endogenous reference gene)

Calculation for delta delta C_T ($\Delta\Delta C_T$):

$\Delta\Delta C_T$ = average ΔC_T (sample of interest) – average ΔC_T (reference sample)

2.3   In-cell Western; VASP phosphorylation assay and DNA staining

In-cell Western (ICW) is a widely used and high throughput assay for the detection of 2 target proteins (as shown in Figure 2-1) in a 96 well plate format. More details on materials and reagents; i.e. primary antibody and secondary antibody are as described in Appendix 3 and Appendix 6.
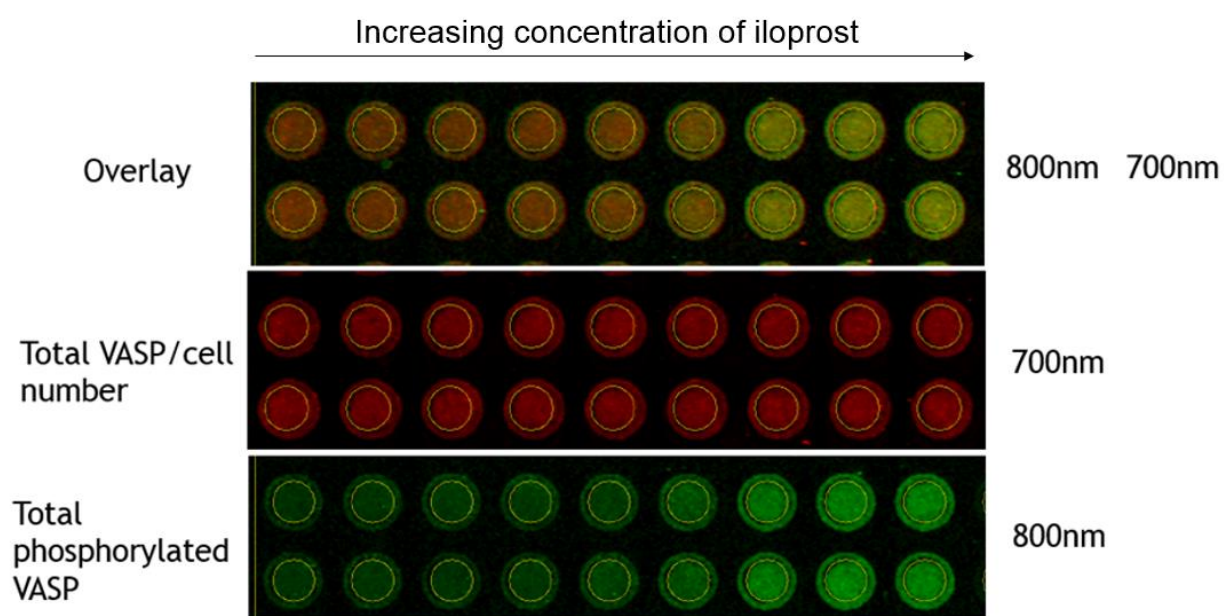
Figure 2-1: Fluorescence image from In-cell Western analysis

Figure 2-1 shows fluorescence image for analysis of VASP phosphorylation normalised to cell number or total VASP. Cell number is stained with DRAQ5 and Sapphire700 and quantified using channel 700, while phosphorylated VASP was detected using 800 channel. Image was recorded using LI-COR Image Studio Software.

2.3.1 PASMCs seeding and stimulation

PASMCs were grown and 5×10^4 cells/ml were seeded in 100 µl per well in 96-well plates (Corning Costar, Sigma, Dorset, UK). Before stimulation, cells were synchronised by using the starve media for 48 hours as described previously. After starvation, cells were stimulated according to the stimulation requirement which involved adenosine diphosphate (ADP) (Sigma-Aldrich), 2MeSADP (TOCRIS), cangrelor (AR-C66931 MX) which was a generous gift received from AstraZeneca R & D Charnwood (Loughborough, UK) and iloprost (Ventavis), together with negative control which was quiescent media. Detailed information on this section can be referred to Appendix 2.

2.3.2 Optimum dose for VASP phosphorylation assay

The first phase of this study was to develop the working model, and the initial step was to identify the optimum concentration of iloprost and 2MeSADP. The concentrations used in this experiment for iloprost were 0.01, 0.03, 0.1, 0.3, 1.0, 3.0, 10.0 and 30.0 µmol/l, and 100, 300, 1000, 3000, 10000, 30000 and 100000 nmol/l for 2MeSADP. 5000 seeded quiescent (72 hours) PASMCs were used for stimulation and phosphorylated VASP was quantified using two antibodies in an independent manner, unless stated otherwise; VASPp antibodies (VASPp[239] and VASPp[157]) (phosphorylated) (pSer239) (product code: ALX-804-240-C100, Enzo Life Sciences), VASP (phosphorylated) (pSer157) (5C6) (product code ALX-804-403 C100, Enzo Life Sciences).

VASP phosphorylation was observed in different concentrations of iloprost treated PASMCs, as shown in Figure 2-2. Effects of VASP phosphorylation on 2MeSADP treated PASMC with and without iloprost were determined after 10 minutes, as shown in Figure 2-3. From the

graph in Figure 2-3, VASP phosphorylation in 2MeSADP stimulated PASMC remained constant without iloprost pre-stimulation.

In the result sections, I have compared the effect of VASP phosphorylation in healthy human and PAH PASMCs as shown in Figure 3-3 at different time points (10 minutes, 20 minutes and 60 minutes). Table 2-2 shows the list of stimulants and time points used for VASP phosphorylation assay.
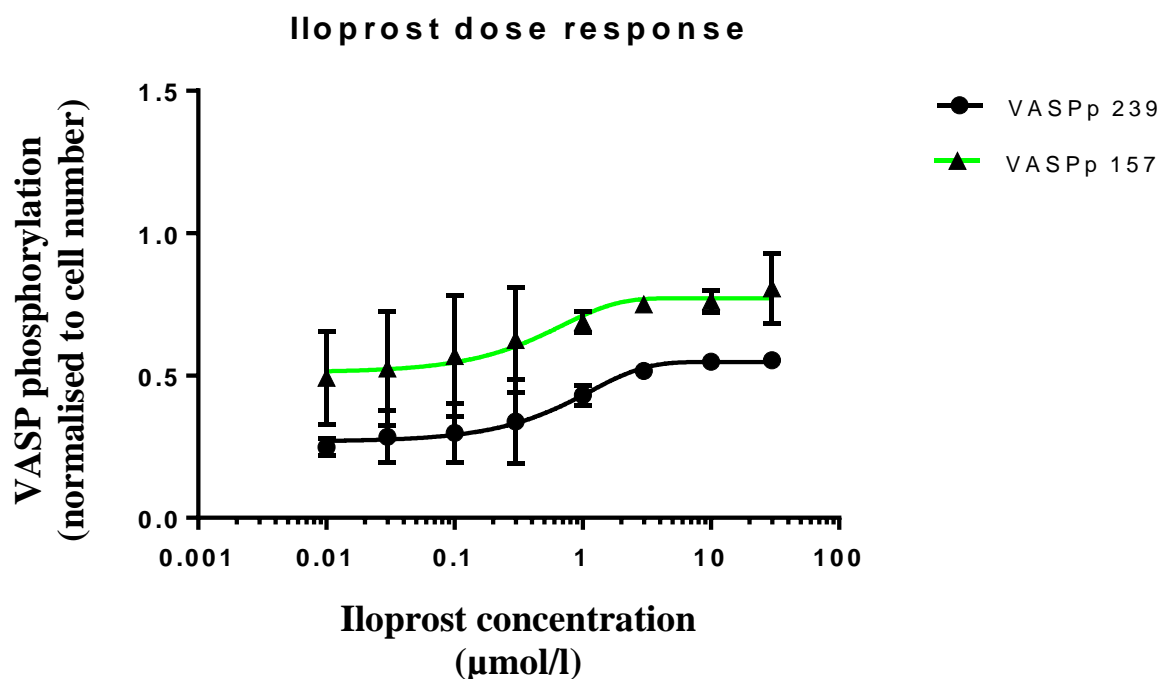
Figure 2-2: Analysis of VASP phosphorylation in different concentrations of iloprost in PASMC

Graph in Figure 2-2 shows the optimisation in different concentrations of iloprost (0.01, 0.03, 0.1, 0.3, 1.0, 3.0, 10.0 and 30.0 µmol/l) for 10 minutes at 37 °C. The cells were stained with VASP-p239 and VASP-p157 antibodies separately and were normalised to cell number (stained with DRAQ5 and Sapphire700). Quantification was done using In-cell Western LI-COR Bioscience. n=2 from different passage of healthy human PASMC (2 donors).
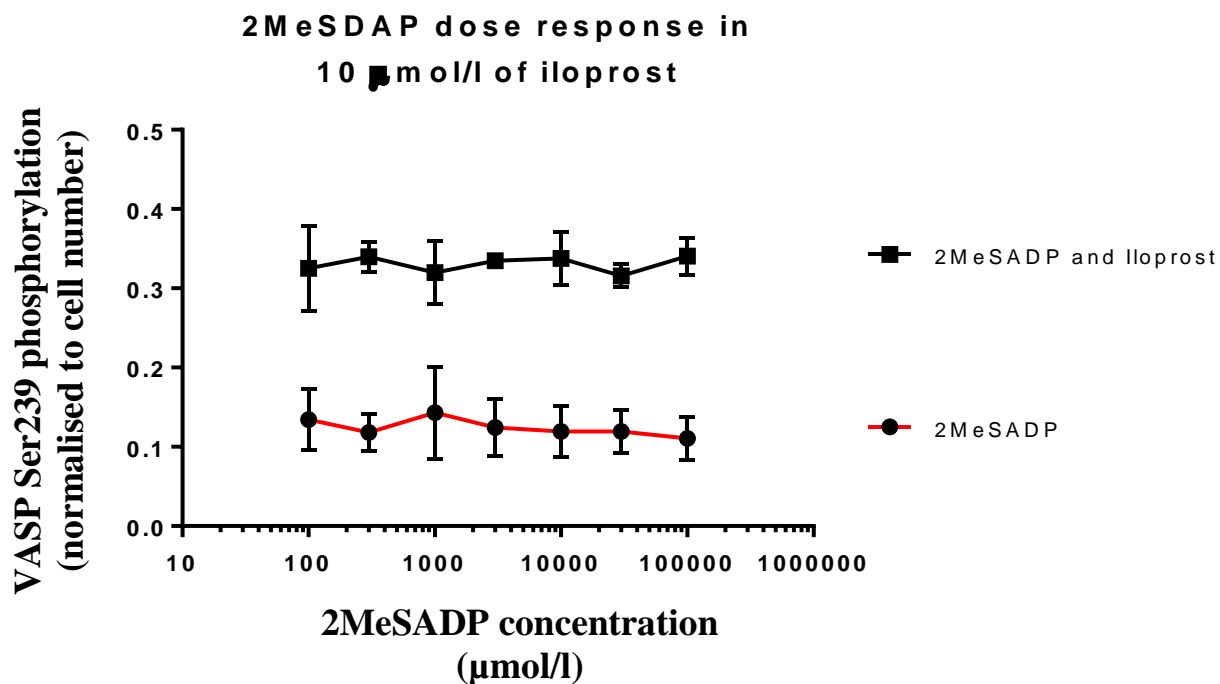
Figure 2-3: Analysis of VASP phosphorylation in different concentrations of 2MeSADP treated PASMCs

Graph in Figure 2-3 shows the optimisation in different concentrations of 2MeSADP (100, 300, 1000, 3000, 10000, 30000 and 100000 nmol/l) for 10 minutes at 37 °C. The cells were stained with VASP-p 239 and VASP-p157 antibodies separately and were normalised to cell number (stained with DRAQ5 and Sapphire700). Quantification was done using In Cell Western LI-COR Bioscience. n=2 from different passage of healthy human PASMC (2 donors).

Table 2-2: List of stimulants, concentrations and time points used for VASP phosphorylation assay for both human and diseased PASMCs.

Stimulants	Concentration (μmol/l)	Duration of stimulation
ADP	100	10minutes
2MesADP	1	
Cangrelor	1	
Iloprost	0.3, 1.0, 3.0, 10.0, 100.0	10, 20, 30 and 60 minutes

2.3.3 Fixation and Permeabilisation of cells

Media was removed from the wells and 150 µl of fixing solution (Tris buffered saline (TBS) containing 3.7% v/v formaldehyde) was added by pipetting to the sides of the well without disturbing the cells. This was incubated for 20 minutes at room temperature. Fixing solution was then removed by dabbing the plate gently to prevent cell detachment. Cell membranes were then permeabilised by washing the cells with TBS 0.1% Triton X-100 with gentle shaking for 5 minutes at room temperature repeated five times. Details for solution preparations are as described in Appendix 1.

2.3.4 Protein detection

Following permeabilisation, non-specific binding was blocked by 1.5 hour incubation with Odyssey Blocking Buffer at room temperature with gentle shaking.

Blocking buffer was then removed and 50 µl of 1:100 dilution of VASP-P (Enzo) antibody in Odyssey blocking buffer was loaded to each well and incubated overnight at 4 °C (gentle shaking). VASP antibodies used in this study are; monoclonal antibody to VASP (phosphorylated) (pSer239) (Product no: ALX-804-240-C100), [pSer157] VASP monoclonal antibody (5C6) (Product no: ALX-804-403 C100) at specific dilution (1:50). Cells were then washed with TBS 0.1% Tween, 5 times for 5 minutes each. Total VASP (942) Rabbit mAb (3132, Cell Signalling Technology), was also incubated for normalisation when necessary. Concentration used was 1:1000 as indicated by manufacturer.

For primary antibody detection and cell number normalisation, 50 µl of Anti-Mouse IRDye 800 (1:800 dilution) and DNA dye DRAQ5 (1:10000 dilution) with Sapphire700 (1:1000) in Odyssey Blocking buffer were added and incubated for 1 hour at room temperature with

gentle shaking. After incubation, cells were washed with TBS 0.1% Tween (3 times for 5 minutes each) and then liquid was removed before analysis. Plates were protected from light while washing.

2.3.5 Plate readout

Plates were analysed using the LiCOR Odyssey Sa system. DNA stain or other protein; i.e. total protein (depending on the assay) was detected using the 700 nm channel while intracellular phosphorylated protein was detected using the 800 nm channel. Signal quantification of phosphorylated proteins were normalised with DNA staining (700 channel) by dividing the signal of the phosphorylated protein by 700 channel and the comparison between stimulated cells and non-stimulated were done by comparing with quiescent cells by using GraphPad Prism (Version 7 or 8, San Diego, CA, USA) statistical analysis.

2.4   Platelet aggregation

Optical platelet aggregometry was performed in human and rat blood samples. This study received ethical approval for platelet study from Ethics Review Committee of Faculty of Medicine Dentistry and Health of the University of Sheffield with the reference number is SMBRER310.

Platelet aggregation tests were done in human blood to validate the reagents used for cell culture work and to rule out the possibility that these reagents have any inhibitory effects. Platelet aggregation was also done to assess pharmacodynamic ($P2Y_{12}$ inhibition) effects on platelet function following clopidogrel administration in Mct rats. In brief, 10 ml of citrated blood (3.13 % w/v tri-sodium citrate) was collected from human volunteers (venepuncture) and from all experimental groups of Sprague Dawley rats (cardiac puncture). Collected blood was centrifuged for platelet rich plasma (PRP) (200 g for 10 minutes at 24 °C). The PRP was then removed and the remaining blood was centrifuged again to obtain platelet poor plasma (PPP) (1500 x g for 10 minutes at 24 ºC). PPP was added to PRP to normalise platelet count. Aggregometry was performed on a Biodata PAP-8 optical aggregometer (Alpha Labs, Eastleigh, UK). Glass cuvettes were prepared, with 240 µl of PRP and a stir bar, for each agonist to be tested. A cuvette containing 240 µl of PPP was used to 'blank' each test well, denoting 100% aggregation. Cuvettes were incubated for 1 minute at 37 °C before being moved to the test wells. Baseline aggregation was recorded for 1 minute before addition of adenosine diphosphate. Platelet aggregation was recorded for a further four minutes. Platelet aggregation analysis was recorded as percentage of maximal aggregation (MA) and final aggregation (FA) responses. An overview of the process of platelet aggregation is shown in Figure 2-4.
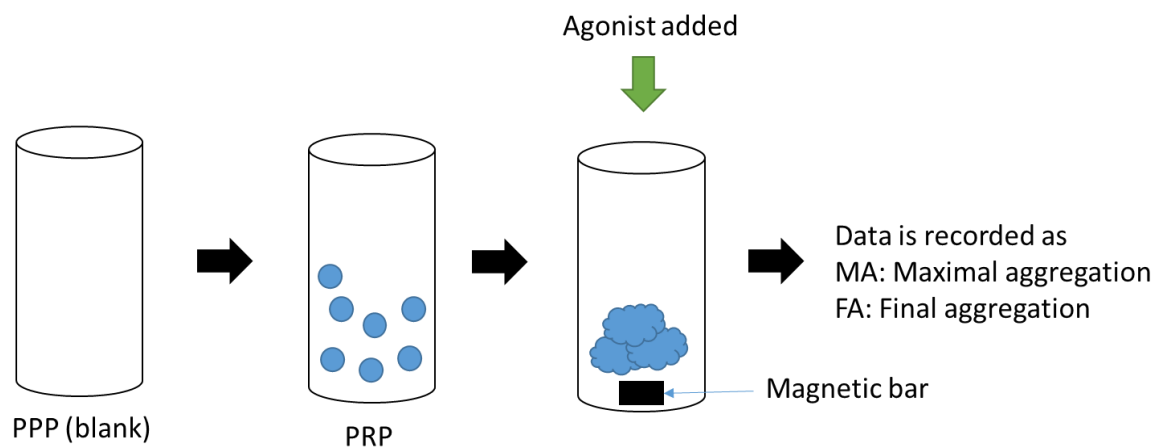
Figure 2-4: Brief overview of platelet aggregation testing principle

Figure 2-4 shows assessment of platelet aggregation using light transmission aggregometry. To obtain accurate results, the instrument was 'blanked' using an autologous sample of PPP. Samples of PRP are stirred by magnetic bar added in the presence of an agonist and as the platelets aggregate together, the light transmission through the sample increases which is a measure of platelet aggregation.

2.5   Radioligand binding study

A Radioligand binding assay was used to quantify the binding of ^{33}P 2MeSADP (Perkin Elmer, Buckinghamshire, UK) to P2Y$_{12}$ receptors on PASMC. A detailed information on materials used and recipes for reagents are as described in Appendix 7 and Appendix 8.

LONZA PASMC and patient cells were grown as described in section 2.1., counted (section 2.1.4) and diluted to 5 x 10^5 per ml for both patient and healthy PASMC. As the positive control in this essay, platelets were obtained from human donors who had not consumed any anti-platelet medication for 7 days prior to blood collection, and anticoagulated with acid citrate dextrose (65 mmol/L citric acid, 80 mmol/L tri-sodium citrate and 110 mmol/L dextrose). PRP was prepared as outlined in the previous section. PRP was centrifuged in the presence of apyrase (0.01 U/ml, Sigma Aldrich), EDTA (4 mmol/L, Fisher Scientific) and PGI2 (100 nmol/L, Cambridge Bioscience) for 20 minutes at 300 x g to prepare washed platelets (WP). The pellet was resuspended in HEPES-tyrodes (HT) buffer and diluted to 1 x 10^9 cells per ml. To assess ^{33}P 2MeSADP binding 200 µl of diluted WP or hPASMC were incubated with 100 µmol/L MRS 2179 (Sigma Aldrich) (to inhibit ^{33}P 2MeSADP binding to P2Y$_1$) and 30 nmol/L ^{33}P 2MeSADP for 5 min. Non-specific binding was assessed using a tube incubated with an excess of unlabelled 2MeSADP (10 µmol/L, Sigma Aldrich). After incubation, the cells were washed with PBS and harvested onto filter paper using a vacuum filtration and semi-automatic cell harvester (Molecular Devices, Sunnyvale, California, USA). The filter papers were added to tubes containing 5ml Ultima Gold MV scintillation fluid (Perkin Elmer, Buckinghamshire, UK) and placed in a scintillation counter (Perkin Elmer, Waltham, Massachusetts, USA) for quantification. P2Y$_{12}$ receptor number was quantified using the formula shown in Equation 1 (adapted from Judge et al.,2015).

We used this assay to demonstrate that PASMC expresses $P2Y_{12}$ receptors. To demonstrate that this assay is specific for $P2Y_{12}$ receptors, all the measurements were done in the presence of a $P2Y_1$ receptor antagonist. The radioligand has a specific activity (supplied by the manufacturer) and was measured relative to a specific date. This is necessary for radioactive decay. The specific activity for the radiochemical is the amount of radioactivity (33P) per molecule of ligand.

For calculation, non-specific binding was subtracted from the test result. Non-specific binding was measured in a sample which contained 100x molar excess of unlabelled 2MeSADP. This measurement provides specific activity for test sample. Then, this number was multiplied by the number of molecules in a mole of any substance which will give the number of molecules of ^{33}P 2MeSADP bound to the cells. In order to calculate this as molecule (receptors) per cell, this value was divided by the number of cells which give the number of $P2Y_{12}$ receptors per cell as shown in Equation 1. To calculate the percentage of functional receptor number and the effects of $P2Y_{12}$ receptor blockade by cangrelor, calculation was done as shown in Equation 2.

Equation 1: Calculation of $P2Y_{12}$ functional receptor number

$$\left((\text{CPM} \div \text{CPM per fmol}) \times 6.02 \times 10^8\right) \div \text{cell number,}$$

Where, CPM per fmol calculation was done as following equation;

$$[(\text{Ci/mmol} \times 2.22 \times 10^{12}) \times \text{counter efficiency}] \div 10^{12}$$

Equation 2: Calculation of percentage of receptor number

Percentage (%) of $P2Y_{12}$ receptor blockade calculation was done as following equation;

$$= \left[\frac{(\text{Total receptor no.} - \text{observed receptor no.})}{\text{Total receptor no.}}\right] \times 100$$

2.6   Flow cytometry: VASP P$^{-Ser239}$

Citrated whole blood (96 µl) was added to 4 µl of either saline (control), PGE1 (10 µmol/L, Cambridge Bioscience) or PGE1 plus ADP (30 µmol/L, Sigma Aldrich, Gillingham, UK) and incubated at room temperature for 5 minutes. 50 µl of fixative solution (9% methanol free formaldehyde in PBS, Thermo Fisher Scientific, Altrincham, UK) was added to each tube, gently mixed, and incubated for a further 5 minutes at room temperature. 125 µl of permeabilisation solution (0.18% (v/v) Triton X100 in PBS, Sigma Aldrich, Gillingham, UK) was then added to all tubes, gently mixed, and incubated at room temperature. 3 ml of PBS was added to all tubes, mixed and 40 µl of the cell suspension added to tubes containing 10 µl of anti-CD42a R-PE antibody (1:10 dilution in PBS, Becton Dickinson, San Jose, California, USA) plus either 10 µl of anti-VASP FITC (phosphorylated) (pSer^{239}) (16C2) (1:50 dilution in PBS, Enzo Life Sciences, Exeter, UK) or FITC mouse IgG control antibody (Enzo Life Sciences, Exeter, UK) as shown in Appendix 9. Tubes were covered with foil and incubated for 20 minutes at room temperature. Samples were diluted with 250 µl of PBS and analysed on an Accuri C6 flow cytometer (Becton Dickinson, San Jose, California, USA). Fixative and permeabilisation solutions were prepared fresh for every two weeks.

2.7 Transwell Migration assay: Optimised for Human PASMC

Cell lines used in this experiment were LONZA hPASMC (Appendix 14) and patient PASMC (Table 2-1) obtained from pulmonary artery. To check the migration assay signal, the positive control used in this experiment was PDGF at 20 ng/ml and full growth media (result is not shown). To check the comparison, PASMCs treated with quiescent media as a negative control were used in this experiment.

Day 1: PASMCs were grown, quiesced and trypsinised as described in section 2.1.

Day 3: Transwell® - Clear Inserts, Polyester (PET) inserts (details on insert size are described in Appendix 10) were coated with Fibronectin 13.5 ng/ml for 30 minutes at 37 ºC (750 µl of fibronectin solution in bottom of well, 100 µl in Insert). Cells were washed with PBS and trypsinised as previously described. Cell suspension was collected and centrifuged as usual (5 minutes at 1000 rpm). Cells were resuspended in starvation medium (quiescent media). Then, cells were counted to make a stock solution of 12×10^4 cells/ml in starvation media.

2.7.1 Pre-incubation of cells with antibodies or inhibitors

Fibronectin was removed from inserts by vacuum/pipette from both top and bottom of the insert. Where required, cells were incubated with cangrelor for 2 minutes prior to addition to the respective wells. Stimulants were prepared in starvation media and pre-loaded (as shown in Figure 2-5) into the lower chamber of the HTS Multiwell Insert system, 8.0 µm pore size, PET membrane, 24-multiwell format (BD Falcon) (REF351185) (750 µl/well). 250 µl of cell suspension (30,000 cells) were added into the insert (refer to Figure 2-5). This was incubated at 37 ºC/5% CO_2 for 4-6 hours.

2.7.2 Cell fixing and cell staining: Diff Quick Staining

After 4-6 hours of incubation, media/stimulus were removed from the inserts and plate wells. Cells were scraped off from the inner membrane of the insert with a cotton bud. Cells were stained with Diff Quick Stain Kit (Solution A = Methyl Alcohol, Solution B = Eosin Y, Solution C = Azure A+ B). The process begins by dipping the insert five times in solution 1, for one second each. Excess stain was allowed to drain after each dip. Insert was dipped five times in solution 2, for one second each. Excess stain was allowed to drain after each dip. Dried insert was dipped five times in solution 3, for one second each dip. Excess stain was allowed to drain after each dip. Insert was rinsed in tap water, blotted and dried in air.

Cell counting: Cells were counted under the microscope. Four fields of vision from each well were chosen for counting. Cell count was normalised to describe percentage of migrated cells where starve media treated cells were baseline and PDGF treated cells were 100% migration for each experiment.
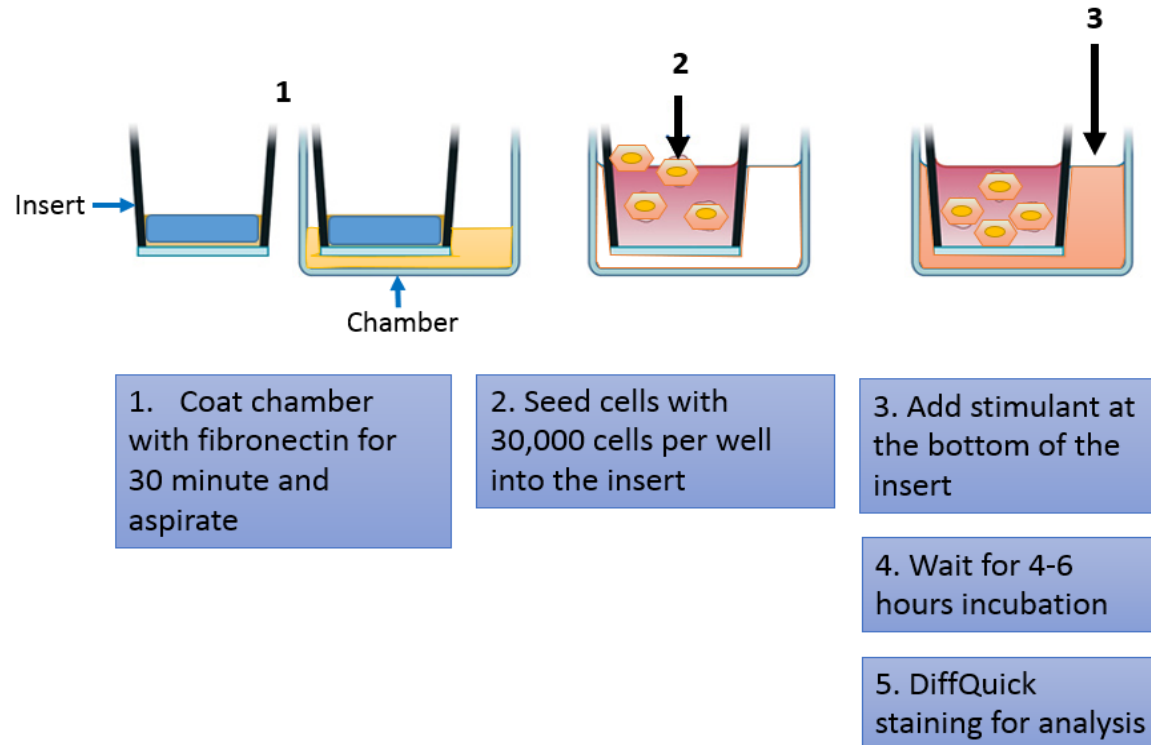
Figure 2-5: Flowchart shows the summarised process of migration assay.

Diagram in Figure 2-5 above shows the flowchart of summarised process of migration assay. The black arrows indicate the locations in the chamber where the cells are seeded (2) and stimulant is added (3).

2.8 Proliferation assay

Proliferation assays on healthy human PASMC and patient cells were done using a standard operating procedure (SOP) generated by Prof Allan Lawrie's laboratory. Details on materials and reagents are as described in Appendix 4. Cryovial containing human PASMC (healthy and PAH patient) was removed from liquid nitrogen storage and maintained in a clean and viable condition in the laboratory. Generally, proliferation assay was done as shown in the timeline in Figure 2-6.
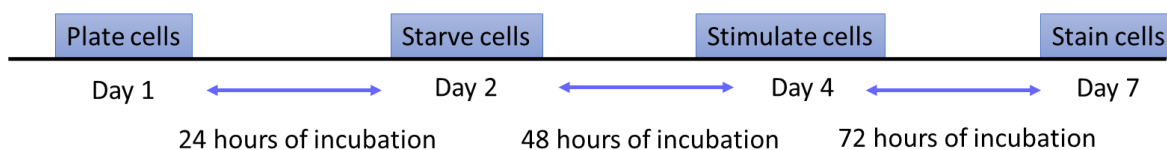
Figure 2-6: Timeline of proliferation assay
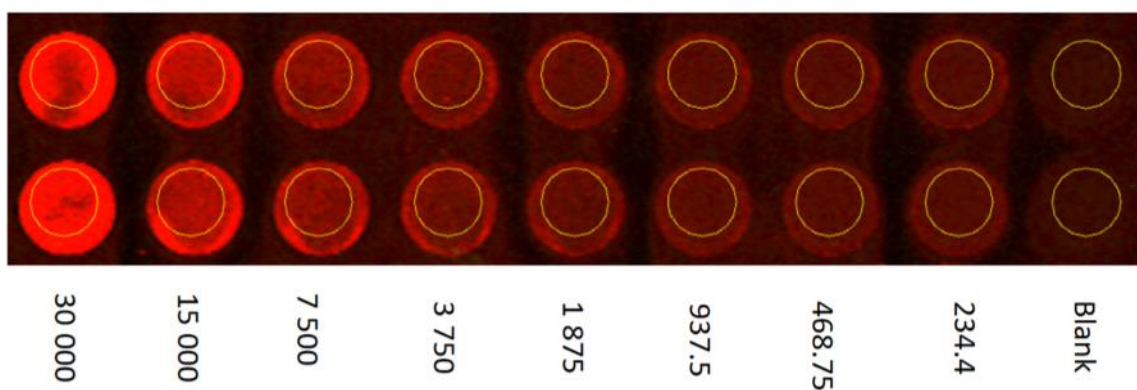
Figure 2-7: Fluorescence image from LICOR analyser

This image captured in Figure 2-7 shows gradient of fluorescence from growth curve of PASMC for proliferation assay.

2.8.1 Protocol

DAY 1: Cells were grown, maintained and trypsinised as described in section 2.1 and plated in a fibronectin coated black walled 96 well plate (Cellstar) at a concentration of 5 x 10^4 cell/ml, in 100 μl per well (5000 cells), by using smooth muscle growth media (SMGM2). Before seeding the cells in the experimental wells, 12 wells were left empty for a standard curve for cell normalisation. Cells were incubated in the CO_2 incubator at 37 ºC overnight.

DAY 2: SMGM2 media was removed and 200 μL of quiescent media (0.5% (v/v) serum) was added. Cells were incubated at 37 ºC for 48 hours.

DAY 4: Media was removed, the cells were washed twice with sterile PBS. Then, cells were stimulated with 2MeSADP, ADP, PDGF-BB (20 μg/ml) and incubated at 37 ºC for 72 hours.

DAY 7: Reference cells for standard curve were seeded as shown in Figure 2-8. For nuclear staining, DRAQ5 and Sapphire700 were used. The gradient of fluorescence intensity is shown in Figure 2-7 and standard curve for cell number is shown in Figure 2-8. Cells were fixed and stained as described in section 2.3.
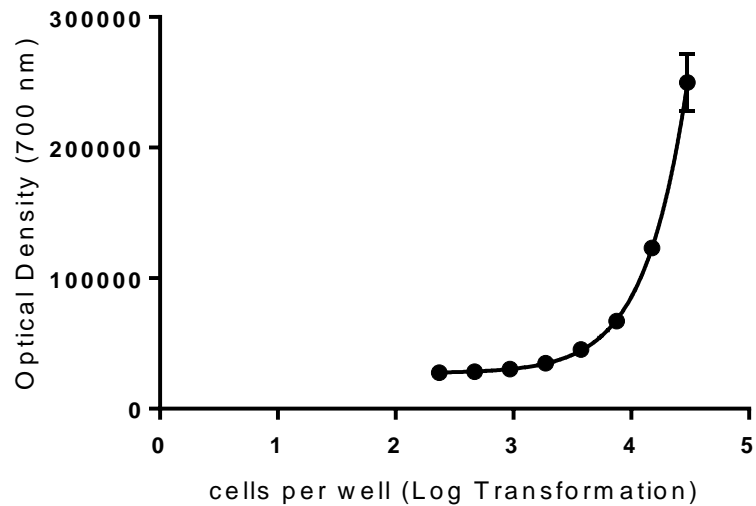
Figure 2-8: Standard curve for cell normalisation in proliferation assay

Graph in Figure 2-8 shows an example of standard curve used for cell normalisation in proliferation assays. Standard curve was done each time of proliferation assay using healthy and PAH PASMC. For each experiment, differences may be present, and normalisation was carried out to minimise these differences in each experiment. Dilutions of PASMCs were plated on a wide range of cell densities (0- 30000 cells) fixed, permeabilised and stained by using DNA staining (DRAQ5 and Sapphire700) as shown in section 2.3 for In-cell Western.

2.9   Animal study: Monocrotaline clopidogrel rat model

2.9.1 Animal license

All animal procedures were performed under the project license of Prof Allan Lawrie (PPL 70/8910) and my personal license, Nur Nabilah Binti Abu Bakar for rat and mice (PIL I8DD5EA6E). This animal study is conducted with approval from The University of Sheffield Ethics Committee and under the Animals (Scientific Procedures) Act 1986. Animal work was conducted with guidance and help from Prof Allan Lawrie and his PVRG group members.

2.9.2 Animal selection

24 Sprague Dawley (SD) male rats (supplied by Charles River) weighing 220 – 250 g were selected for this study and divided into 4 groups as shown in Figure 2-9. Animals were housed at the Biological Service Unit (BSU) with 2-3 rats per cage in a controlled environment (12 hours dark/light cycle), temperature and humidity. Animals were fed with standard chow diet and water ad libitum.

2.9.3 Monocrotaline clopidogrel rat model
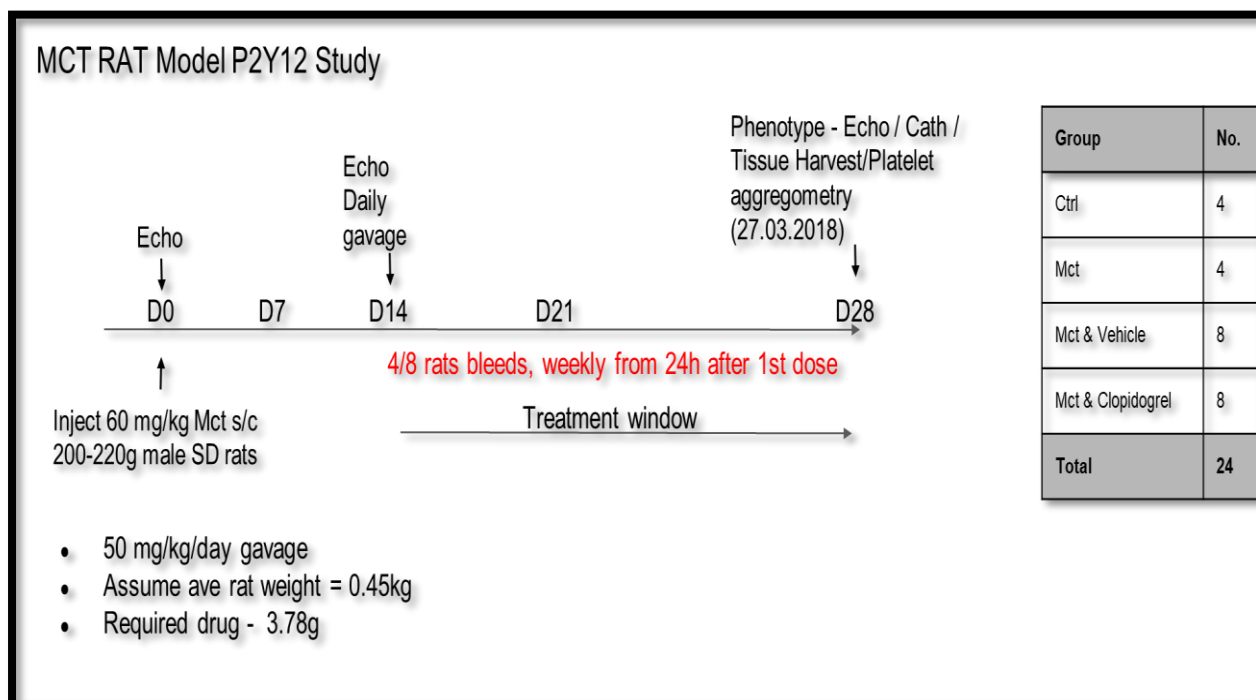
Figure 2-9: Clopidogrel monocrotaline rat model

Figure 2-9 shows the timeline of clopidogrel treatment in monocrotaline PH rat model. Rats derived from external sources were weighed and half of the rats had a baseline echocardiograph performed on day 0. Rats were allocated into experimental groups. Monocrotaline (Mct) rats received a single injection of monocrotaline (60 mg/kg) which was given subcutaneously. To see the effect of $P2Y_{12}$ inhibition, clopidogrel was gavaged daily in the respective group for 14 days and echocardiography was performed at day 14 to show disease progression.

2.9.4 Monocrotaline injection

Monocrotaline injection was done by Ms Nadine Arnold. The dosage of monocrotaline used in this study was 60 mg/kg of rat's body weight, which ranged between 220 g - 250 g. 200 mg of Mct was dissolved in 0.6 ml of 1M HCL. Then, the solution was vortexed for 15-20 minutes and water was added to total of 5 ml. The pH was then adjusted to 7.0 with NaOH. Each rat was injected with 0.6 ml solution subcutaneously into the left flank.

2.9.5 Oral dosing of clopidogrel in rats by gavaging

Gavaging was done with the help of Dr Laura E West, Ms Nadine Arnold, Dr Amira Zawia and Jianhui Lin. To inhibit $P2Y_{12}$ receptor, rats were treated with an irreversible $P2Y_{12}$ antagonist, clopidogrel. For the monocrotaline placebo control group, rats were given water. The dosage of clopidogrel suitable for rats was determined and approved by a certified officer. The preparation of clopidogrel suspension was done by scraping away the coating of the tablet, crushing it and preparing a suspension in sterilised water, which was given to the rat at a dose of 50 mg/kg by oral gavage. Oral gavage is a safe procedure and has been widely used to deliver substances/drugs precisely to the stomach. Rats were restrained and oral gavage was performed using a long-curved plastic feeding tube (supplied by Instech Laboratories, United States), measured for the correct length to access the stomach. Sterilised water was used in the placebo group (n=8). The gavage procedure was carried out in the morning between the hours 0800 – 1000. The process of gavaging was done with caution to minimise any pain that might cause to the rat. First, the needle used was measured from mouth to the length of the stomach (measured from the outside). Then, the rat was scruffed in an upright position and its head was held in a vertical position aligned to the oesophagus. The tip of blunt curved flexible canula (feeding tube) was tipped gently on the rat's mouth. Then, approximately 3 inches length of canula was passed

slowly through oesophagus straight to stomach. The canula was carefully removed after administration. Resistance should not appear if the needle was properly placed during gavaging. The treatment window for clopidogrel administration was done for 2 weeks. Gavage didn't start until 14 days after the Mct injection and disease progression was monitored in the rats by echocardiography. The rats were gavaged once daily for the duration of 14 days and were culled/sacrificed 28 days after the study period.

2.9.6 Echocardiography

Transthoracic echocardiography was performed by Ms Nadine Arnold.

The reason for performing echocardiography on the rats was to assess the live images of cardiac anatomy and function by using high frequency sound waves. This was done at the beginning, mid-point, and the final termination of the study. The outputs of this procedure include heart ultrasound visual, right ventricle (RV) and left ventricle (LV) parameters.

Rat preparation: Rats were exposed to 0.5-2% (v/v) isoflurane, 2 L/min oxygen. Anaesthetised rats were taken from the isoflurane chamber and were transferred to the heated platform, with maintenance of isoflurane at 2% (v/v) supplied through nose cone and rats were checked for pedal reflex. Rat's paws were secured with tape and placed symmetrically on the platform secured with cushion support so that heart can be visualised better by transducer for ECG reading. Rat's hair was clipped dry to allow hair trimming carried out. Nair cream was applied and wiped after 20 – 30 seconds. This was done until all the hair on the chest was removed with a warmed wet gauze to avoid heat loss as this affects cardiac cycle and this step is important to obtain a clear visual and optimal measurement of heart echocardiography.

Echocardiography scanning: Echocardiography was carried out using a Vevo 770™ High-Resolution In Vivo Imaging System (Visual Sonics, Canada) and the scan head RMV7108 probe. After the rat was placed on the heated platform, respiratory rate (85 breaths per minute), heart rate (330-480 beats per minute) and temperature (35.9 – 37.5 °C) of the anaesthetised rat were monitored throughout the procedure using the ECG amplifier and Visual Sonic temperature control.

The visualisation of echocardiography consists of two different modes: M-mode and B-mode. Right ventricle free wall view was visualised using the right parasternal long axis view by M-mode. Left ventricle parameters were visualised in the short axis view and long axis view by M-mode at the level of papillary muscle. From this analysis, RV free wall thickening and enlargement in both dimensions (B-mode and M-mode) will determine PAH disease development.

Pulse wave Doppler was taken from the parasternal short axis view at the pulmonary valve for the measurement of pulmonary artery flow; PA acceleration time (PAAT), PA ejection time (PAET) and velocity time interval (VTI). For the measurement of cardiac output, pulse wave Doppler was taken from the right axis view of the aortic valve and left axis view of the left ventricle outflow tract diameter (LVOT).

2.9.7 Clopidogrel pharmacodynamic analysis

To inhibit $P2Y_{12}$ receptor, rats were administered with clopidogrel for 14 days. After 14 days, rats were tested for drug delivery efficacy. Rats were culled and 10 ml of blood was collected from nearly each rat for platelet aggregation analysis. This was done to analyse the efficacy of drug treatment since clopidogrel is an anti-platelet drug and will cause inhibition of platelet aggregation. The technique of platelet aggregation has been described as shown in section 2.4. Concentrations of TRAP and ADP used for this analysis were 0.3, 1.0, 3.0, and 10.0 µmol/l for TRAP and 10 and 30 µmol/l for ADP. In this present study, data of pharmacodynamic analysis shown in the results section is only for 10 µmol/l of ADP. Data was analysed using GraphPad Prism 7 and expressed as percentage of platelet aggregation.

2.9.8 Cardiac catheterisation

Cardiac catheterisation was performed by Prof Allan Lawrie. The purpose of cardiac catheterisation is to measure the dynamic function of the heart and right heart catheterisation is also a reference test to diagnose PAH. Cardiac catheterisation performed was based on the closed chest method. The principle of RHC is to insert a very small, flexible, and hollow tube into the pulmonary artery and guide it to the chamber of right heart side. RHC was done during mid and after the development of right heart hypertrophy. After 14 days of daily administration of clopidogrel, rats were measured for right ventricular systemic pressure (RVSP). The Sprague Dawley rats were anaesthetised with 0.5-2% (v/v) of isoflurane and the depth of anaesthetisation was measured visibly looking at the leg movement of the rats. After rat was fully anaesthetised on stage, the catheter was connected to the computer/machine that analysed the parameters. The flexible catheter was inserted in the jugular vein. First, a small cut was done next to the neck of the rat and surrounding tissue was dissected to ease the process of inserting the catheter and to make the jugular vein more visible. Fine curved forceps were used to dissect any fat or tissue surrounding the jugular vein and using a bent (prepared manually) 25G needle, jugular vein was lifted. After that, catheter was inserted carefully and directed to the right heart chamber until established reading of right heart chamber was detected. This was confirmed by the reading of haemodynamic parameters shown by the aid of PowerLab system version 7, AD instruments (Oxford, UK).

2.9.9 Tissue harvesting

Tissue harvesting was done by Dr Laura E West. Since platelet aggregation needs fresh blood to perform the test, Dr Laura West helped me to harvest the organs/tissues from the rats. The process was started by cutting the low part of the rib cage. Skin was dissected and the rib cage

93

was lifted. After identifying the rib cage, it was cut carefully up to the collar bones to expose the lung. Extra blood was aspirated for sample collection. Then the rib cage was opened to avoid cutting the vessel of the lung. Phosphate-buffered saline (PBS) was injected into the right ventricle and other parts of the heart. This was done to flush the blood out from the heart. Excessive blood was taken into a tube. The ribs were then opened as wide as possible and the end of the trachea was identified (under the chin). The trachea was cut/diced and pulled out slowly (avoiding damage to the lung). The aorta and oesophagus were cut and placed in formalin. The right lung (multiple lobe) was tied with a suture and was cut before putting into the prepared formalin. To inflate the lung with formalin, a suture was tied around the catheter. This catheter was connected to a syringe filled of formalin. The suture was then pulled slowly towards the trachea and tied without causing any damage to the trachea. Formalin was injected to inflate the lungs and the tip of the trachea was tied tightly. Then, lungs were kept in the formalin together with other organs that might be usable in future experiments; i.e. spleen and liver.

2.9.10 Quantification of right ventricular hypertrophy

The quantification of right ventricular hypertrophy (RVH) is essential in identifying the effects of the drug in reversing heart hypertrophy. A quantitative evaluation of RV can be identified by weighing the right ventricle, septum and left ventricle. The right ventricular hypertrophy was calculated by using the formula as shown in Equation 3. First, the formalin fixed heart (at least 24 hours of fixation) was taken out from the formalin solution and put on a dry tissue. The first step was to remove the atria, any pericardial fat and valvular tissues, outflow vessels that were visibly obvious. To dissect the RV from left ventricle (LV) and septum (S), first, the right ventricle was identified from the interventricular septum and cut by using a sharp scissors. This can be done by inserting a sharp tiny scissors into the RV compartment where the pulmonary valve is

prominent. In reference to the anatomy of the heart, the RV is located behind the sternum and opposite of the left ventricle. By feeling the resistance against the septum wall, RV free wall was cut. Plus, the LV was cut and opened to make sure there was no blood clots left that might alter or bias the weight. The whole heart looked like a crescent shape and the right ventricle itself when separated from the whole heart looked like a moon shape. The extent of right ventricular hypertrophy was measured by calculating the ratio of right ventricle weight in relative to left ventricle and septum weight. The formula for right ventricular hypertrophy quantification is modification of Fulton index (Lawrie et al., 2011) as shown in Equation 3 and was measured in gram units:

Equation 3: Right ventricular hypertrophy calculation

$$RVH = \frac{RV}{(LV + S)}$$

2.9.11 Tissue processing and embedding for histology analysis

The purpose of tissue processing is to dehydrate the tissue and prepare for tissue sectioning, which can be stored for many years. After tissue harvesting as shown in section 2.9.9, each tissue was cut in 3 pieces and placed in a cassette for tissue processing. Tissue processing was done using the automated tissue processor (LEICA TP 1020). The dehydration process starts with ascending concentrations of ethanol (50% v/v, 70% v/v, 90% v/v and 100% v/v) which each step requires 1 hour of incubation. Then, the next step involved incubation in 50% (v/v) of xylene and two times of 100% (v/v) xylene for 1 hour each.

Following overnight fixation and complete penetration of fixative, lung tissue located in the cassette was taken out and placed on the heated platform of the embedding machine. Before starting to embed the tissue with paraffin wax, the wax was placed in the tank and waited until it was fully melted (approximate 61 ºC). Embedding process begins by placing the lung horizontally facing upwards in a metal mould as shown in Figure 2-10. Accurate orientation of the lung tissue is important for the pulmonary artery muscularisation microscopy examination. To begin, a small amount of wax is placed in a mould filled with lung tissue. Wax was cooled and flattened as required. Then, cassette cover (labelled) was added, the mould was filled with paraffin wax until it fully covered the mould and tissue (most important) and left overnight to solidify on the cold plate.

Tissue sectioning: The formalin fixed paraffin embedded section was trimmed at a thickness between the size of 5 µm – 10 µm for further histology analysis; alcian blue van gieson (ABEVG), smooth muscle actin (α-SMA), von Willebrand factor (VWF), proliferating cell nuclear antigen (PCNA), Caspase3, and $P2Y_{12}$ immunofluorescence staining. The protocol of IHC was as described in the section 2.10 on histology analysis of tissue samples.
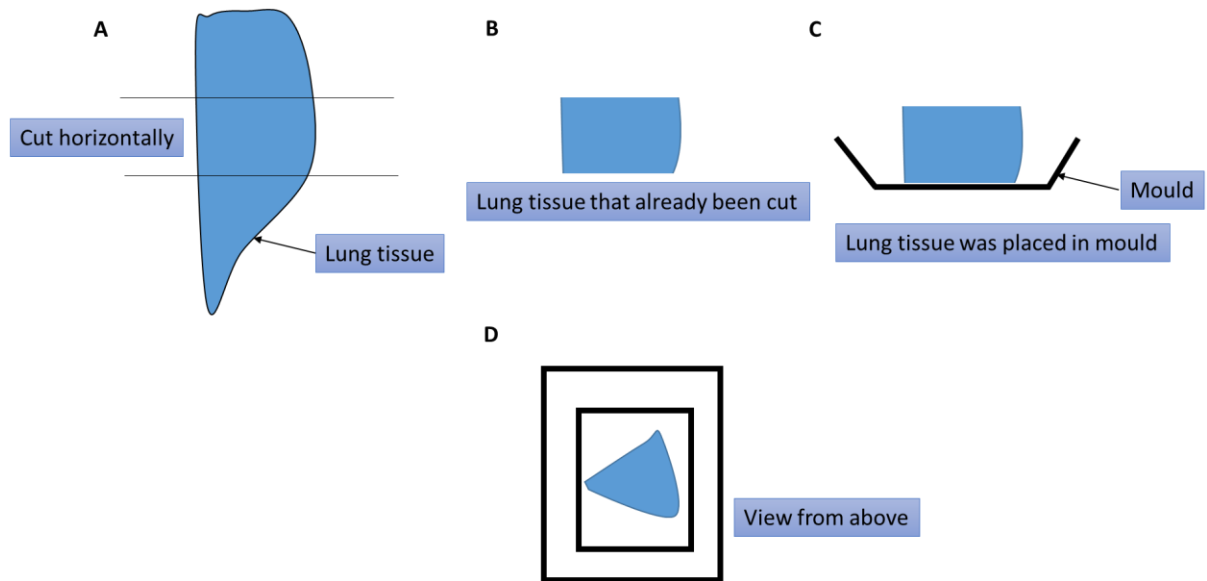
Figure 2-10: Orientation of lung in mould for histology analysis

Figure above shows correct orientation of tissue position for embedding process. (A) Lung tissue was cut horizontally. (B) This image shows one part of the lung tissue that has been cut before placing in the steel mould. (C) All three lung tissues were placed in the centre. (D) View from above shows cross section of the lung tissues.

2.9.12 Quantification of pulmonary artery vascular remodelling

The severity of pulmonary artery muscularisation was measured as a percentage of total muscularised vessel and non-muscularised vessel in all 24 rat lung tissue samples obtained from different groups, which consist of 4 control rats (no treatment), 8 placebo monocrotaline, 4 monocrotaline, and 8 clopidogrel monocrotaline treated rats.

Slide scanning was done using Zeiss Axio imager Z2 microscope. Slides were arranged on 8 - slide stage and all slides were labelled before scanning. The digital images were scanned using a 20x objective. Microscopy images were scanned and compressed to 80% using the Axiocam 506 Color System (Zeiss) and analysis for pulmonary artery muscularisation was done using Zen2 Blue Edition (Zeiss).

VWF staining was used to stain endothelial cells lining on vessel, allowing identification of pulmonary artery vessel for scoring. ABEVG staining was done to identify muscularised vessels (as shown in Figure 2-11) and α-SMA (Figure 2-12) staining was done to observe muscle content of vessel.

Scoring was done in a blinded manner. Vessels were grouped based on size; 20 – 70 µm in diameter representing small vessel, while 71 – 150 µm in diameter representing large vessel. For each group, 45- 50 vessels were selected. The vessel muscularisation analysis was done by selecting a grid area on a scanned slide, using the Zeiss scanning software. For each rat, 4 images of lung were used. The marking and vessels selection were maintained consistent for each lung tissue sample.

Two types of analysis were done for vessel muscularisation:

Number of muscularised vessels versus non-muscularised – identified by ABEVG staining. The circle was drawn from one point of elastic lamina to another point of elastic lamina as shown in Figure 2-11 .
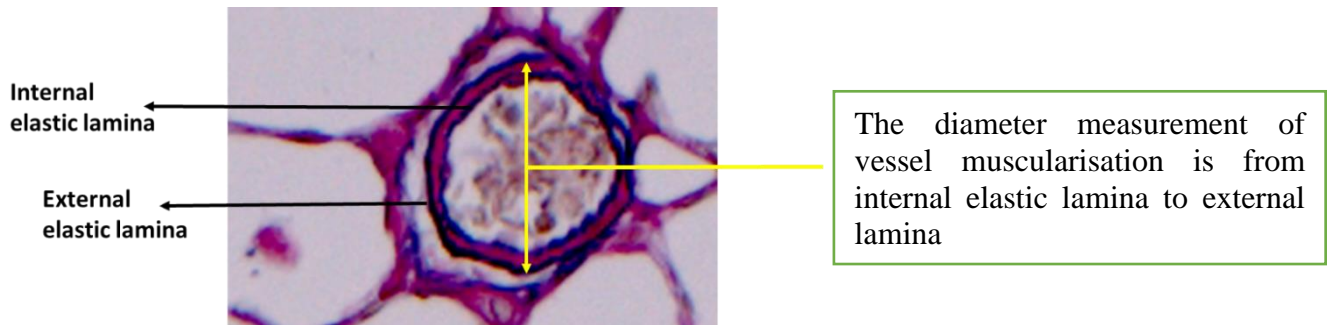
Figure 2-11: Muscularised versus non-muscularised vessel quantification

The media/CSA measurement was identified by αSMA staining as shown in Figure 2-12. Rigid area of muscularisation was drawn using the Zeiss scanning software.
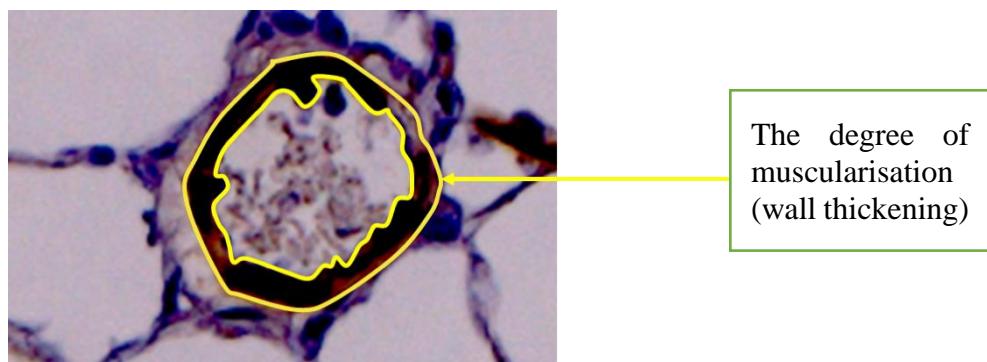
Figure 2-12: Quantification of total area of muscularisation

2.10   Histology analysis of lung tissue

Information on primary antibodies and secondary antibodies for histology staining are as described in Appendix 11.

2.10.1   Alcian Blue/Van Gieson

ABEVG staining was started by dewaxing the slides, using steps as described; (a) 10 minutes xylene, (b) 10 minutes xylene in separate tank, (c) 2 minutes absolute alcohol, (d) 2 minutes absolute alcohol, (e) 1 minute 95% (v/v) alcohol, and (f) 1 minute 70% (v/v) alcohol. First, slides containing tissue were rinsed with water for 5 minutes. Second, the slides containing lung tissue were oxidised using potassium permanganate (0.25% (w/v) aqueous potassium permanganate) for 3 minutes followed by rinsing with distilled water for 5 minutes. After bleaching with oxalic acid, slides were immersed in distilled water. For nuclei staining, slides were immersed in haematoxylin (carazzi's haematoxylin) for 2 minutes. After that, slides were differentiated with acid alcohol for 30 seconds of 1% hydrochloric acid (HCL) in 70% (v/v) industrial methylated spirit (IMS), followed by rinsing under tap water for 5 minutes. Slides were then stained with Alcian blue (pH 2.5) (1% (w/v) [CI 74240] in 3% aqueous acetic acid), Miller's Elastin stain (Merck) for 5 minutes. After that, slides were rinsed with distilled water and then with 95% IMS. Slides were rinsed with distilled water again and stained with Curtis reagent [Curtis' Modified Van Gieson (add 10 ml 1% w/v Ponceau [aq] to 90 ml saturated aq)]. Picric acid, add 1 ml acetic acid] for 6 minutes. Finally, slides were rinsed with tap water and blotted dry to dehydrate before mounting them on coverslips by using DPX mount as described in these steps: 70% (v/v) alcohol, 95% (v/v) alcohol, 2 minutes of absolute alcohol, 2 minutes of absolute alcohol and Xylene.

2.10.2 Smooth Muscle Actin

Primary antibody used was Dako monoclonal anti-human smooth muscle actin (cat number M0851) (1:150 dilution in PBS) and secondary antibody used was biotinylated anti-mouse (1:200 dilution in PBS).

Staining was started by dewaxing and rehydrating the slides containing paraffin wax tissue through graded alcohol to water as described in these steps: Xylene (10 minutes minimum), 100% ethanol (EtOH) (2 minutes), 100% EtOH (2 minutes), 90% (v/v) EtOH (2 minutes), 70% (v/v) EtOH (2 minutes), 50% (v/v) EtOH (2 minutes), and rinsed with running water.

To block the endogenous peroxidase in tissue, slides were incubated with 3% (v/v) of hydrogen peroxide for 10 minutes and then rinsed with tap water. To avoid nonspecific binding of secondary antibody, slides were blocked with 1% milk buffer (commercial dried skimmed milk) for 30 minutes at room temperature. Then, excess milk was tipped off and blotted away. After blocking with milk buffer, slides were incubated with primary antibody (1:150 dilutions) for 1 hour at room temperature. The slides were then washed in three changes of PBS, for 5 minutes in each wash.

DAB (SIGMAFAST™ 3,3' -Diamino-benzidine; Sigma-Aldrich) substrate was added on the slides and reaction was stopped before colour development becomes too strong. Then, slides were rinsed in tap water for 5 minutes before counterstaining with Carazzi's Haematoxylin for 1 minute. After counterstaining step, slides were dehydrated in the following steps: water, 50% EtOH, 70% EtOH, 90% EtOH, 100% EtOH, 100% EtOH (v/v) and xylene.

After slides were dehydrated through graded alcohols and xylene, slides were mounted on to coverslips by using DPX mountant. Staining will be in pinkish red hue, detecting smooth muscle content.

2.10.3 Von Willebrand factor

Primary antibody used for vWF staining was Dako rabbit anti-human vWF (cat number A082), (1:300 dilution in PBS). Secondary antibody used was biotinylated anti-rabbit (1:200 dilution in PBS).

Slides containing tissue sample were de-waxed and rehydrated through graded alcohols to water per the following steps: Xylene (10 minutes minimum), 2 minutes respectively for 100% EtOH, 100% EtOH, 90% EtOH, 70% EtOH, 50% EtOH (v/v) and water. Then, the slides were incubated in 3% (v/v) of hydrogen peroxide for 10 minutes before rinsing in water. After rinsing, for antigen retrieval step, slides were trypsinised by incubating in 0.1% (w/v) trypsin in Tris buffer pH 7.8, pre-heated to 37 ºC for 10 minutes. Trypsinisation was stopped by immersing the slides in running tap water for 5 minutes. Then, the slides were incubated in 1% milk buffer (commercial dried skimmed milk was prepared in PBS) for 30 minutes. This was done to block non-specific binding of secondary antibody. After incubation period, excess milk was tipped and blotted away. After that, slides were incubated with primary antibody for 1 hour at room temperature. Before incubating with biotinylated secondary antibody, slides were washed with PBS, for 5 minutes. Then, slides were incubated with biotinylated secondary antibody (1:200) for 30 minutes at room temperature. After incubating with secondary antibody, slides were washed with three changes of PBS for 5 minutes. Slides were incubated with Vectastain Avidin-biotin complex (ABC) (Vector Laboratories) reagent, for 30 minutes at room temperature, before washing again with PBS for three times =(5 minutes each). Next, DAB substrate (SIGMAFAST™ 3,3' -Diamino-benzidine; Sigma-Aldrich) was added on slides for 5 minutes and the reaction was stopped by rinsing/pipetting with tap water if colour development becomes too strong. Slides were rinsed in tap water and counterstained

using Carazzi's Haematoxylin for 1 minute. After counterstaining, slides were washed with water before being dehydrated with graded alcohols to xylene as described: Water, 50% EtOH, 70% EtOH, 90% EtOH, 100% EtOH, 100% EtOH and Xylene. Finally, slides were mounted on cover slips using DPX mount.

2.10.4 Proliferating cell nuclear antigen

Primary antibody used was Dako mouse monoclonal anti human PCNA (cat number M0879) (1:125 dilution in PBS). Secondary antibody used was biotinylated anti-mouse (1:200 dilution in PBS). To begin the procedure, slides were dehydrated through graded alcohol and xylene. Then, the slides were blocked with 3% (v/v) of hydrogen peroxide for 10 minutes, followed by rinsing with tap water. For antigen retrieval, slides were incubated with citrate buffer at pH 6, 20 minutes, 95 °C. Slides were cooled for 20 minutes before being blocked with 1% milk buffer (commercial dried skimmed milk) for 30 minutes at room temperature. After blocking with milk, excess milk on the slides was removed by tipping the end of the slides on a tissue paper. The slides were then washed in PBS (three changes and 5 minutes each). After washing, slides were incubated with PCNA monoclonal antibody (1:125) at room temperature for 1 hour and washed with three changes of PBS. Slides were then incubated with secondary antibody (1:200) for 30 minutes and washed again in three changes of PBS. Next, slides were incubated with Vectastain ABC (Vector Laboratories) complex for 30 minutes, at room temperature. After incubating with ABC complex, slides were washed with three changes of PBS for 5 minutes each. Slides were incubated with DAB (SIGMAFAST™ 3,3' -Diamino-benzidine; Sigma-Aldrich) substrate for 5 minutes depending on the colour development. Incubation was stopped early, and the slides were rinsed in tap water before the colour

development becomes too strong. Finally, slides were counterstained using Carazzi's Haematoxylin for 1 minute. Then, slides were washed with water and mounted using DPX.

2.10.5 Caspase-3

Primary antibody used was Abcam rabbit anti-Caspase-3 (cat number ab4051, 1:100 dilution in PBS). Secondary antibody used was biotinylated anti-rabbit (1:200 dilution in PBS).

Dewaxing and rehydration using different concentrations of alcohol and xylene were performed as described in other staining protocols. Slides containing paraffin wax embedded tissue were blocked from endogenous peroxidases using 3% (v/v) of hydrogen peroxide for 10 minutes. Then, slides were rinsed under running tap water for a few minutes before transferring the rack (filled with slides) and was moved into a black box containing citrate buffer. For the antigen retrieval step, slides were incubated for 20 minutes at 95 °C. After 20 minutes of incubation in citrate buffer, the slides were cooled to room temperature for 20 minutes. Slides were blocked from non-specific binding of secondary antibody by incubating in 1% milk buffer for half an hour at RT. The excess milk was blotted and shaken on clean paper. The end of the slides was tipped on a tissue (do not wipe on the slide surface containing tissue). Only the back of the slides was wiped. Then the slides were incubated with primary antibody (1:100 dilution), overnight at 4 °C. Slides were washed with three changes of PBS (5 minutes each). Next, slides were incubated with biotinylated secondary anti-rabbit antibody (1:200), 30 minutes at RT. Slides were washed with PBS for three times (5 minutes each). Slides were incubated with ABC complex in metal racks for 30 minutes. Slides were washed again with PBS as before. Then, the most crucial step was to incubate with DAB (SIGMAFAST™ 3,3' -Diamino-benzidine; Sigma-Aldrich) substrate for 10 minutes. Slides were observed under the microscope to avoid strong colour development. Finally, slides were rinsed in tap water

and slides were counterstained with Carazzi's Haematoxylin for 1 – 1.5 minutes. Then, slides were washed with water and mounted using DPX.

2.10.6 Immunofluorescence - P2Y$_{12}$/Smooth Muscle Actin

Primary and secondary antibody used were Dako mouse monoclonal anti-human smooth muscle actin α-SMA (M0851) (1:150 dilution), Rabbit polyclonal anti-P2Y$_{12}$ (Sigma, P4871) (1:100 dilution), Alexa fluor 488 goat anti-mouse immunoglobulin G (IgG) (H+L) (1:200 dilution), highly cross adsorbed (cat number A-11034), Alexa fluor 594 goat anti-rabbit IgG (H+L) (1:200), highly cross adsorbed (cat number A-11037). Further information on primary and secondary antibodies can be referred to Appendix 12.

Slides were dewaxed and rehydrated through graded alcohols (xylene for 10 mins, 100%, 100%, 90%, 70%, and 50% of ETOH for 2 minutes each). Then, the slides were rinsed with running tap water for 5 minutes. After rinsing, slides were blocked with prepared bovine serum albumin (BSA) as described: 5% goat serum/1% BSA/0.5% triton/PBS for 30 minutes at RT. Excess blocking buffer was tipped off by using a clean tissue paper. Then slides containing embedded tissue were incubated with primary antibodies (SMA: 1: 150 and P2Y$_{12}$: 1:100) in 1% BSA/0.5% triton/PBS overnight at 4 °C. After that, slides were washed in three changes of PBS (5 minutes each). The next incubation involved secondary antibodies (1:200) in 1% of BSA/PBS. Incubation was done in the dark for 2 hours at room temperature. Then, the final wash of PBS (3 changes, 5 minutes each) was done before mounting the slides using Vectashield mounting medium with DAPI (Vector Labs H-1200). The mounting was sealed with nail varnish and kept in the dark. Human brain tissue was used as positive staining as shown in Figure 2-13.

P2Y$_{12}$ immunofluorescence staining on human brain (positive control)

DAPI   **P2Y$_{12}$**   **SMAα**
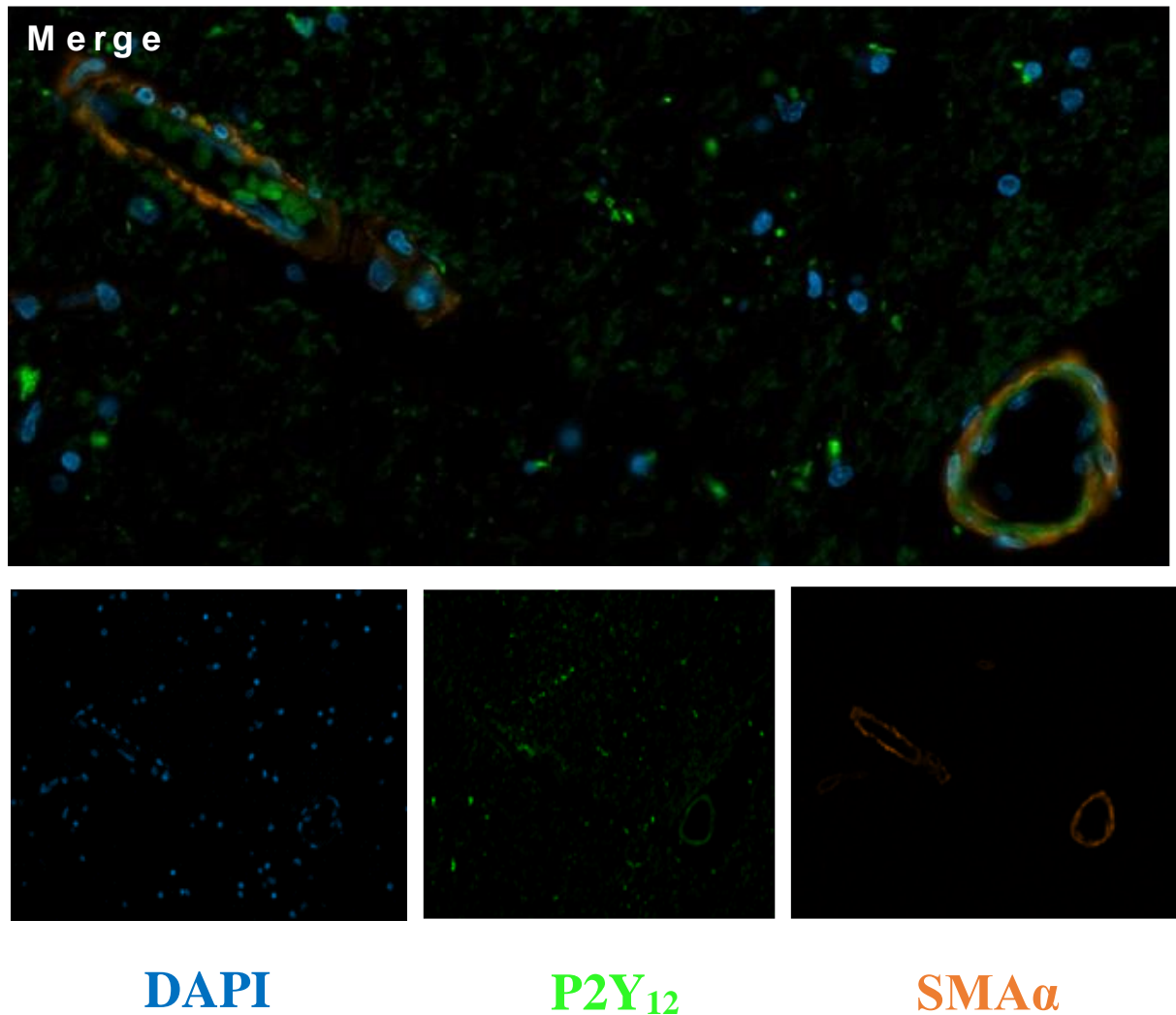
Figure 2-13: Dual Immunofluorescence staining images of smooth muscle actin and P2Y$_{12}$ expression in human brain

Fluorescence images shown in Figure 2-13 indicate clear expression of P2Y$_{12}$ and SMAα staining on human brain tissue. P2Y$_{12}$ (green) and SMAα (orange). Human brain was used as positive control and supportive monitor for P2Y$_{12}$/SMA expression in PASMC.

2.11   Western Blot

Western blotting is a semi-quantitative method used in research to identify or characterise a protein of interest by electrophoretic separation of proteins based on their molecular weight. It is done by transferring proteins to a membrane for antibody probing which is done to identify proteins by their size relative to a protein ladder. Materials utilised in Western Blot are listed in Appendix 13. The western blotting protocol is described in more detail below:

2.11.1 Preparation of lysate from PASMC cell culture

Cells were grown in T25 flasks as shown in section 2.1. Cells in T25 flasks were grown to approximately 80% confluency. Then, cells were quiesced for 48 hours and stimulated according to the experimental design; non-treated, PDGF (20 ng/ml), 2MeSADP (1000 nmol/l), cangrelor (1 µmol/l), combination of 2MeSADP and cangrelor. Cells were washed with PBS and lysed with 500 µl of Mammalian Protein Extraction Reagent (M-PER), containing Halt ™ Protease Inhibitor Cocktail and Halt ™ Phosphatase (1:100 dilution in M-PER). Cell lysates were then kept in the -80 °C until the day of gel electrophoresis.

2.11.2 Sample preparation

25 µl of loading buffer (LI-COR Biosciences, UK), 10 µl of reducing agent (Invitrogen, UK), and 65 µl of sample (cell lysate) were mixed and heated in 95 °C for 2 minutes to denature the protein. Details on materials utilised are as described in Appendix 13.

2.11.3 Gel electrophoresis and sample loading

NuPAGE 4-12% Bis-Tris Mini gels, (Invitrogen, UK) were used with the Bolt mini tank system to perform all electrophoresis experiments. 10 µl of pre-stained ladder (Chameleon Duo Pre-stained Protein Ladder) and 40 µl from the sample mix prepared were added respectively into

the wells. This protein ladder provides detection from small to medium sized proteins; 8 to 260 kDA as shown in Figure 2-14. After samples were loaded, gel electrophoresis was run in running buffer (500 µl of anti-oxidant added into 25 ml of 20x running buffer) (Invitrogen, UK) for 30 minutes at 200 V. Details on materials and reagents are as described in Appendix 13.
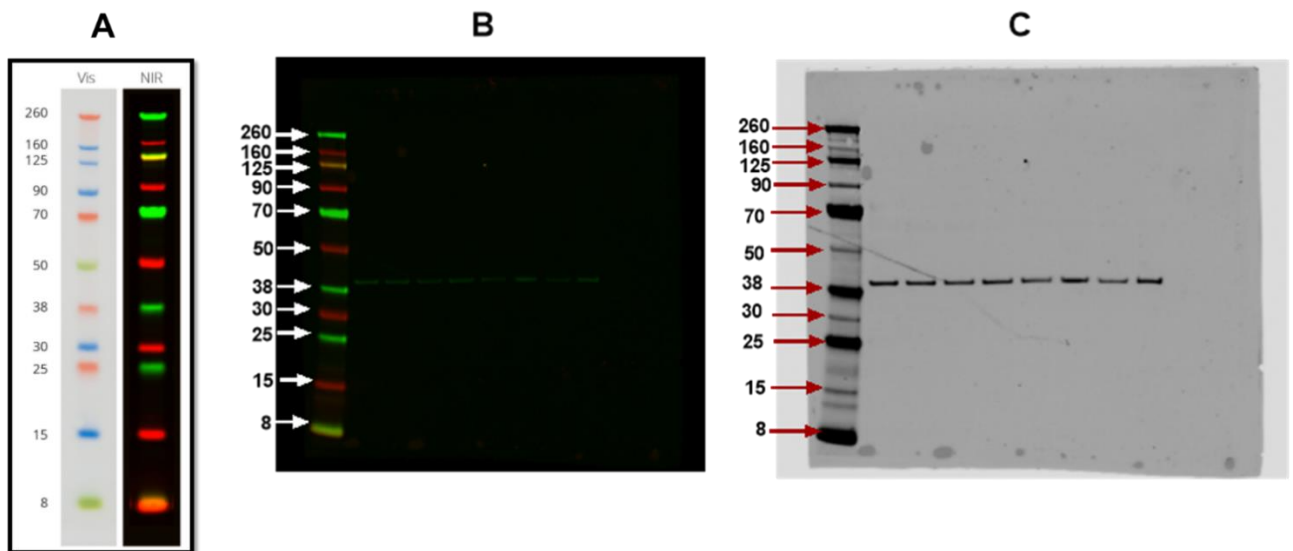
Figure 2-14: Pre-stained protein ladder

Figure 2-14 shows pre-stained protein ladder, (A) Chameleon Duo Pre-stained protein ladder (LI-COR P/N 928-60000) used in Western Blot (image from LICOR), (B) Western blotting in NIR format using the chameleon duo pre-stained protein ladder used in the assay (C) Western Blotting in grey scale format using the chameleon duo pre-stained protein ladder used in the assay. In the gel B and C also showing the detection of p38 MAPK protein is observed.

2.11.4 Nitrocellulose membrane transfer

Membrane transfer was conducted using the iBlot™ 2 Dry Blotting System. After electrophoresis, the gel was placed on the bottom stack and a soaked filter paper was placed on the gel. Gel was placed onto the nitrocellulose membrane according to the iBlot™ 2 Dry Blotting system manufacturer guidelines. The manufacturer's guidelines describe the

preparation of the stack membrane and filter paper arrangement. After gel was placed accordingly, a blotting roller was used to remove any bubbles. Transfer time was run for approximate 7 minutes, 20 V – 25 V as described in the manufacturer guidelines.

2.11.5 Primary antibody staining and detection

Nitrocellulose membrane was taken out from the iBlot and washed once in deionised water, non-specific binding was then blocked by incubation of the membrane in 30% Odyssey blocking buffer for 1 hour of rocking at room temperature. Primary antibody (refer to Appendix 3) and universal antibody detection reagent (Quick Western Kit IRDye 680RD, LI-COR, Biosciences, UK) were prepared for 1 in 1000 dilution in 30% Odyssey Blocking Buffer and incubated overnight at 4°C on a rocking platform. The membrane was then washed three times with 0.1% Tris buffered saline with Tween 20 (TBST) for 10 minutes each before scanning using the LICOR Odyssey Sa System (LI-COR, Biosciences, UK). Details on primary and secondary antibodies are as described in Appendix 3 and Appendix 13.

2.11.6 Re-probe membrane

For multiple protein immunoblotting, the membrane could be stripped by using stripping buffer (1 ml of 10X Reblot Mild Solution in 9 ml of distilled water) for 15 minutes at room temperature on a rocking platform. After stripping, membrane was scanned to make sure blots were stripped completely and no signal was detected. Then, the membrane was blocked and incubated with primary antibody and detection reagent as described previously.

2.12 Statistical analysis

Data presented considering each cell vial used as an independent experiment. The n number refer to separate reagents prepared for each experiment, different donor cells or passages and was performed at least in triplicate, then averaged to give n=1. All data were presented as mean ± SEM. Normality test was performed to determine the distribution of the data. Independent sample T-test was used to compare two groups (parameters) of data; i.e. different time points or concentrations. One way or Two-way ANOVA using Tukey's and Bonferroni's multiple comparison were used for large number of parameters (more than two). Data and statistical analysis were performed by using Prism 7 or Prism 8 (GraphPad, San Diego, CA, USA).

3. P2Y$_{12}$ expression and VASP phosphorylation in pulmonary artery smooth muscle cells.

3.1   Introduction

The first report identifying the expression of P2Y$_{12}$ in vascular smooth muscle cells was in 2004 by Wihlborg and colleagues, in which they demonstrated that ADP induced contraction was inhibited by the P2Y$_{12}$ inhibitor, ARC67085 (Wihlborg et al., 2004). Subsequently, a study by Kylhammar and colleagues showed that treatment with the P2Y$_{12}$ inhibitor (Cangrelor) transiently lowered pulmonary artery pressure in an acute pulmonary hypertension hypoxia *in vivo* pig model (Kylhammar et al.*,* 2014).

The role of P2Y$_{12}$ in mediating vasoconstriction has henceforth been well documented but its involvement, if any, in the pulmonary vascular remodelling remains unclear. Interestingly, using chimeric mice, West et al., (2014) showed a role for P2Y$_{12}$ expressed within the vessel wall, and platelets in early atherogenesis (West et al., 2014). These data suggest that the P2Y$_{12}$ receptor may have multiple functions and play an important role in different cells and tissues.

The main P2Y$_{12}$ receptor mediated signalling event is the inhibition of adenylate cyclase via the Gi signalling pathway, resulting in a reduction of cAMP (Hardy et al., 2004). The inhibition of cAMP leads to a reduction of the phosphorylation of vasodilator-stimulated phosphoprotein (VASP) phosphorylation. Patients with severe PAH have reduced circulating levels of prostacyclin (Tuder et al., 1999) leading to a reduction of cAMP production.

Subsequently, treatment with prostacyclin analogues such as Iloprost (ventavis) are widely used to treat PAH.

Less is known about the contribution of P2Y$_{12}$ receptor signalling in pulmonary artery smooth muscle cell (PASMC). This chapter will therefore determine the expression of P2Y$_{12}$ in healthy versus diseased human and rat cells as well as the influence of P2Y$_{12}$ on Iloprost induced VASP phosphorylation. Finally, since VASP has been identified as a substrate of both cAMP dependent kinases (PKA) at serine 157 and cGMP dependent protein kinase G (PKG) at serine 239 (Butt et al., 1994), I will examine whether P2Y$_{12}$ signalling has a specific effect on either cAMP/cGMP signalling.

3.2   Hypothesis

I hypothesised that ADP induced P2Y$_{12}$ receptor activation will inhibit prostacyclin/Iloprost signalling in PASMC, and that blocking P2Y$_{12}$ signalling will, therefore, result in dysregulation of Iloprost induced VASP phosphorylation.

3.3 Working model
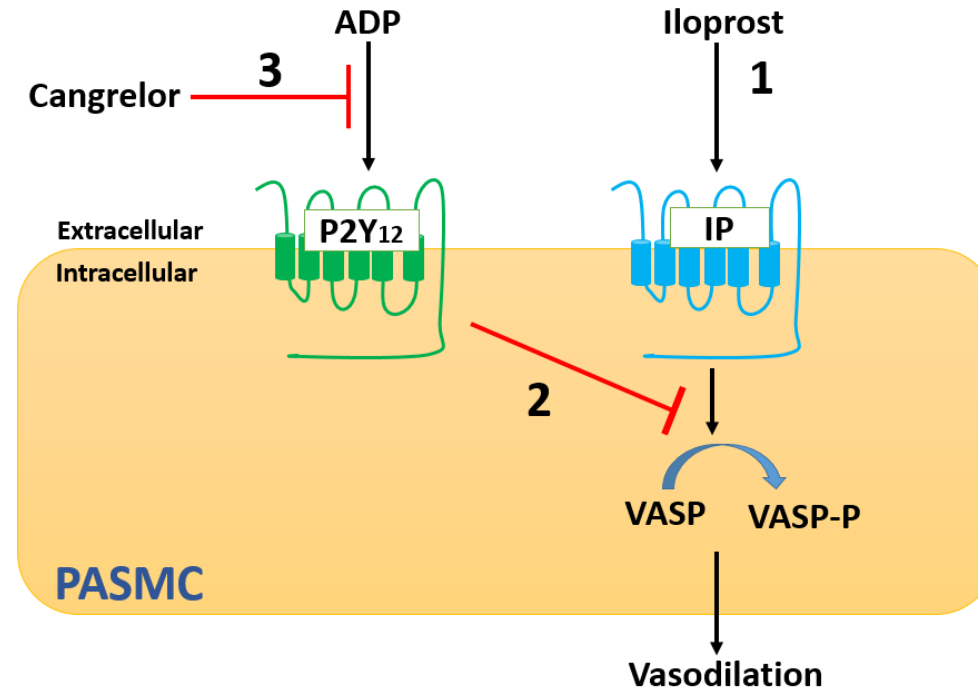
Figure 3-1: Working model of VASP phosphorylation assay

Figure 3-1 above shows the working model used in this chapter. (1) Iloprost binds to IP receptor resulting in vasodilator stimulated protein (VASP)

phosphorylation and vasodilation. (2) Binding of adenosine diphosphate (ADP) to P2Y$_{12}$ receptor decreases pVASP and vasodilation. (3) Addition

of cangrelor will prevent P2Y$_{12}$ binding to ADP and therefore, 1 continues being uninhibited by 2.

3.4 Materials and Methods

3.4.1 Cell culture

Detailed protocol on cell culture can be referred to section 2.1.

3.4.2 Taqman RT-PCR

Healthy lung tissue samples were obtained from Lonza, whereas 2 sex matched lung tissues from PAH patients (Table 2-1) were obtained from Prof Allan Lawrie laboratory. The (healthy controls and PAH patient PASMCs) were grown in T25 flasks and RNA extraction was done once cells were confluent. RNA samples from rat's lung were obtained with courtesy from Prof Allan Lawrie, that were used in PH study. Expression of *P2RY12* mRNA was quantified by Taqman RT-qPCR. Taqman probes; *P2RY12* (Hs591281) and *18S* (Hs03003631_g118S) were used as the endogenous controls. Detailed protocol can be referred in the method section 2.2.

3.4.3 Stimulants

2MeSADP (1000 nmol/l) (1624, Tocris), ADP (30 µM) (A2754, Sigma), Iloprost (10 – 100 µM) (Ventavis) and cangrelor (1 µM) (STH pharmacy) were diluted in sterile phosphate-buffered saline.

3.4.4 VASP phosphorylation by In-cell Western

Vasodilator-stimulated phosphoprotein phosphorylation (VASPp) was quantified using In-cell Western assay. Cells were grown in 96-well plates coated with fibronectin, stimulated with different concentrations of Iloprost (0.3 – 100 µmol/L) alone for 10, 20, or 60 minutes and for

10 minutes in the presence of 2MeSADP (1 μM). Primary antibodies used: VASP (phosphorylated) (pSer239) (product code: ALX-804-240-C100, Enzo Life Sciences), VASP (phosphorylated) (pSer157) (5C6) (product code ALX-804-403 C100, Enzo Life Sciences) and Total VASP (942) Rabbit mAb (product code 3132S, Cell Signalling Technology) as detailed in the method section 2.3.

3.4.5 VASP phosphorylation quantification by flowcytometry

As described in the method section 2.6, 100 μl of whole blood was incubated with Prostaglandin E_I (PGE_I) (10 μmol/l) or PGE_I with/without ADP (30 μmol/L). Methanol-free formaldehyde (final concentration 3%) was then added and incubated for 5 minutes. Permeabilising solution was added (final concentration 0.18%), incubated for 10 minutes and then 3 ml of PBS was added. A 40 μl aliquot was then incubated with 162C-FITC/isotype control antibody and anti-CD42 R-PE for 20 minutes and analysed by flowcytometry.

3.4.6 Platelet aggregation by optical aggregometry assay

Platelet rich plasma (PRP) aliquots were prepared as detailed in the method section 2.4. PRP was then diluted to 250 x 10^9/L with platelet poor plasma (PPP). Solutions of 2MeSADP (100-1000 nmol/l) were prepared in three different buffers; serum starved media (SM), full growth media (FG) and phosphate buffer saline (PBS). Prepared PRP was incubated with 2MeSADP for 4 minutes. BioData PAP-4 aggregometer (Alpha Labs, Eastleigh, UK) was used to calculate platelet aggregation response. Data was recorded as final aggregation (FA) and maximal aggregation (MA).

3.4.7 P2Y$_{12}$ antagonism assay by radioligand binding assay

PASMC cells were obtained, counted using Neubauer chamber and diluted to 5×10^5 cells/ml in a quiescent media. Blood samples were obtained from healthy volunteers who had not taken any medications or anti platelet therapy for 24 hours prior to their blood collection and kept in a tube containing tri-sodium citrate (0.1 mol/l). This experiment was performed as described in method section 2.5 with the kind help of Dr Heather Judge as I was not certified to work with radioligands.

3.4.8 Statistical analysis

Data are presented as mean ± SEM. T-test was used to compare between two groups of data. For data with more than 2 groups, each parameter; time point and concentration were compared by One-Way ANOVA or Two-Way ANOVA followed by Tukey's multiple comparison. Each n is derived from a different passage of cells and were performed in at least triplicates, the results of which were averaged to give an n=1. Donor number is derived from different patients.

3.5 Results

3.5.1 *P2RY12* mRNA expression is increased in PAH-PASMC and lung tissue from a rat model of PAH

Quantification of *P2RY12* mRNA expression was performed in human PASMC from LONZA and cells isolated from PAH, and in whole lung lysates from control (saline) or monocrotaline-treated rats 28-days after stimulation of disease. Taqman qPCR assay showed that *P2RY12* mRNA expression was significantly increased in human PAH PASMCs compared to healthy controls (relative quantitative (RQ) (5.9 ± 0.9 vs 1.1 ± 0.06, n=4-9 from 2 distinct donors in each case, p=<0.01) (figure 3.2A). *P2RY12* was also significantly increased in Mct-treated compared to healthy rat lungs (1.9 ± 0.1 vs 1.3 ± 0.4 n=9, p=<0.05) (figure 3.2b).

As different passages have different concentrations of *P2RY12* mRNA, the variations in expression observed in different PASMC samples obtained from the same patient can be caused by the passage number.
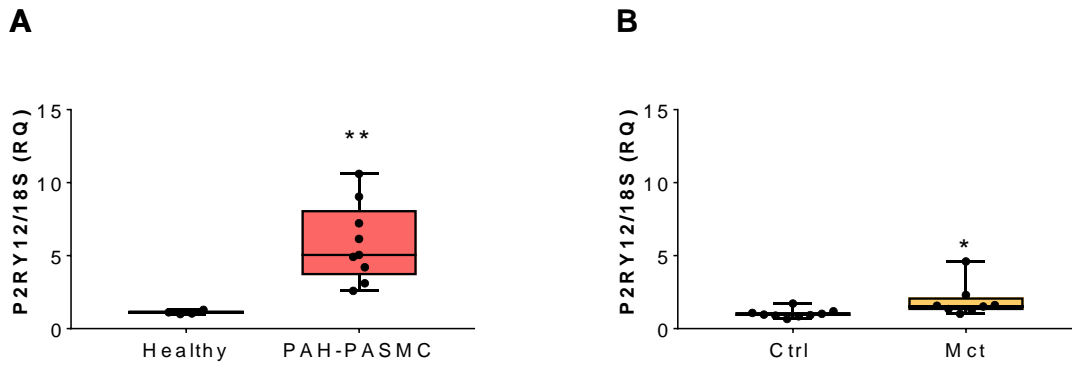
Figure 3-2: P2RY12 expression in healthy PASMC and PAH-patient PASMC

*Quantification of P2RY12 mRNA expression in (A) human healthy and PAH-patient PASMC, (B) whole lung RNA from control (Ctrl) and monocrotaline (Mct) treated rats. Graph shows relative quantity (RQ) of P2RY12 expression normalised to 18S ribosomal RNA. Bar represents mean ± SEM, n=4 Healthy (2 different passages from 2 Lonza distinct donors), 9 PAH PASMC (minimum of 4 passages from 2 distinct donors), 9 saline treated Ctrl rats, and 8 Mct treated rats at d28. * = p<0.05, ** =p<0.01 using an unpaired T-test.*

3.5.2 VASP phosphorylation assay in PASMC

Since *P2RY12* expression was significantly increased in PAH derived human cells and rat whole lung, next I investigated the effect of *P2RY12* activation on Iloprost induced VASP phosphorylation in control and PAH-PASMC. Prior to examining the influence of *P2RY12*, I first determined the optimal concentration and time course of Iloprost induced VASP phosphorylation in control and PAH-PASMC. Figure 3-3 (A-C) shows that there are significant differences between patient and commercially available PASMC in their response to Iloprost. Five concentrations of iloprost were used to make the curves as shown in Figure 3-3 and from the statistical analysis of two-way ANOVA, there are significance dosage effects observed in iloprost-induced VASP phosphorylation derived from the samples of PAH patient-derived PASMCs compared to healthy controls PASMC. Statistical analysis was summarised in Table 3-1.
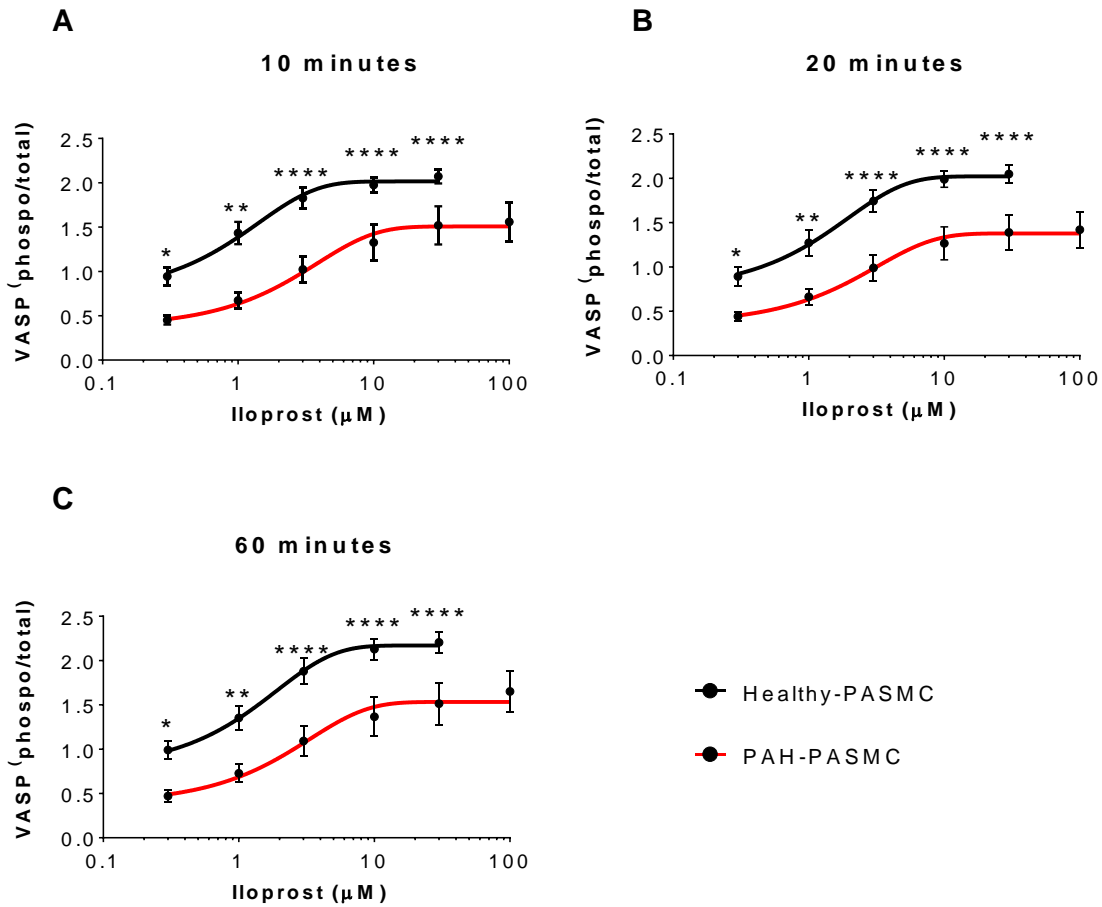
Figure 3-3: VASP phosphorylation mediated by a concentration curve of iloprost at different time points.

VASP phosphorylation mediated by a concentration curve of Iloprost (0.3, 1.0, 3.0, 10 and 30 µM) for normal LONZA and PAH patient-derived PASMCs (0.3, 1.0, 3.0, 10, 30 and 100 µM) respectively at different time points: (A) 10 minutes, (B) 20 minutes and (C) 60 minutes. Normal LONZA hPASMC n=5 (3 donors), PAH patient-derived PASMCs (2 donors) n=7. Black line (hPASMC), red line (PAH PASMC). VASP phosphorylation was measured by In-cell Western. * p =<0.05, ** p=<0.01, ***p =<0.001, ****p =<0.0001.

Table 3-1: Statistical analysis of Iloprost-induced VASP phosphorylation in healthy and PAH-

PASMC

Timepoint	Concentration	P -value	Asterix
10 minutes	0	0.0167	*
	0.3	0.031	**
	1.0	0.0001	****
	3.0	0.0001	****
	10.0	0.0001	****
	30	0.0001	****
20 minutes	0	0.0097	*
	0.3	0.003	**
	1.0	<0.0001	****
	3.0	<0.0001	****
	10.0	<0.0001	****
	30	<0.0001	****
60 minutes	0	0.0293	*
	0.3	0.00273	**
	1.0	<0.0001	****
	3.0	<0.0001	****
	10.0	<0.0001	****
	30	<0.0001	****

Table 3-1 shows statistical analysis of VASP phosphorylation induced by iloprost. Comparison

between healthy and PAH PASMC at different time points (10, 20, and 60 minutes) and varying

concentrations (0.3, 1.0, 3.0, 10, 30 and 100 μM) of iloprost. Two-way ANOVA. Mean ± SEM.

*N=5. * p =<0.05, ** p=<0.01, ***p =<0.001, ****p =<0.0001.*

3.5.3 2MeSADP does not inhibit VASP phosphorylation induced by iloprost in control or PAH-PASMC

In the previous section, I demonstrated that stimulation for 10 minutes with 10 µmol/l of Iloprost optimally induced VASP phosphorylation. I therefore continued with this time point and concentration for the remaining experiments in this chapter. To ensure we accounted for alteration in phosphorylation of both cAMP dependent kinases (PKA) at serine 157, and cGMP dependent protein kinase (PKG) at serine 239, I examined these independently and combined, measured using In-cell Western assay. There was however, no significant reduction in VASP phosphorylation with 2MeSADP stimulation at ser 157, ser 239 and at both ser 157 and ser 239 in PAH-PASMC and healthy PASMC, as shown in Figure 3-4.

A Phospho VASP (Ser 239 and 157)

B Phospho VASP (Ser 157)

C Phospho VASP (Ser 239)

☐ No Agonist
■ 2MeSADP
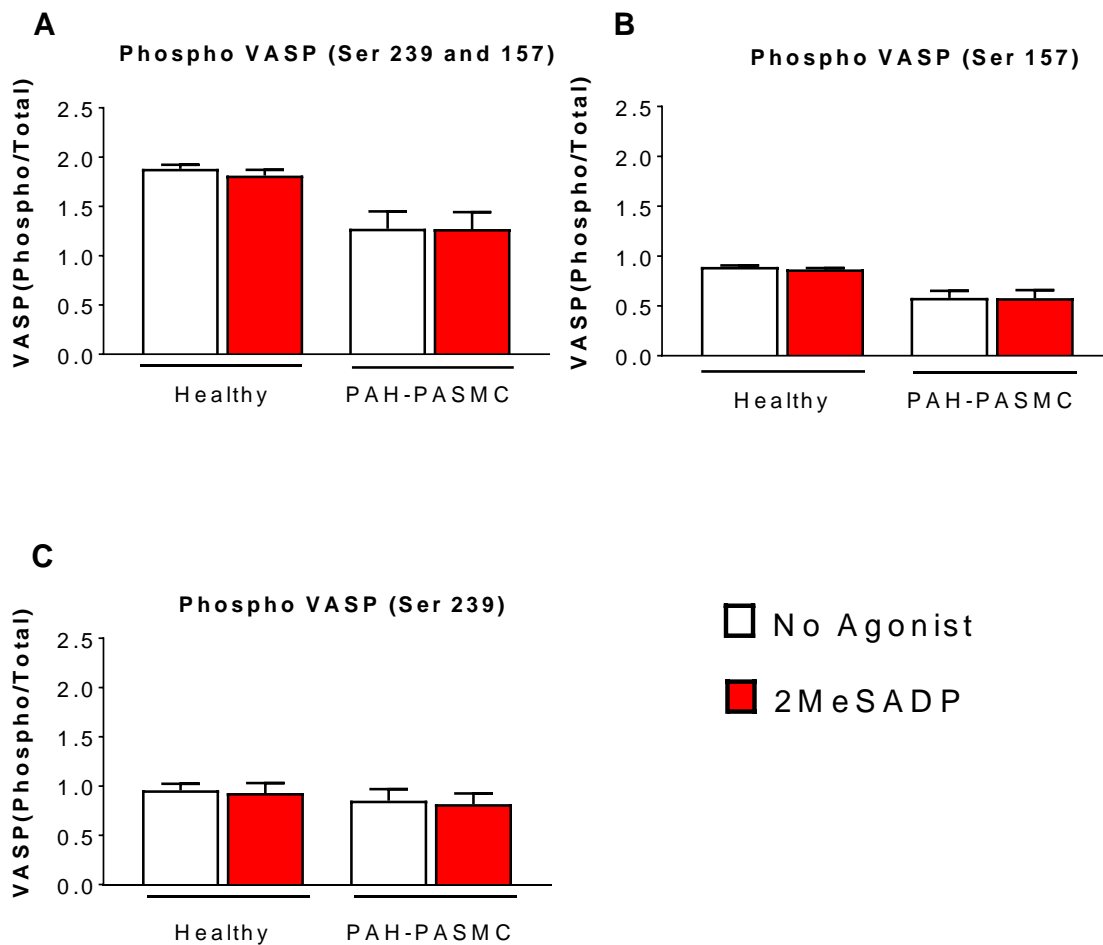
Figure 3-4: VASP phosphorylation with addition of 2MeSADP

Figure 3.4 shows graphs of In-cell Western analysis for VASP phosphorylation in 10 minutes from human healthy PASMC (3 donors) and patient's cell (2 donors). VASP phosphorylation marker used: (A) both VASP-p 239 and VASP-p 157, (B) VASP-p157, and (C) VASP-p239. All experiments done in the presence of 10 μmol/l Iloprost with 1 μM of 2MeSADP added to the relevant wells. N=5 of human PASMC and n= 5-8 of PAH-PASMC, Two-way ANOVA, Tukey's multiple comparison test. ns

As this result was unexpected, I next attempted to rule out that loss of cells due to toxicity was the reason that the addition of 2MeSADP did not inhibit VASP phosphorylation. Compared to untreated and PDGF stimulated (negative control), cells treated with staurosporine (positive control) induced cell death and cell toxicity but there was no significant effect of 2MeSADP (Figure 3-5) in either control or PAH-PASMC as visualised under the microscope.

This assay was done for only n=1. However, the cells were always observed using microscope before and after, in all In-cell Western assays. There was no cell toxicity or cell death observed.

Staurosporine   Untreated   PDGF

Iloprost   Iloprost and 2MeSADP   2MeSADP
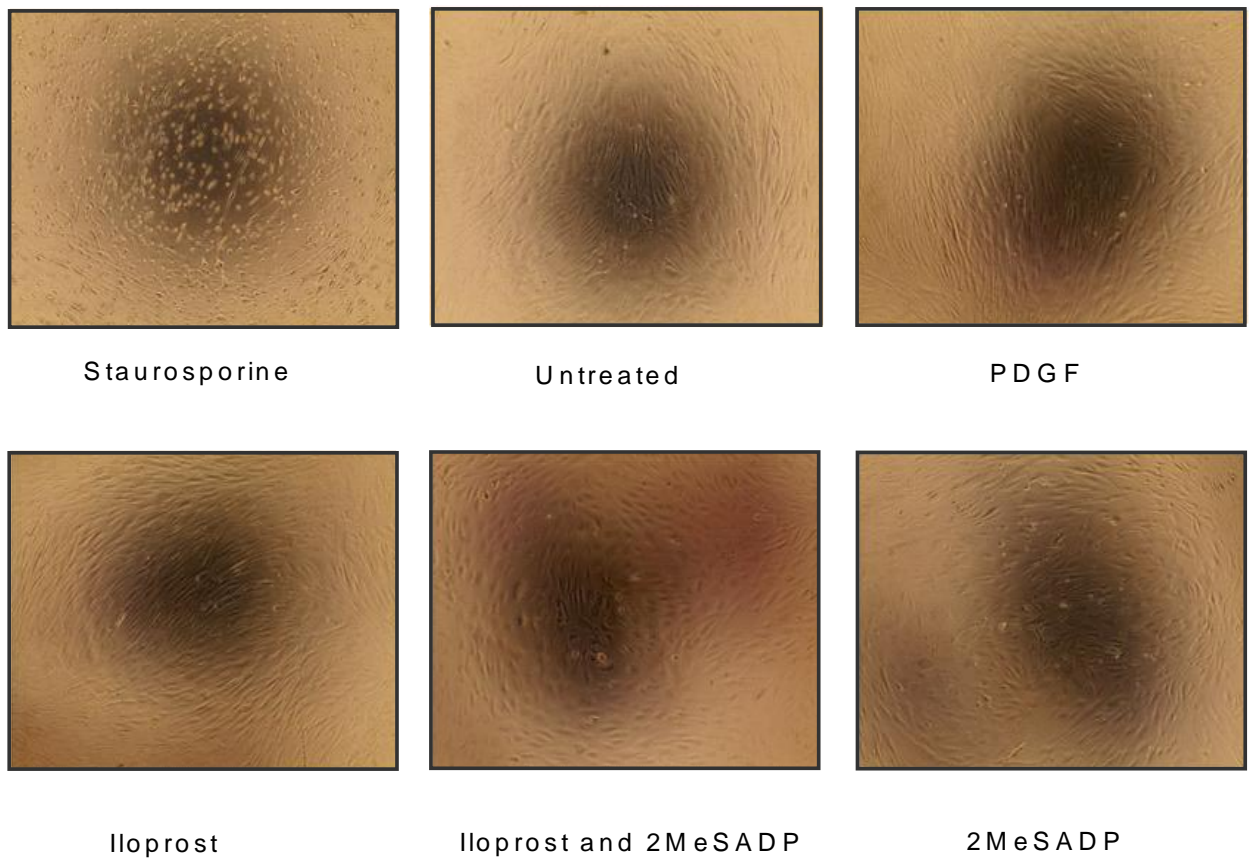
Figure 3-5: Iloprost and 2MeSADP do not cause toxicity to PASMC

Images taken from microscope show that 2MeSADP (1000 nmol/l) and iloprost (10 µmol/l) stimulation did not cause cell death or cell toxicity. 1 µM of staurosporine (Sigma) was used as an indicator for cell toxicity. Untreated PASMC and PDGF treated PASMC were also included to confirm this assay. N=1

3.5.4 2MeSADP inhibits iloprost/prostacyclin induced VASP phosphorylation in platelets

As I observed, there was no significant effect of 2MeSADP on VASP phosphorylation in either control or PAH-PASMCs. Hence, I next used well-established platelet function protocols to measure VASP phosphorylation and validate that all reagents were working as expected. Platelets were stimulated with 10 µM Iloprost or 30 µM prostacyclin for 20 minutes to induce VASP phosphorylation in platelets. This was inhibited by the addition of either 2MeSADP (1000 nmol/l) or ADP (10 µmol/l) (figure 3.6) confirming that the reagents worked. To verify the lack of response to 2MeSADP in PASMC, I next investigated whether there was any interference of the PASMC growth media on platelet aggregation.
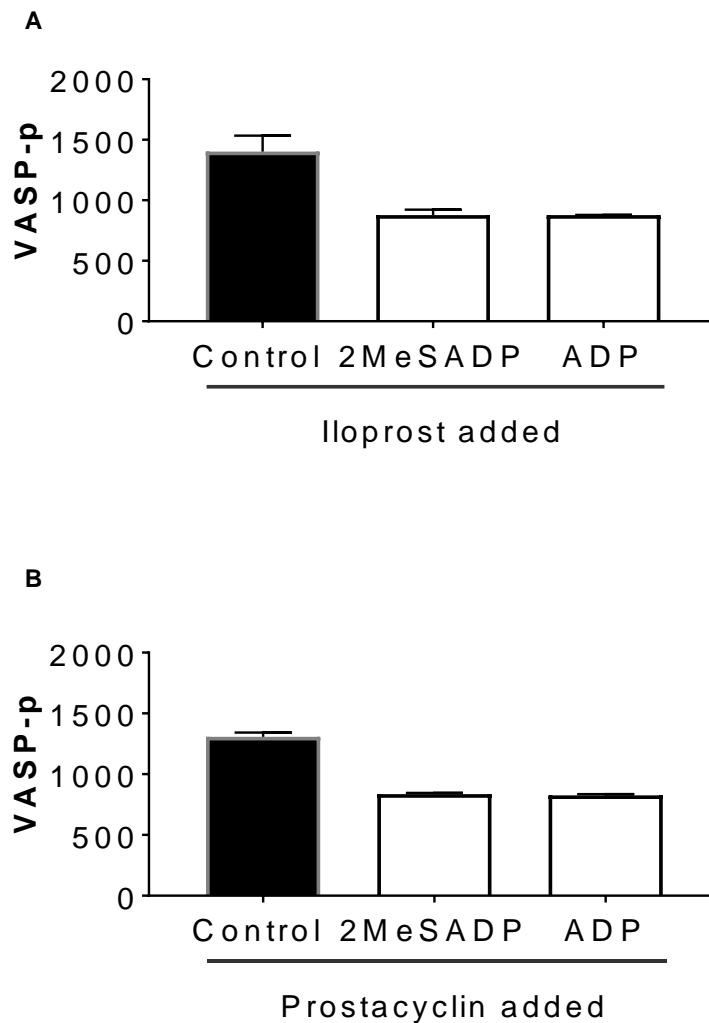
Figure 3-6: 2MeSADP and ADP inhibit VASP phosphorylation in platelets

Graphs in Figure 3-6 show VASP phosphorylation inhibition in platelets stimulated by 2MeSADP and ADP. Platelet activation responses to ADP (10 μmol/l), and 2MeSADP (1000 nmol/l). Agonists used in this experiment: (A) PGI$_2$ (Prostacylin) and (B) Iloprost (prostacyclin analog). Platelet activation (phosphorylated VASP) was measured by flow cytometry. Bars shown are from experiment of n=2 from healthy donor.

3.5.5 PASMC growth media does not affect 2MeSADP stimulated platelet aggregation

It is well demonstrated in literature that activation of $P2Y_{12}$ causes platelets to aggregate. I therefore used platelet aggregometry assays to analyse the platelet aggregation rate induced when stimulated with different concentrations of 2MeSADP. Data is recorded as final aggregation and maximal aggregation. Platelet aggregation assays were carried out in the presence of the PASMC cell culture reagents to rule them out as inhibitors of the assay in SMCs (figure 3.7).
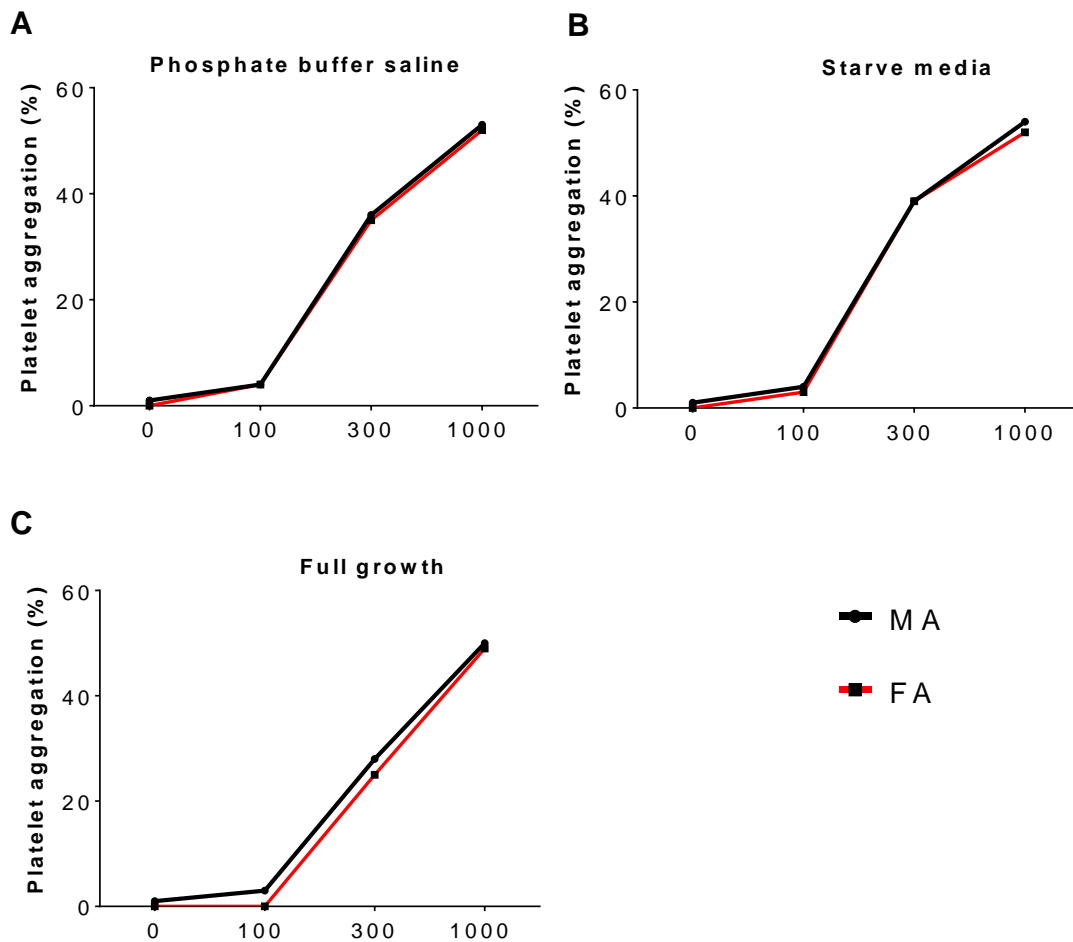
Figure 3-7: Platelet aggregation response stimulated by 2MeSADP in different buffer/media.

Graphs in Figure 3-7 show platelet aggregation responses after stimulation with different concentrations of 2MeSADP (100 - 1000 nmol/l) measured by platelet aggregometry in the presence of (A) Phosphate-buffered saline (PBS), (B) Serum starved media (SM), and (C) Full growth media (FG). MA= maximal aggregation, FA = final aggregation. Graphs shown are from experiment of n=2 blood from healthy donor.

3.5.6 Cangrelor (P2Y$_{12}$ inhibitor) inhibits the action of 2MeSADP in platelets but not in healthy PASMC.

After validating the antibodies and reagents used in the cell culture experiments, the next step was to confirm the presence of P2Y$_{12}$ receptor on PASMC with platelets being used as a positive control. In this section, a radioligand binding assay was used to detect the binding affinity of P2Y$_{12}$ receptor expressed in control and PAH-PASMC.

In this experiment, platelets were used as a positive control and cangrelor (1 µmol/l) was used to verify that the binding was specific to P2Y$_{12}$ and functional P2Y$_{12}$ receptor is expressed in PASMC. In this experiment, I used P2Y$_1$ antagonist to exclude any effect of P2Y$_1$ receptor binding to ^{33}P 2MeSADP. It should be noted that P2Y$_1$ antagonist inhibits ^{33}P 2MeSADP binding to P2Y$_1$.

Non-specific binding was determined using samples with the excessive addition of a potent unlabelled P2Y$_{12}$ agonist, 2MeSADP. The results show that cangrelor is a non-competitive antagonist for platelets but has no effect on the P2Y$_{12}$ receptor number in either patient or healthy SMCs (figure 3.8). The radioligand binding assay demonstrates that cangrelor has a binding site for platelets, whereas for PASMC, it is still unknown as more n number is required to draw conclusion.
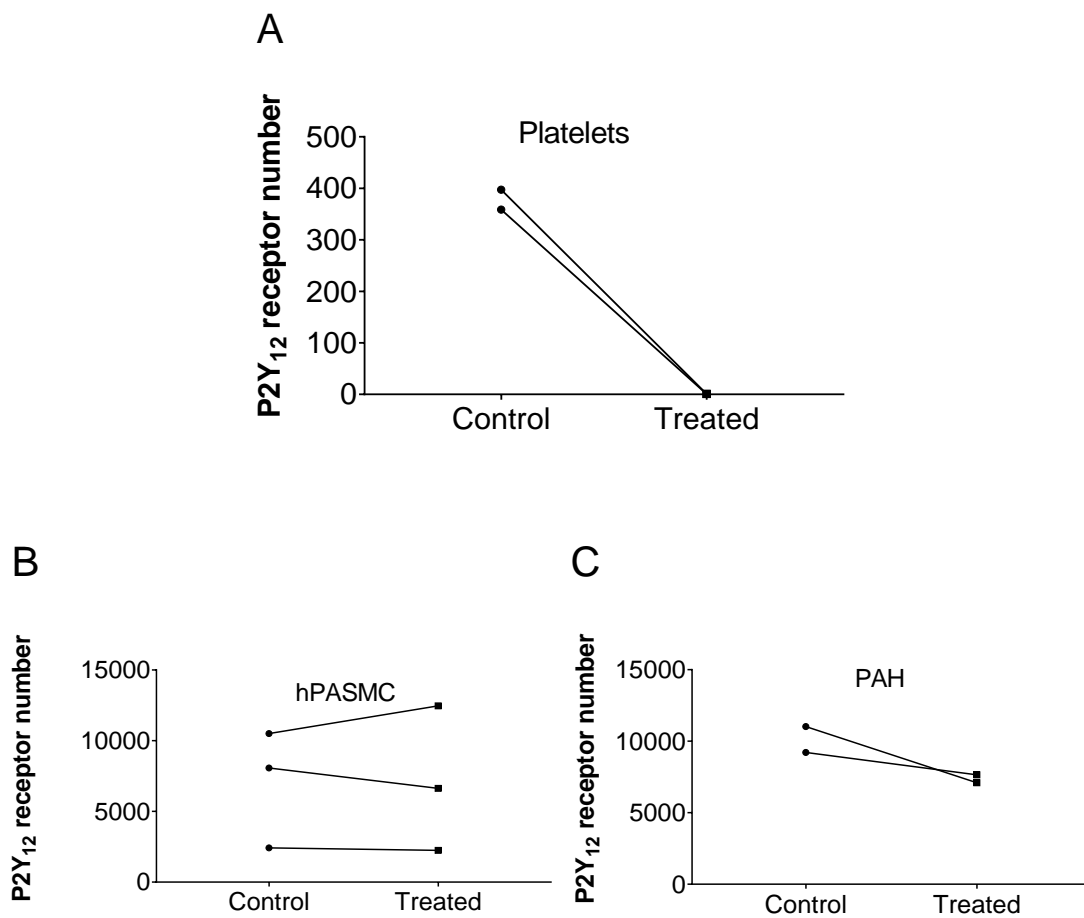
Figure 3-8: Quantification of the P2Y$_{12}$ functional receptor with high affinity radiolabelled ^{33}P 2-MeSADP binding.

Graphs in Figure 3-8 show the quantification of P2Y$_{12}$ functional receptor number. The ^{33}P 2-MeSADP binding was quantified in the presence of cangrelor (1 µmol/L) (treated) and saline (control). Platelets n=2, healthy PASMC (hPASMC) n=3, PAH-PASMC n=2.

3.6 Summary of key findings

- *P2RY12* is highly expressed in patient cells compared to healthy hPASMC.

- *P2RY12* is highly expressed in monocrotaline rat model compared to control.

- From the VASP phosphorylation assay, optimum VASP phosphorylation induced by Iloprost starting at 10 µmol/L at 10 minutes was observed.

- Patient PAH PASMCs show significantly lower effect of VASP phosphorylation induced by iloprost compared to control hPASMC.

- No inhibition of VASP phosphorylation were observed when induced with 1000 nmol/l of 2MeSADP (P2Y$_{12}$ agonist) for all type of PASMCs.

- Full inhibition of P2Y$_{12}$ was observed in platelets.

3.7 Discussion

The results in this chapter show that *P2RY12* is increased in PAH human and pre-clinical Mct model. Besides PASMC, previous findings have shown that P2Y$_{12}$ receptor is expressed in other cells including vascular cells. P2Y$_{12}$ receptor expression has been shown in endothelial cells (Shanker et al., 2006), smooth muscle cells from internal mammary artery and vein (Rauch et al., 2010; Wihlborg et al., 2004) and intrapulmonary artery (Mitchell et al., 2012). I postulated that increased expression of P2Y$_{12}$ in diseased cells contributes to vasoconstriction in PAH patients and it is mediated by P2Y$_{12}$ signalling pathway.

P2Y$_{12}$ has been shown to play a role in vasoconstriction. A study by Wihlborg et al., (2004) showed that P2Y$_{12}$ induced vasoconstriction in internal mammary arteries, and P2Y$_{12}$ inhibitor (AR-C69085) inhibits vasoconstriction induced by 2MeSADP (Wihlborg et al., 2004). They have shown in their *in vitro* model that P2Y$_{12}$ receptor has the highest expression amongst the P2

receptors in VSMC. A different study showed that contractile effect is mediated by $P2Y_{12}$ receptor, and that cangrelor, a potent $P2Y_{12}$ inhibitor, prevents vasoconstriction in hypoxia acute pulmonary hypertension pig model (Kylhammar et al., 2014). To date, there is no established signalling pathway showing $P2Y_{12}$ mediating vasoconstriction in VSMC, but all the evidence have led to the idea of identifying a potential signalling pathway related to $P2Y_{12}$ receptor in the vascular endothelium.

In PAH patients, abnormal levels of vasodilators such as prostacyclin have been documented and iloprost is one of the prostacyclin analogues used as a treatment in PAH. This supports the findings in my study that lower levels of VASP phosphorylation were observed in patient's cells compared to healthy control.

VASP phosphorylation is a validated substrate for cAMP in vasodilation pathway. Following the activation of cAMP, VASP phosphorylation will be increased and leads to vasodilation. VASP phosphorylation has been a promising tool for studying the cAMP pathway and monitoring $P2Y_{12}$ receptor activation in platelets. In this study, VASP phosphorylation is first raised by iloprost and since I observed lower levels of VASP phosphorylation in patient cells, I speculated that 2MeSADP will inhibit VASP phosphorylation induced by iloprost more than in healthy cells. Data from scientific literature indicates that the ADP receptor $P2Y_{12}$ is involved in the inhibition of VASP phosphorylation in platelets. I hypothesised that the same may also apply in pulmonary artery smooth muscle cells vasodilation pathway.

Vasoconstriction affects PAH pathogenesis and smooth muscle cells have been associated with contraction via nitric oxide or prostacyclin. Clinical relevance of testing this in PASMC is that $P2Y_{12}$ and VASP phosphorylation may potentially be a critical mediator in modulating

SMC contraction. As previously shown in the results section, VASP phosphorylation induced by iloprost was observed in PASMC but no inhibition by 2MeSADP was observed.

As it was unexpected that PASMCs did not respond to 2MeSADP, I wanted to exclude any potential reasons for failure caused by cell culture reagents. Therefore, efficacy of 2MeSADP was tested by platelet aggregation and reagents used in cell culture were also tested and I excluded any reagent causing the 2MeSADP to fail inhibiting VASP phosphorylation in PASMC. We tested VASP phosphorylation at residue serine 239 efficacy by flowcytometry. This was done to test the working model in PASMC.

In this study, I have designed an experimental model where iloprost induces VASP phosphorylation and with the addition of 2MeSADP, I was expecting 2MeSADP to reduce VASP phosphorylation induced by iloprost. To my knowledge, this is the first *in vitro* model of VASP phosphorylation related to $P2Y_{12}$ activation by 2MeSDAP in vascular cells. Other vascular cell VASP phosphorylation assay has assessed vasoconstriction pathway and other functional pathways related to VASP phosphoprotein (i.e. motility and actin polymerisation). One of the studies was by Schafer et al., (2003) in an *ex vivo* model that demonstrated the correlation between vascular relaxation and VASP phosphorylation (Schäfer et al., 2003). They have demonstrated the endothelium dependant cAMP pathway in rat aorta. Their findings showed dose dependant VASP phosphorylation and vasorelaxation and these actions were inhibited after removal of the endothelium (Schäfer et al., 2003). Besides that, a study by Defawe et al., (2010) showed that VASP phosphorylation at residue serine 239 mediates collagen matrix contraction (Defawe et al., 2010). It is known that VASP Serine 239 is a preferred site for nitric oxide (NO)/cGMP/PKG pathway and VASP serine 157 is a preferred

site for cAMP kinase C in platelets and other intact cells (Smolenski et al., 1998). VASP protein phosphorylation has been shown in other cells with different functions (Butt et al., 1994; Mülsch et al., 2001; Smolenski et al., 1998). VASP serine 239 has also been studied extensively by other researchers on vasodilation pathway in vascular cells; VASP phosphorylation in endothelial cells and smooth muscle cells from aorta of hyperlipidaemic Watanabe rabbits (Oelze et al., 2000), other cell studies and animal models (Defawe et al., 2010; Schulz et al., 2002).

As no inhibition was seen of VASP phosphorylation at ser239, ser157 was investigated along with the combination of both. Data presented by Schafer et al., (2002) have shown that VASP serine 157 phosphorylation is also a good marker with specificity for cAMP to study vasorelaxation pathway in vascular cells. In my study, I used Iloprost activated VASP phosphorylation whilst Schafer et al., (2002) used forskolin demonstrating VASP phosphorylation via differing receptors. Even when both sites were combined, 2MeSADP showed no inhibition of VASP phosphorylation at ser239 or ser157.

At this point, I speculated that *P2RY12* (P2Y$_{12}$) mRNA is highly expressed in PASMC but not functional at protein level. An alternative hypothesis could be that there is another pathway inhibiting P2Y$_{12}$ Gi signalling in PASMC. Further experiments might give an insight on this issue.

To check if P2Y$_{12}$ was functional, I did a radioligand binding assay using ^{33}P 2MeSADP in PASMC. Radioactive ^{33}P 2MeSADP binding was inhibited in platelets stimulated with cangrelor but not in healthy PASMC. However, 2MeSADP was still able to bind to the receptor. My

results show that ADP can bind to PASMC $P2Y_{12}$ but has no effect on VASP phosphorylation, therefore, suggesting that $P2Y_{12}$ in PASMCs does not activate similar pathways as it does in platelets. This assay is routinely performed in platelets (Judge et al., 2008) but to my knowledge, this has not been performed on PASMC prior to this study.

There are established clinical trials on $P2Y_{12}$ antagonist in PH targeting vasodilation pathway or markers related to vasodilation. In situ thrombosis has been reported to be one of the pathogenesis in PH and clinical trial targeting antiplatelet therapy in PH has established (Robbins et al., 2006). No antiplatelet therapy clinical trial on IPAH was documented until 2006. In 2006, Robbins and colleagues investigated the effect of aspirin and clopidogrel in idiopathic pulmonary arterial hypertension patients. Clopidogrel inhibited platelet aggregation but has no effect on thromboxane metabolite production (vasoconstrictor) as well as Eicasanoid metabolites; i.e. prostacyclin (Robbins et al., 2006). Also, COPD patients has also been associated with PH. Recently, randomised clinical trial by Campo et al., (2017) showed the effect of ticagrelor and clopidogrel on endothelial function by testing biochemical profile related to endothelial dysfunction; chemokines/cytokines release, the rate of apoptosis, nitric oxide levels and etc. Interestingly, according to their findings, reduced endothelial apoptosis rate was observed in COPD patients treated with ticagrelor compared to clopidogrel (Campo et al., 2017). This shows that the potential value of $P2Y_{12}$ antagonist in pulmonary hypertension as endothelial dysfunction play role in PAH pathogenesis. Also, this suggests that $P2Y_{12}$ antagonist has a potential in modulating PAH disease. These evidence on clinical trials further supports my effort on testing the effect of activation and inhibition of $P2Y_{12}$ in PASMC focusing on vasodilation pathway. Data presented in this chapter demonstrated an increase in *P2RY12* expression, however, no effect of 2MeSADP on Iloprost

induced VASP phosphorylation was observed. Thus, the results presented in this chapter have concluded that high expression of $P2Y_{12}$ receptor on PASMC does not play a role in vasodilation via 2MeSADP/$P2Y_{12}$/VASP signalling pathway.

4. Investigating the role of P2Y$_{12}$/ADP signalling on human PASMC phenotype

4.1 Introduction

In chapter 3, I have showed that there was no effect of P2Y$_{12}$ on VASP phosphorylation in PASMC. Next, I sought to investigate the role of PASMC expressed P2Y$_{12}$ on PASMC proliferation and migration. *In vivo* studies have shown that P2Y$_{12}$ activation and inhibition functionally influence disease progression such as atherogenesis (West et al., 2014), acute pulmonary hypertension (Kylhammar et al., 2014) and inflammatory diseases (Satonaka et al., 2015). Progressive proliferative and/or migratory responses are associated with pulmonary vascular remodelling in PAH.

4.2 Hypothesis and Aims

I hypothesised that P2Y$_{12}$ plays a role in PASMC phenotype; proliferation and migration.

To test this, I aimed to determine the effect of 2MeSADP and cangrelor on 1) proliferation, and 2) migration to identify whether P2Y$_{12}$ activation (with 2MeSADP) or blocking (with cangrelor) drives cell migration in healthy or PAH PASMCs. Finally, I investigated the signalling involved which mediated the phenotypic changes.

4.3   Materials and methods

Human pulmonary artery smooth muscle cells (PASMC) were isolated and used as described in the method section 2.1.

4.3.1 Proliferation assay

5000 cells of PASMC were grown per well and plated in 96-well plates. Then, after 48 hours of starvation, quiescent cells were stimulated with 2MeSADP (1000 nmol/l) in the presence and absence of cangrelor (1 µM). The time points used in this experiment was 72 hours, with two different stimulation delivery protocols. In one protocol cells were given new media containing 2MeSADP and cangrelor every 24 hours and the other were just given one dose of 2MeSADP and cangrelor at time 0 and incubated without disturbance for 72 hours. Where cangrelor was present this was pre-added to cells for 2-5 minutes prior to stimulation. To display cell growth of PASMC, PDGF (20 ng/ml) was used as positive control. After 72 hours of incubation, cells were then fixed and stained with Sapphire700 and DRAQ5 and cell number was measured using the LI-COR imaging system. Detailed methodology is described in method sections 2.3 and 2.8.

4.3.2 Migration assay

PASMCs were cultured to about 70 – 80% confluence. Cultured PASMCs were treated with trypsin. Cells were quiesced in starvation medium (0.5% FCS) for 48 hours. Migration of PASMC was done using the Transwell migration method where cells are seeded into the boyden chamber insert. Before seeding, stimulus 2MeSADP (1000 nmol/l), cangrelor (1 µM), combination 2MeSADP and cangrelor were prepared and added into 24-well plates. Cells

were pre-incubated for at least of 2 minutes with cangrelor where necessary. Then, inserts were placed into 24-well plate containing stimulus. 24-well plate with inserts was incubated at 37 ºC and 5% CO_2 for 4-6 hours. Following migration assay membranes were cleaned, fixed, and stained, using Kwiff Diff staining kit. For analysis, 24-well plate with inserts containing migrated cells were counted under microscope (10-20x). Four random fields were selected, and number of migrated cells in each field was averaged to get the mean number of migrated cells as described in method section 2.7.

4.3.3 ERK phosphorylation by In-cell Western

ERK phosphorylation was performed using In-cell Western technique as used in chapter 3 section 3.1.4. Cells were stimulated with 2MeSADP (1000 nmol/L), ADPβS (10 µmol/L), and cangrelor (1µM) at different time points (10 minutes, 20 minutes, 30 minutes, and 60 minutes). Detailed information for the method used can be referred to section 2.3.

4.3.4 Identification of other protein changes by Western Blotting

ERK and other proteins were identified by western blot as detailed in method section 2.11. Cell lysates were stimulated with PDGF (20 ng/ml) (positive control), 0.2% FCS (unstimulated), 2MeSADP (1000 nmol/l), cangrelor (1 µM) ($P2Y_{12}$ inhibitor), and combination of 2MeSADP and cangrelor for 15 minutes. Antibodies used for protein detection: p-AKT, p-cofilin, p38 MAPK, p-ERK, and PI3K. Protein detection for all proteins was conducted on the same blot and the same GAPDH was used for each protein. Details on antibody used in this experiment can be referred to Appendix 3.

4.4 Results

4.4.1 The effect of ADP and cangrelor on proliferation in human PASMC

Enhanced proliferation and increased migratory cells have been observed in PAH pulmonary artery and smooth muscle cells which are vital in vascular remodelling development (Chazova et al., 1995; Fernandez et al., 2015; Voelkel et al., 2014). These cells possess fibres of myosin and actin which support other proteins in regulating contractility and vascular remodelling. $P2Y_{12}$ has been shown to be involved in cell proliferation (Czajkowski et al., 2004; Korybalska et al., 2018). Therefore, I aimed to identify the role of $P2Y_{12}$ and 2MeSADP play in proliferation. To test this aim, PASMC and PAH patient's PASMC were stimulated with 2MeSADP and ADPβS to see $P2Y_{12}$ activation and cells were stimulated with cangrelor to inhibit $P2Y_{12}$. Cells were assessed 72 hours after stimulation following either a single treatment with ADP±cangrelor at 0 hours, or treatment every 24 hours at 0, 24 and 48 hours. Figure 4-1 (A) representing cell number results from proliferation assay for healthy PASMC while Figure 4-1 (B) representing PAH PASMC. 20 ng/ml PDGF (positive control) induced a significant increase in cell number as expected, demonstrating that the assay has worked effectively. Cells stimulated with 1000 nmol/l 2MeSADP and 10 μmol/l ADPβS show no proliferative effect on patient or commercial PASMCs, whether alone or in combination with 1 μmol/l cangrelor, or the reagents were given once or daily for 3 days as shown in Figure 4-1.

A. Healthy PASMC
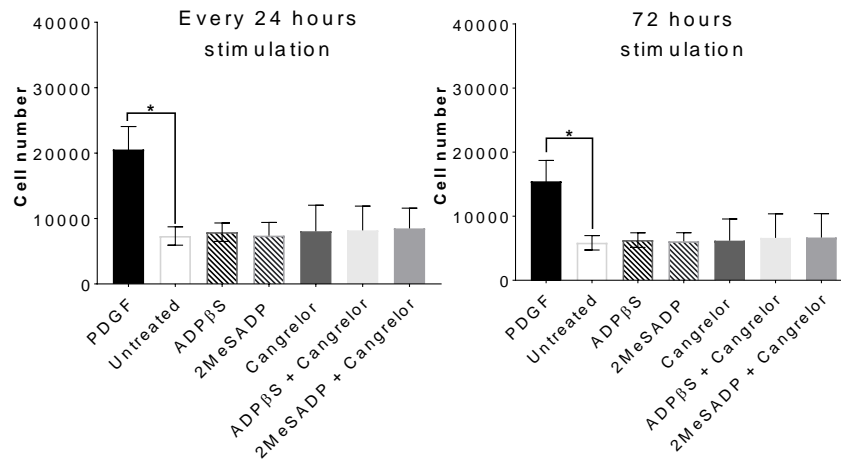
B. PAH PASMC
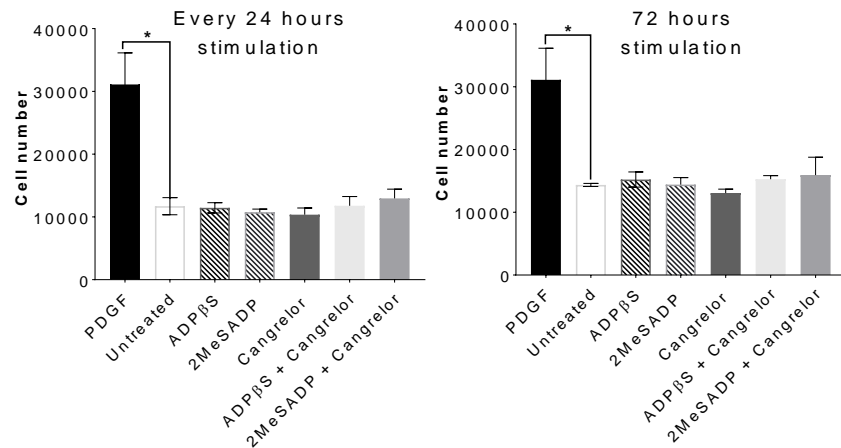
Figure 4-1: 2MeSADP does not increase proliferation of healthy or patient PASMC

Graphs in Figure 4-1 show 2MeSADP does not increase proliferation compared to untreated

control in healthy (A) and patient PAH (B) PASMCs. Time course of 2MeSADP and ADPβS

stimulations; 24 hours stimulation (one-time stimulation) and every 24 hours for 72 hours

(three-time stimulations). Comparison between PDGF (20 ng/ml) (positive control), untreated,

ADPβS (10 μmol/l), 2MeSADP (1000 nmol/l), cangrelor (1 μmol/l), combination of ADPβS and

cangrelor, and combination of 2MeSADP and cangrelor. Cell were stained using DRAQ5 and

Sapphire700 and measured using In-cell Western assay. Bar graphs represent mean ± SEM,

*healthy PASMC (N=5 -8), PAH PASMC (N=3). * p =<0.05.*

4.4.2 The effect of ADP and cangrelor (P2Y$_{12}$ inhibition) on migration in healthy PASMC and PAH-PASMC

Migration is another key cellular phenotypic response driving PAH pathogenesis. The migratory response to 2MeSADP was assessed using the Transwell migration assay and statistically analysed using GraphPad Prism 7. PASMC migration was normalised and assessed relative to control values, where unstimulated as 0% and PDGF as 100%. Transwell migration assay results (Figure 4-2) show that treatment with 2MeSADP significantly increases cell migration to around one third in healthy PASMC (33.32% ± 10.66%, n=5, p<0.001). Although there was also a significant reduction in migration with cangrelor alone (6.875% ± 2.477%), this result shows that P2Y$_{12}$ blockade by cangrelor almost completely abolished 2MeSADP-induced migration (1.088% ± 1.948%, n=5, p=<0.001).

Referring to the results in Figure 4-3, available PAH-PASMCs that were used in proliferation assay were also used in this migration assay. The results of the migration assay shows that treatment of PAH-PASMC with 2MeSADP induced significant migration compared to untreated cells (13.00% ± 7.803%, N=3, p= <0.05) and the effect was significantly decreased with addition of cangrelor (3.647% ± 4.506%, N=3, p= <0.05).
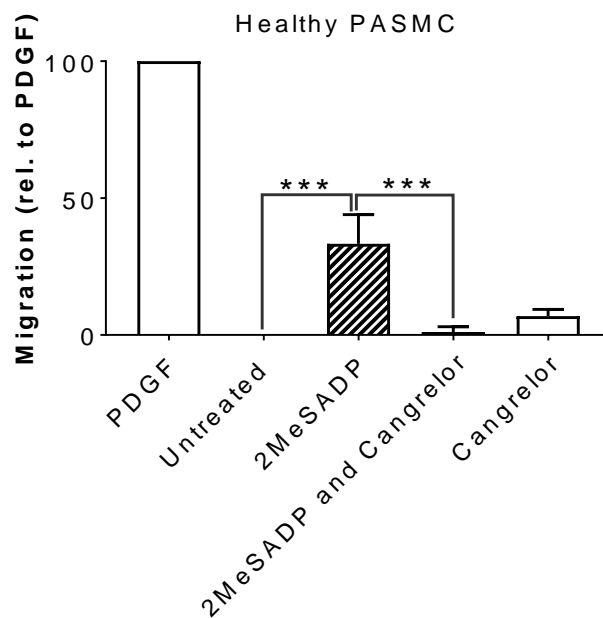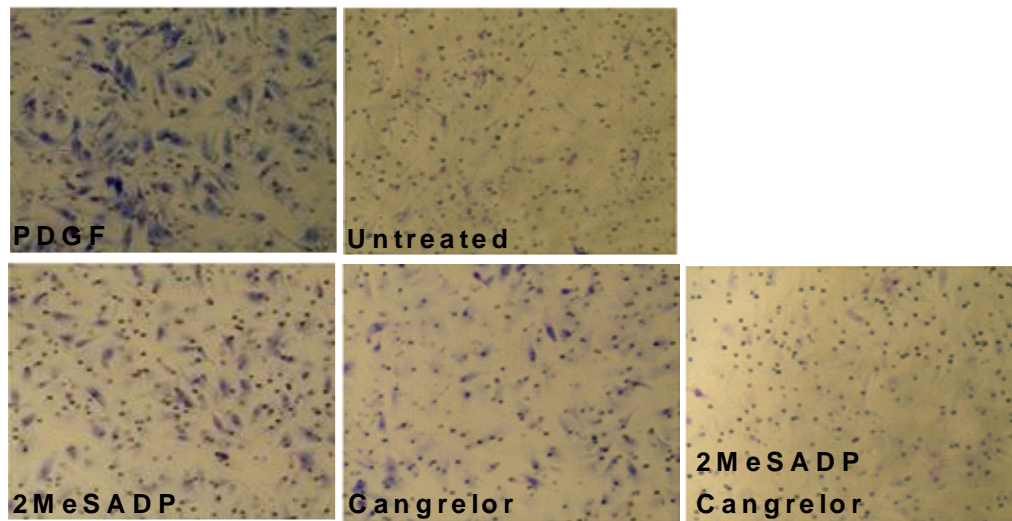
Figure 4-2: 2MeSADP increases migration in healthy PASMC.

Graph in Figure 4-2 shows PASMC were incubated with either PDGF (20 ng/ml), untreated (0.2% FCS), 2MeSADP (1 μM), and cangrelor (1 μM). Representative photomicrographs x40 show the comparison of migrated PASMC between positive control (PDGF), negative control (untreated) and tested stimulus (2MeSADP and cangrelor). Bar represents mean ± SEM. N=5, *** p=<0.001.

.
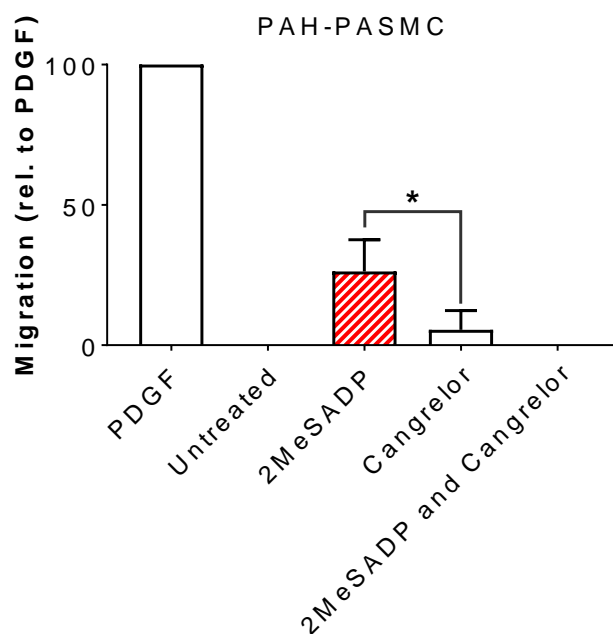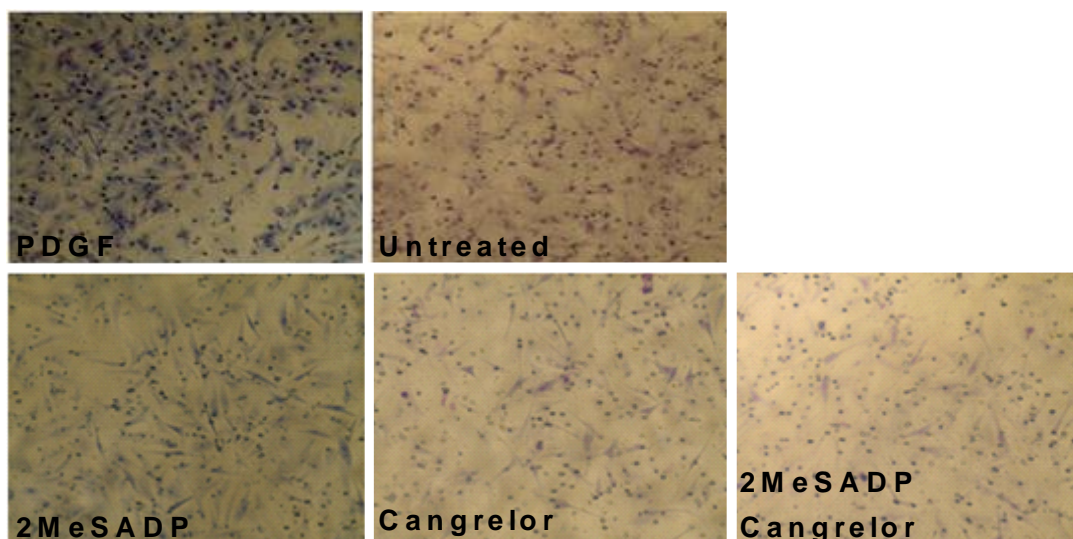
Figure 4-3: Cell migration in PAH-PASMC stimulated with 2MeSADP

Graph in Figure 4-3 shows PAH PASMC stimulated with either untreated (0.2% FCS), PDGF (20 ng/ml), 2MeSADP (1 μM), and cangrelor (1 μM). Representative photomicrographs show the comparison of migrated PASMCs between positive control (PDGF), negative control (untreated) and tested stimulus (2MeSADP and cangrelor). Bar represents mean ± SEM. N=3, * p= <0.05.

4.4.3 2MeSADP does not affect ERK phosphorylation in healthy human PASMC

PASMCs proliferation and migration have been shown to be mediated by ERK1/2 and recently, studies showed that $P2Y_{12}$ activation by ADP induced migration in C6 glioma cells and ERK1/2 play a role in this mechanism (Czajkowski et al., 2004). In previous section, I have shown that 2MeSADP induced migration and was inhibited in the presence of cangrelor. Thus, initial thoughts led me to investigate ERK1/2 as a potential mediator of this response due to its integral role in migration and cell function. To measure the effects of ERK phosphorylation in 2MeSADP and cangrelor treated PASMC, the cells were treated with PDGF (20 ng/ml), 2MeSADP (1000 nmol/l), and cangrelor (1 µmol/l) for different timepoints (10, 20, 30 and 60 minutes) and In-cell Western assay was used to detect the difference in levels of ERK phosphorylation due to $P2Y_{12}$ activation by 2MeSADP. The In-cell Western results, however, showed that treatment with 2MeSADP cause no increase in ERK1/2 phosphorylation in any of the cell types or timepoints that I investigated as shown in Figure 4-4 and

Figure 4-5. Treatment with PDGF resulted in an increase in ERK phosphorylation; 10 minutes (0.48 ± 0.03), 20 minutes (0.49 ± 0.03), 30 minutes (0.49 ± 0.1) and 60 minutes (0.36 ± 0.03) and low levels of ERK phosphorylation was detected in untreated PASMCs (negative control). Both PDGF and untreated validate this experiment. This experiment was also repeated in PAH PASMC as shown in Figure 4-5.
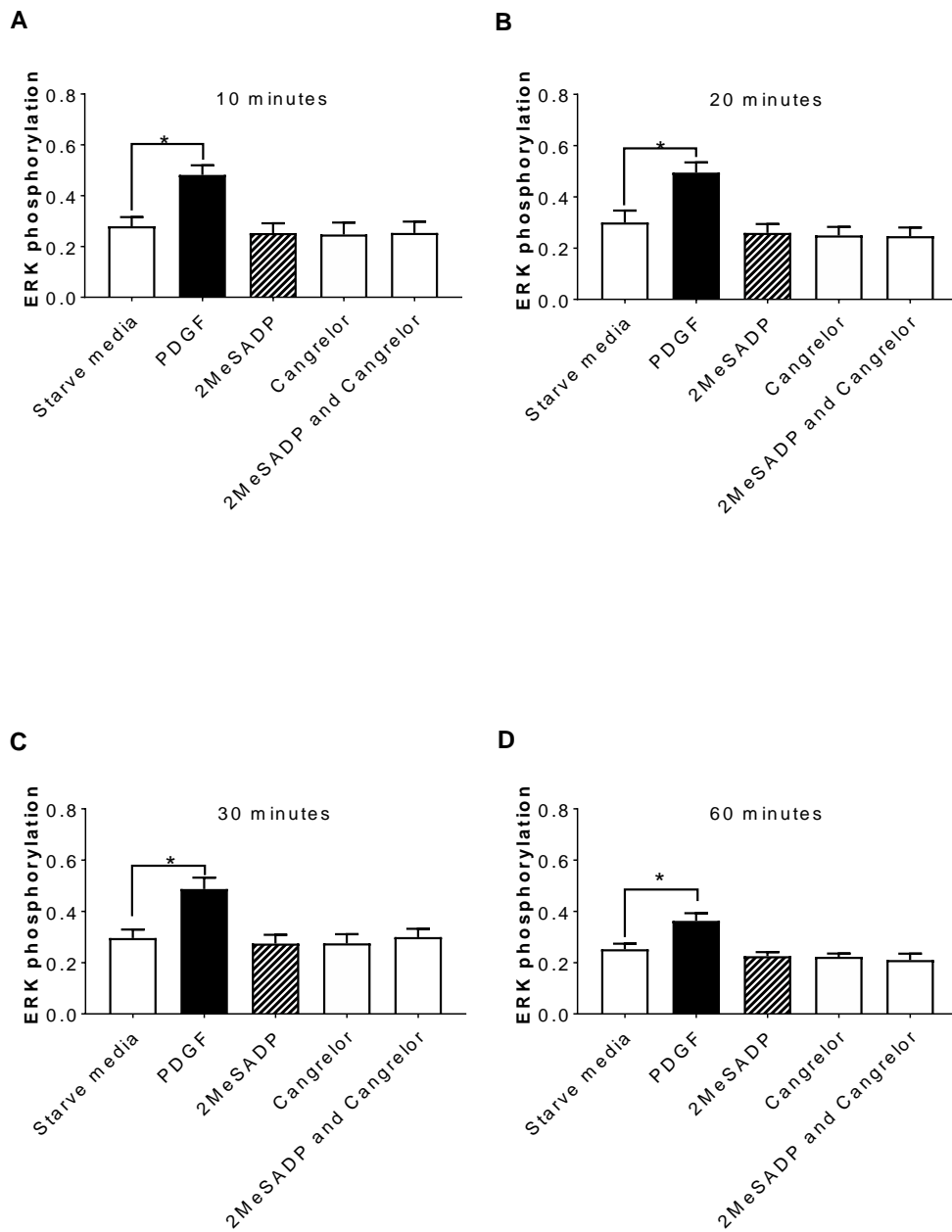
Figure 4-4: ERK phosphorylation in human PASMC

Graphs in Figure 4-4 show ERK phosphorylation in human PASMC in a time course manner: (A) 10 minutes, (B) 20 minutes, (C) 30 minutes, and (D) 60 minutes. Healthy PASMC were stimulated with starve media (0.2% FCS), PDGF (20 ng/ml), 2MeSADP (1000 nmol/l), Cangrelor (1 umol/l). These results were obtained using In-cell Western assay. Bars represent mean ± SEM. N=6 (2 donors). * p = <0.05.

4.4.4 2MeSADP does not affect ERK phosphorylation in PAH-PASMC
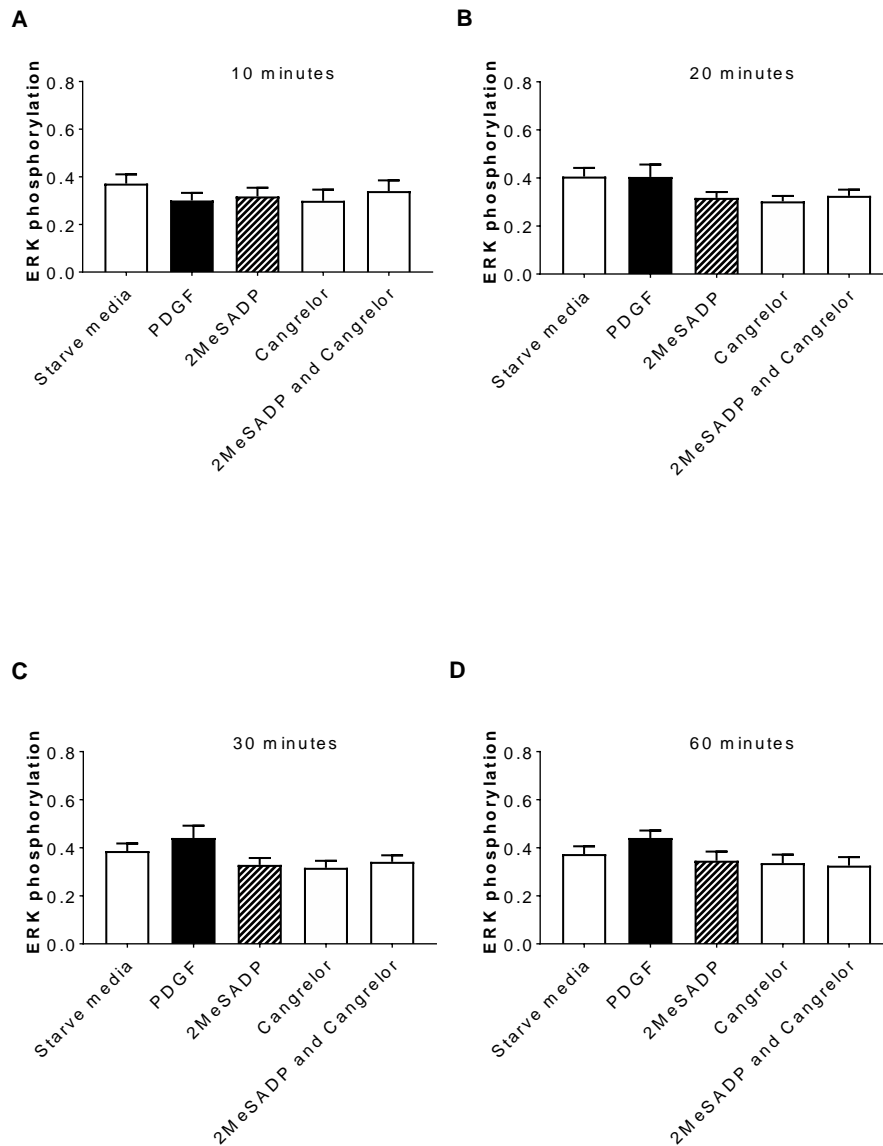
Figure 4-5: ERK phosphorylation in patient PASMC

Graphs in Figure 4-5 show ERK phosphorylation in PAH-PASMC in a time course manner: (A) 10 minutes, (B) 20 minutes, (C) 30 minutes, and (D) 60 minutes. PAH patient cells were stimulated with starve media (0.2% FCS), PDGF (20 ng/ml), 2MeSADP (1000 nmol/l), Cangrelor (1 umol/l). These results were obtained using In-cell Western assays. Bars represent mean ± SEM. N=5 (2 donors). Ns.

4.4.5 Other proteins that may play role in the signalling pathway linked to P2Y$_{12}$

After my first attempt on ERK phosphorylation detection by In-cell Western assay showed no response, I search on signalling pathways related to ADP or P2Y$_{12}$ receptor on the vascular pathway, as shown in Table 4-1.

From there, I selected few proteins to identify any effect of 2MeSADP activation on PASMC by Western Blot assay. ERK, cofilin, PI3K, Akt and p38 MAPK proteins were selected to assess whether they contributed to ADP/P2Y$_{12}$ induced migration or other phenotypic changes in cells. This was done to see the effect of 2MeSADP on activation of protein (phosphorylation or dephosphorylation) or changes in total protein. From Figure 4-6, it can be seen that ADP was found to show no effect on (de)phosphorylation or total protein in any of the proteins tested.

4.4.6 P2Y$_{12}$ signalling associated with endothelium phenotypic changes

These findings are related to proliferation, migration, and vascular remodelling in human and animal models. Table 4-1 shows the study findings and effects of protein mediator that was tested in comparison to controls.

Table 4-1: List of P2Y$_{12}$ associated protein related to vascular phenotypic changes in human and animal.

Protein	Cell	Related disease/mechanism	Study	Pathway	Findings	P2Y$_{12}$ antagonist used	Sources
Activated Rac	Rat pulmonary cultured microglial	Microglial responses towards brain injury	*In vitro* assay on; chemokinesis, chemotaxis assay, Rac staining and activated Rac quantification.	Gi/o-coupled P2Y receptors	ADP and ATP activate Rac ADP and ATP enhance chemokinesis. AR-C69931MX inhibited microglial ADP/ATP induced membrane ruffling.	AR-C69931MX	(Honda et al., 2001)
P44/42 MAPK (ERK1/2)	C6 glioma cells	Cellular growth	*In vitro* assay on ERK1/2 phosphorylation, and cell proliferation	Gi signalling	ADP activates P42/44 MAPK ERK1/2 in time dependant manner. P2Y$_{12}$ inhibition causes inhibitory effect to ERK1/2 phosphorylation. ERK1/2 was also positively associated with glioma C6 cells proliferation	AR-C69931 MX	(Czajkowski et al., 2004)
PI3K	C6 glioma cells	Receptor expression and signalling pathway	PI3K activity, intracellular calcium activity	P2Y$_{12}$-PI3K P2Y$_{12}$-ERK1/2	PI3-K activity was decreased in non-starved cells compared to serum-starved cells. Serum-starved cells causes an increase activity of PI3K. P2Y$_1$ inhibition increases PI3K activity which leads to the findings that P2Y$_{12}$ has a stimulatory effect on PI3K.	AR-C69931 MX	(Czajkowski et al., 2004)

p38 MAPK	Spinal microglial	Neuropathic pain model	Rat peripheral nerve injury model	Rho/ROCK	2MeSADP administration via intrathecal injection induced mechanical sensitivity and induced phosphorylation of MAPK in spinal cord. ROCK inhibition caused reduced of 2MeSADP induced mechanical sensitivity and MAPK phosphorylation reduction was observed. P38 MAPK activation was suppressed, and morphological changes was observed after $P2Y_{12}$ inhibitor administration	MRS2395	(Tatsumi et al., 2015)
JNK (c –Jun NH2- terminal kinase)	Vascular smooth muscle cells	Inflammation	*In vitro* rat's VSMC culture	Not mentioned	JNK inhibition causes reduced level of ADP induced MCP-1 mRNA and protein expression. $P2Y_{12}$ inhibition by $P2Y_{12}$ inhibition by small interference RNA (siRNA) and R-138727 reduced JNK activation	R-138727	(Satonaka et al., 2015)

monocyte chemoattractant protein-1 (MCP-1)	Smooth muscle like cells (SMLCs) from bone marrow derived cells	Transplant atherosclerosis; Orthotopic carotid artery transplantation.	Animal $P2Y_{12}$ deficient knockout mice and *in vitro* assay	MCP pathway	SMLCs from bone marrow derived cells and CD45+ leukocytes were decreased in 2MeSADP/ADP stimulated $P2Y_{12}$ knockout mice. MCP-1 alone did not induced migration but 2MeSADP plus MCP-1 induced migration and expression of MCP-1 in wild type compared to knockout mice.	None	(Harada et al., 2011)
monocyte chemoattractant protein-1 (MCP-1)	Vascular smooth muscle cells	Inflammation	Rats VSMC culture	Not mentioned	$P2Y_{12}$ involved in increase of MCP-1 expression.	R-138727	(Satonaka et al., 2015)
Cofilin	Vascular smooth muscle cells from mice	Atherogenesis	Animal; apolipoprotein mice study	Cofilin dephosphorylation	Cofilin dephosphorylation causes migration in VSMCs.	Clopidogrel	(Niu et al., 2017)
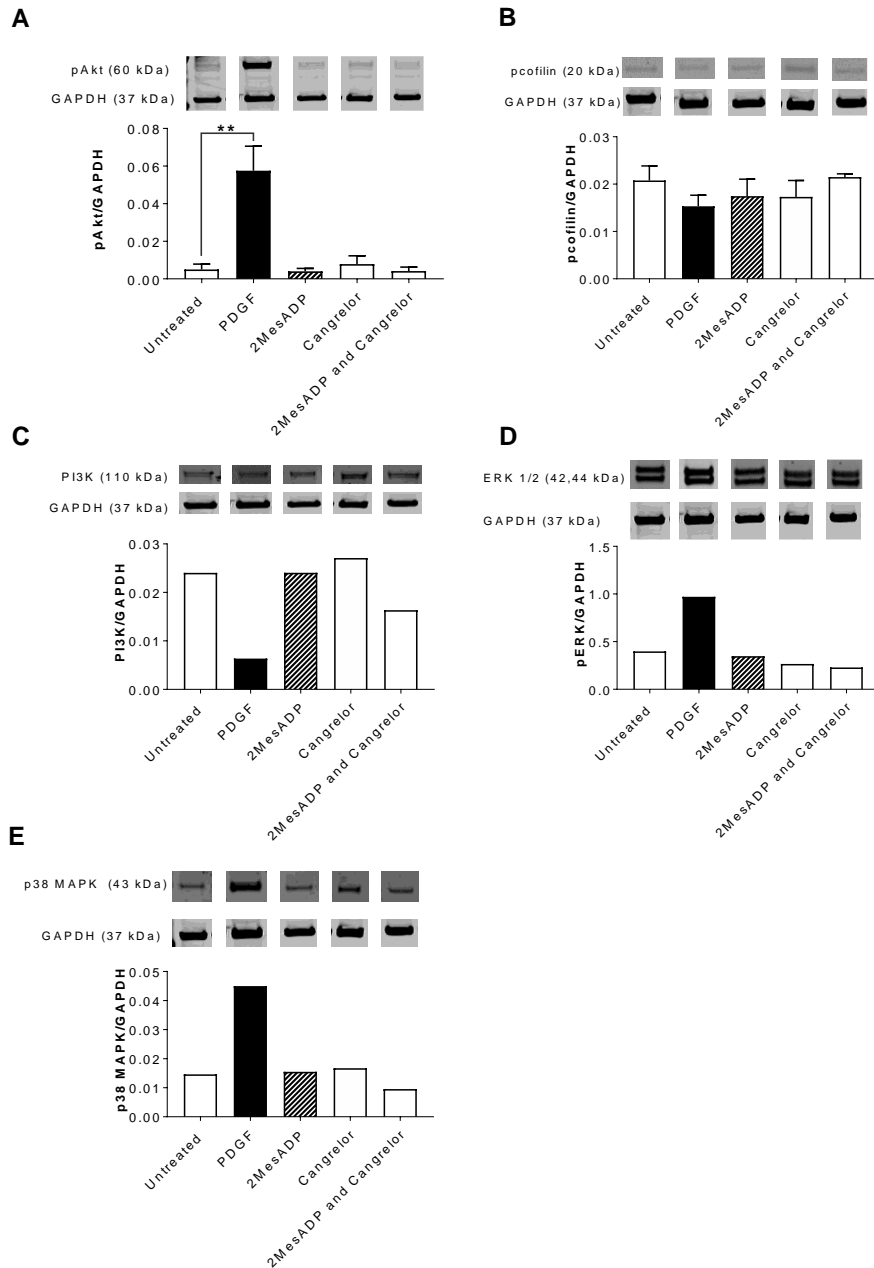
Figure 4-6: 2MeSADP induced protein phosphorylation in healthy PASMC

Graphs in Figure 4-6 show the effect of ADP stimulation at 15 minutes time point on different proteins; (A) pAkt, (B) pcofillin, (C) PI3K, (D) ERK1/2, and (E) P38 MAPK in healthy PASMCs. All proteins are normalised to GAPDH. Controls used: unstimulated and PDGF. N=3 for (A) pAkt and (B) cofilin and N=1 for (C) PI3K, (D) ERK1/2, and (E) P38 MAPK respectively. Western blotting band images expressing proteins are from the same experiment. Error bar represents mean ± SEM.

154

4.5   Summary

In this chapter, I aimed to answer whether $P2Y_{12}$ activation by 2MeSADP modulates phenotypic changes in PASMC and unveil possible signalling pathway involved mediating $P2Y_{12}$ induced phenotypic changes. Below bullet points show the main findings that I have achieved in this chapter.

- 2MeSADP and cangrelor have no effect on proliferation in healthy and PAH patient's PASMC.
- 2MeSADP causes migration of PASMC.
- Cangrelor inhibits 2MeSADP dependant migration of PASMC.
- ERK phosphorylation shows no response to 2MeSADP.

4.6   Discussion

It is well documented that PAH pathogenesis involves sustained vasoconstriction and vascular remodelling due to PASMC proliferation and migration. $P2Y_{12}$ has been shown to contribute to vascular remodelling (Giachini et al., 2014; West et al., 2014), however, its exact role in modulating vascular remodelling still remains elusive.

In the previous chapter, I discussed the effect of $P2Y_{12}$ in the vasodilation pathway in normal PASMC and PAH PASMC and from there, I have identified that $P2Y_{12}$ plays no role in inhibiting iloprost induced VASP phosphorylation in PASMC. Therefore, in this chapter, I have designed *in vitro* experiment to see the effect of $P2Y_{12}$ activation and blockade by 2MeSADP and cangrelor in the phenotypic changes, respectively.

Recent study by Korybalska et al., (2018) shows that P2Y$_{12}$ antagonist reduced cell proliferation. Adding to that, their results show that P2Y$_{12}$ antagonist is safe to be used in endothelial cells and is linked to the following angiogenic factors; bFGF, MMP-2 and angiostatic mediators such as Ang-2, which is related to VEGF. This shows that P2Y$_{12}$ inhibitor has not only inhibits platelet aggregation and been used as a treatment for acute coronary syndrome treatment, but has also been proven to have effects on endothelial cell proliferation and is safe for vascular cells which further support my study in investigating the role of P2Y$_{12}$ receptor for therapeutic value in PAH (Korybalska et al., 2018).

The first aim was to see the effect of P2Y$_{12}$ receptor in proliferation pathway. In this chapter, I aimed to determine whether P2Y$_{12}$ activation causes changes in PASMC migration and proliferation. I examined the cellular response towards 2MeSADP in the absence and presence of cangrelor. Results in this chapter demonstrate that, in these conditions, 2MeSADP does not induce proliferation in healthy control or PAH-PASMC. This is in contradiction with reports in the literature that 2MeSADP causes proliferation and migration in brain and vascular cells (Czajkowski et al., 2004, Niu et al., 2017).

The role of P2Y$_{12}$ in proliferation has been noted in several studies. Rauch et al., (2010) shows that expressed P2Y$_{12}$ on human carotid plaque influences Smc mitogenesis and IL6 expression and they were further increased after pre-stimulation with thrombin. Due to that, they have concluded that pre-stimulation with thrombin helps IL-6 expression and SMC mitogenesis (Rauch et al., 2010). I have tried to pre-stimulate PASMC with thrombin, however qPCR

analysis and In-cell Western (data not shown) showed no difference in mRNA level and PASMC cell number.

I began to speculate that another factor which might stop 2MeSADP to cause proliferation is that 2MeSADP was being broken down to adenosine due to prolonged incubation (72 hours). Therefore, I altered the stimulation protocol to renew the reagents every 24 hours but with no effect and due to that, I concluded that this was not the cause of the lack of proliferation.

After knowing that 2MeSADP does not cause any changes to proliferation, I moved to see the effect of 2MeSADP and cangrelor in migration. Harada et al., (2011) have also shown that ADP promotes migration in cells derived from orthotopic carotid artery transplantation from $P2Y_{12}$ deficient knockout mice which shows that not only in cell culture study, but this animal study also proved that $P2Y_{12}$ receptor plays a role in migration and other diseases (Harada et al., 2011).

I have concluded that 2MeSADP induces migration that was inhibited by the addition of cangrelor. In support of these findings, study by Niu et al., (2014) has shown that 2MeSADP has caused migration but not proliferation. Interestingly, I found that healthy PASMCs had an increased migratory response compared to diseased cells. This result is in contrast with observations in the previous chapter, where I showed increased expression of *P2RY12* expression in diseased cells compared to healthy controls. This was an unexpected result as it would be anticipated that diseased cells would have an increased migratory phenotype, in line with the increased $P2Y_{12}$ expression and the known process of PAH pathogenesis. It is

difficult to explain this finding with current knowledge in the field and therefore further experiments are required to understand the process leading to this conflicting result.

I therefore postulate there must be a specific molecular pathway involved in inducing migration, but my results suggest no such link to ADP induced proliferation through P2Y$_{12}$. Therefore, inhibiting ADP induced migration with cangrelor may be beneficial in PAH.

P2Y$_{12}$ signalling has been well established in platelets but is still in the process of discovery for other cells. There are several signalling pathways which have been shown to be related to vascular changes, inflammatory cell migration and proliferation; activated Rac (Honda et al., 2001), P44/42 ERK 1/2 (Czajkowski et al., 2004), PI3K (Czajkowski et al., 2004; Sapey et al., 2014), P38 MAPK (Tatsumi et al., 2015), JNK (Satonaka et al., 2015), cofilin (Niu et al., 2017). Other findings from human and animal studies are listed in Table 4-1. I performed a broad spectrum of assays to examine several intracellular signalling pathways that might be mediating 2MeSADP induced migration. Unfortunately, I failed to see any changes to phosphorylation levels of PI3K, p38 MAPK, pAKt, pERK1/2, p38 or pCofilin that could explain this phenotype. One of the potential reasons could be that the changes in the protein level is at a very low concentration, or that cellular location of the protein at the leading edge is more critical that the absolute expression level.

2MeSADP causes migration and cangrelor inhibits migration in PASMC.
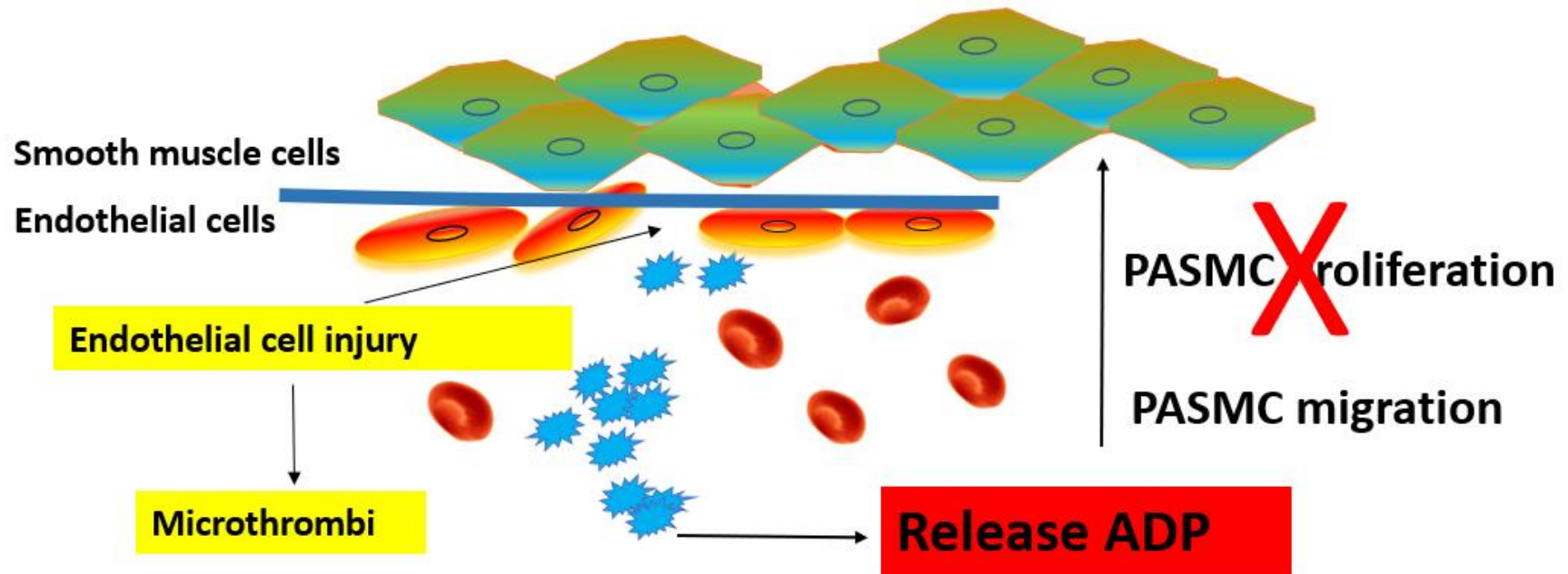
Figure 4-7: 2MeSADP stimulates migration but not proliferation

The diagram above shows the chronology from endothelial injury causing platelet activation and microthrombi formation in PAH. This coagulation process results in release of ADP from platelets. Thus, this section is to identify the effects of endogenous ADP on vascular cells such as PASMCs proliferation and migration that contribute to vascular remodelling in PAH. Results in this study show that ADP stimulations does not influence PASMC proliferation but does have an impact on PASMC migration.

5. Investigating the effect of clopidogrel in PAH monocrotaline rat model.

5.1   Introduction

As a result of the finding that 2MeSADP influences PASMC migration *in vitro*, a key cellular process in the pathogenesis of PAH, I next looked into determining the effect of $P2Y_{12}$ inhibition in the monocrotaline rat model where *P2RY12* expression was shown to be increased.

Clopidogrel is an antiplatelet agent which functions by inhibiting $P2Y_{12}$/ADP activation. Apart from clopidogrel's well known role in platelet aggregation, it has been shown to also influence vascular remodelling in the aorta (Giachini et al., 2014) and in other animal models (Niu et al., 2017). Studying the effects of clopidogrel in vascular remodelling may contribute to determining an effective therapeutic strategy in PAH.

5.2 Hypothesis and aims

I hypothesised that $P2Y_{12}$ inhibition by treatment with clopidogrel would reduce pulmonary vascular remodelling in the monocrotaline rat model of PAH.

Thus, the aims of this study are to assess the therapeutic effect of this $P2Y_{12}$ inhibition on pulmonary arterial muscularisation, pulmonary artery pressure (mPAP) and other haemodynamic analysis.

5.3   Method

5.3.1   Animal preparation

24 male Sprague Dawley rats were randomly divided into groups. All the rats were grouped by weight (220g – 250g). Baseline weights and echocardiograph measurements were taken prior to the start of the experiment.

Groups are as follows:

<u>Groups:</u>

1. **4 Normal control rats**: No clopidogrel treatment and no monocrotaline injection were given.

2. **4 Monocrotaline rats**: No clopidogrel treatment but monocrotaline injection were given.

3. **8 Monocrotaline placebo rats**: No clopidogrel treatment but vehicle which is only water were given.

4. **8 Monocrotaline clopidogrel rats**: Clopidogrel treatment and monocrotaline injection were given.

5.3.2 Study design
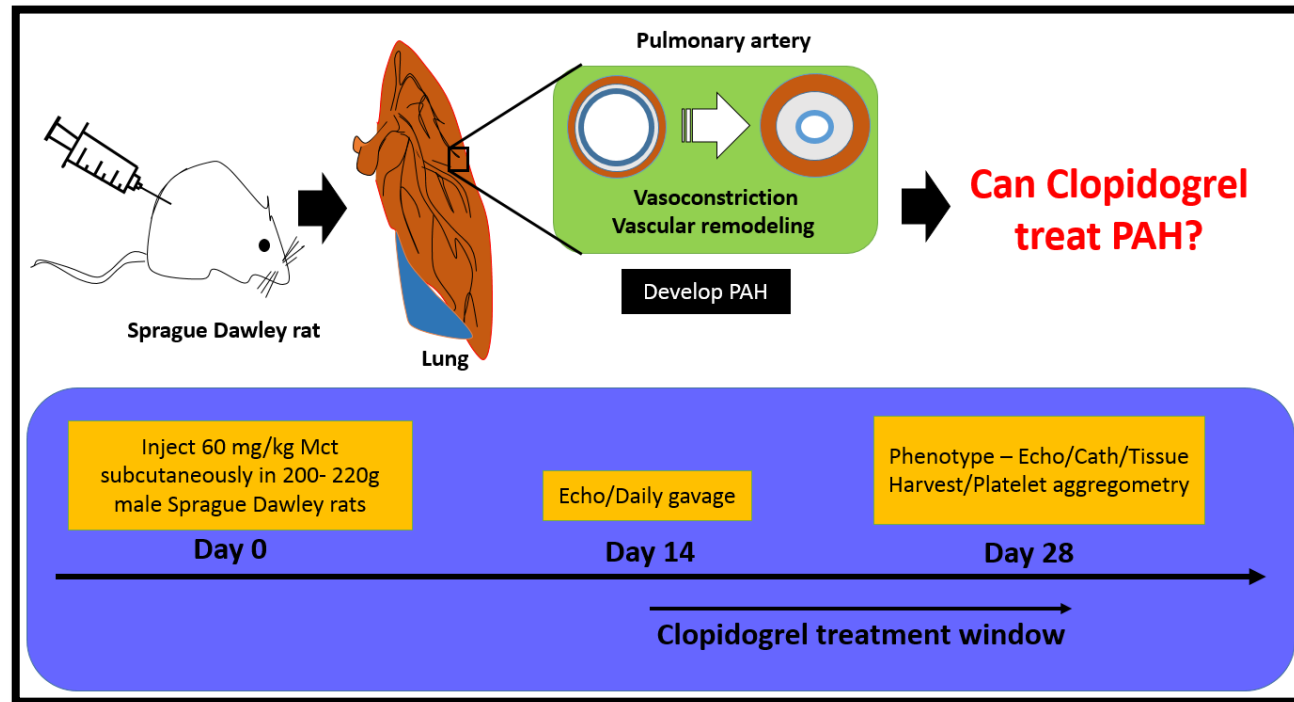
Figure 5-1: Summary of the clopidogrel monocrotaline (MCT) PAH pre-clinical model

Diagram above shows the flowchart and time point of clopidogrel monocrotaline PAH pre-clinical model from day 0 until day 28. Monocrotaline (MCT) was injected on Day 0 (start date). Rats were assessed for pulmonary hypertension by echocardiography (echo). Then, rats were given clopidogrel treatment for approximate of 14 days. On day 28 (last day), rats were sacrificed for catheterisation, tissue harvesting and blood sampling.

5.3.3 Clopidogrel efficacy by platelet aggregometry

Platelet aggregation assays measure platelet activation and final platelet aggregation. In this study, platelet aggregation was assessed using a BioData PAP-8 aggregometer (Alpha Labs, Eastleigh, UK) as described in section 2.4.

5.3.4 Echocardiography

Echocardiography was kindly performed by Ms Nadine Arnold. Echocardiography was performed to assess heart function including right ventricular hypertrophy. Echocardiography was performed as described in method section 2.9.6 (chapter 2).

5.3.5 Cardiac catheterisation

Jugular vein catheterisation was kindly performed by Prof Allan Lawrie. The procedure was done for haemodynamic assessment. Detailed protocol can be obtained from method section 2.9.8.

5.3.6 Tissue harvesting

Tissue harvesting was performed with the help of Dr Laura West. Tissue was perfused for blood removal, harvested and stored for future analysis as described in more detail in the method section 2.9.9.

5.3.7 Tissue processing and tissue embedding

Tissue processing involved multiple steps and it was done by using automated technique provided in the lab. Detailed protocol can be referred in the method section 2.9.11.

5.3.8 Tissue sectioning

Paraffin embedded tissue was sectioned using the microtome. Tissue was sectioned into 5 µm slices.

5.3.9 Immunohistochemistry staining

Tissue section was stained using immunohistochemistry staining for histology analysis as shown in method section 2.10; ABEVG, vWF, α-SMA, PCNA and Caspase-3. The purpose of doing the ABEVG staining is to differentiate the layers of collagen and connective tissues, vWF staining is to stain the endothelial cells, α- SMA staining is to stain the smooth muscle cells, PCNA staining is to see cell proliferation and, Caspase-3 staining is to detect the activated caspase 3 for apoptotic process.

5.3.10 Fluorescence staining

Tissue was processed according to the method section 2.10.6. Then, tissue was stained with primary antibody $P2Y_{12}$ rabbit (P4871, Sigma) and Dako mouse monoclonal anti human smooth muscle actin (cat number M0851). Then, tissue was incubated with secondary antibodies, Alexa fluor 488 goat anti-rabbit (H +L) (cat number A-11034) and Alexa fluor 594 goat anti-rabbit IgG (H+L), highly cross adsorbed (cat number A-11037).

5.3.11 Analysis of pulmonary vascular remodelling

Vessels were counted and grouped according to different sizes; 0 – 70 µM and 71- 150 µM. Statistical analysis from R software was used to group the vessels according to two different sizes. Vascular remodelling was assessed by the number of elastic lamina layers and the amount of α-SMA positive staining present in the vessel wall. Detailed protocol can be referred in the method section 2.9.12.

5.4 Results

5.4.1 Pharmacodynamic effect of clopidogrel in MCT-induced PAH rats.

Clopidogrel 50 mg/kg was given daily by gavage and the drug delivery was validated by platelet aggregation. ADP was used in this experiment to induce platelet aggregation. In this section, I will describe the efficacy of clopidogrel treatment for 14 days and pharmacodynamic effect of clopidogrel in monocrotaline PAH rats.

Figure 5-2 demonstrates that ADP stimulated platelet aggregation and is significantly inhibited by clopidogrel treatment ($p < 0.001$), confirming effective delivery of clopidogrel at therapeutic concentrations.
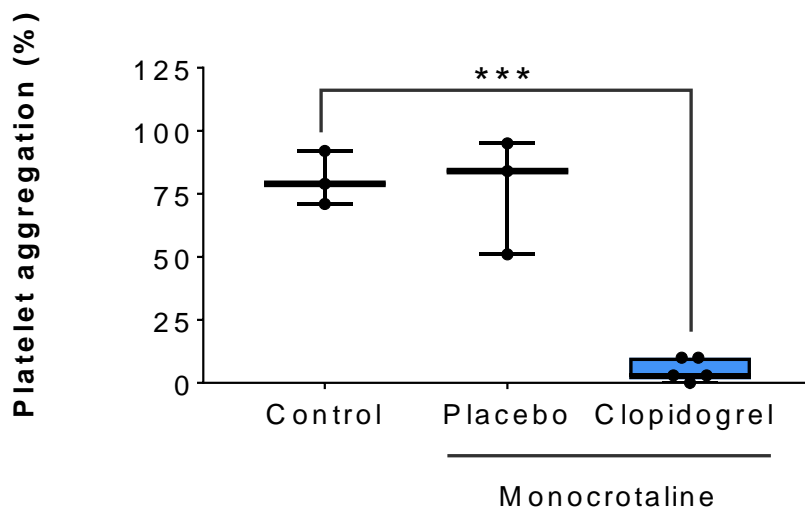
Figure 5-2: Clopidogrel monocrotaline treated shows decrease level of platelet aggregation

Graph in Figure 5-2 shows the results of platelet aggregation in response to clopidogrel treatment. Effect of clopidogrel treatment was analysed using ADP (10 μM) treatment on platelets rich plasma from rat's whole blood. Data was recorded as percentage from platelet aggregation analysis of control, MCT placebo and MCT clopidogrel rats. Plots show median, IQR and Max-Min data points. N=4 -8 rats per group, *** p< 0.001.

5.4.2 Haemodynamic characterisation: Right and left heart pressures

Baseline, mid-point and end point of echocardiography, and end point right heart catheterisation results were recorded. Right ventricular systolic pressure (RVSP) was taken to quantify the pressure inside the artery. This was done to investigate the effect of clopidogrel on pulmonary artery pressure in the right ventricle. From Figure 5-3 (A), it can be seen that the model of disease worked well with monocrotaline dosing causing an increase in RVSP, however this was unaffected by clopidogrel treatment.

Furthermore, Figure 5-3 (B) demonstrates that the left ventricular end systolic pressure shows no statistical difference in any of the groups indicating that clopidogrel treatment does not affect systemic pressure.
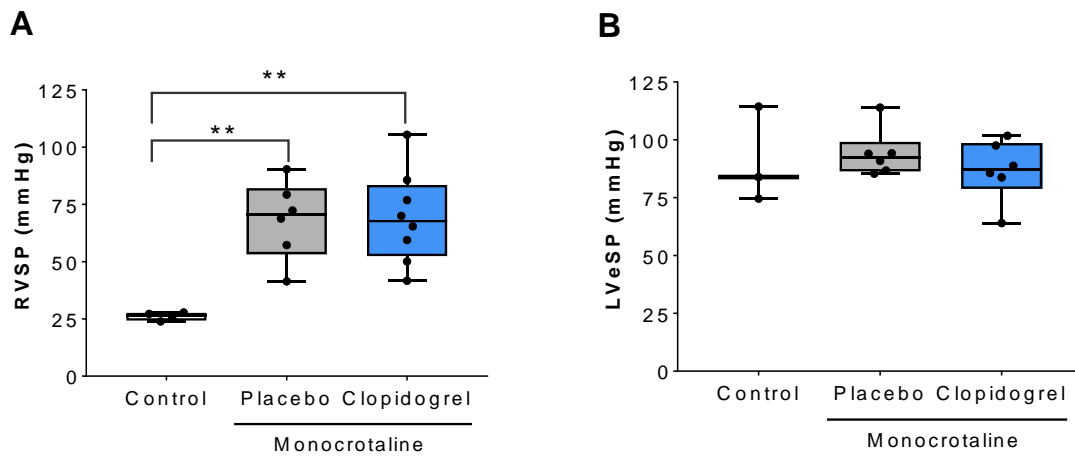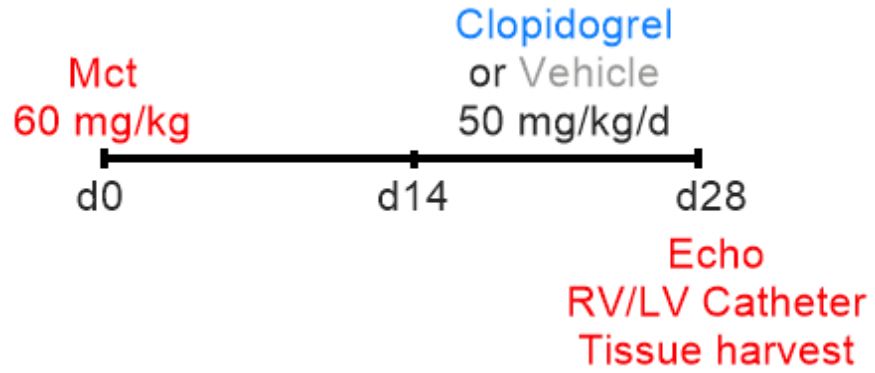
Figure 5-3: Right ventricle systolic pressure and left ventricular end systolic pressure

*Graphs in Figure 5-3 show right ventricle systolic pressure (RVSP,A), and left ventricular end-systolic pressure (LVeSP,B). Box plot represents mean ± SEM, 4 saline treated Ctrl rats (control), and 8 monocrotaline placebo treated rats (placebo), and 8 clopidogrel monocrotaline treated rats (clopidogrel) at d28. ** = p<0.01 compared to control rats. Box plots show median, interquartile range (IQR) and Max-Min data points.*

5.4.3 Haemodynamic characterisation: pulmonary vascular resistance and cardiac output

Haemodynamic assessment of pulmonary arterial hypertension also includes pulmonary vascular resistance (PVR). PVR is use to see the changes in RVSP during disease progression or effect of the treatment. Calculation for PVR is based on three parameters; mean pulmonary artery pressure (mPAP), capillary wedge pressure (CWP) and cardiac output (CO). Figure 5-4 (A) shows the estimated pulmonary vascular resistance which shows no statistical differences compared to monocrotaline placebo and monocrotaline clopidogrel treatment. Cardiac output can be described as the volume of blood pumped by the heart per minute through the circulatory system. It depends on the heart rate, preload, afterload, and contractility. It is an important indicator on cardiac function and the delivery oxygen to the cells. Cardiac output is the multiplication of two variables which are the stroke volume and heart rate. In Figure 5-4 (B) can be seen that there is no statistically significant evidence that clopidogrel has any effect on cardiac output in comparison to control. Trend from the graph shows that cardiac output is slightly increased in comparison to placebo control. However, these data are suggestive of a slightly milder phenotype in pulmonary vascular remodelling as shown in the photomicrograph and result in Figure 5-6, Figure 5-7 and Figure 5-8.
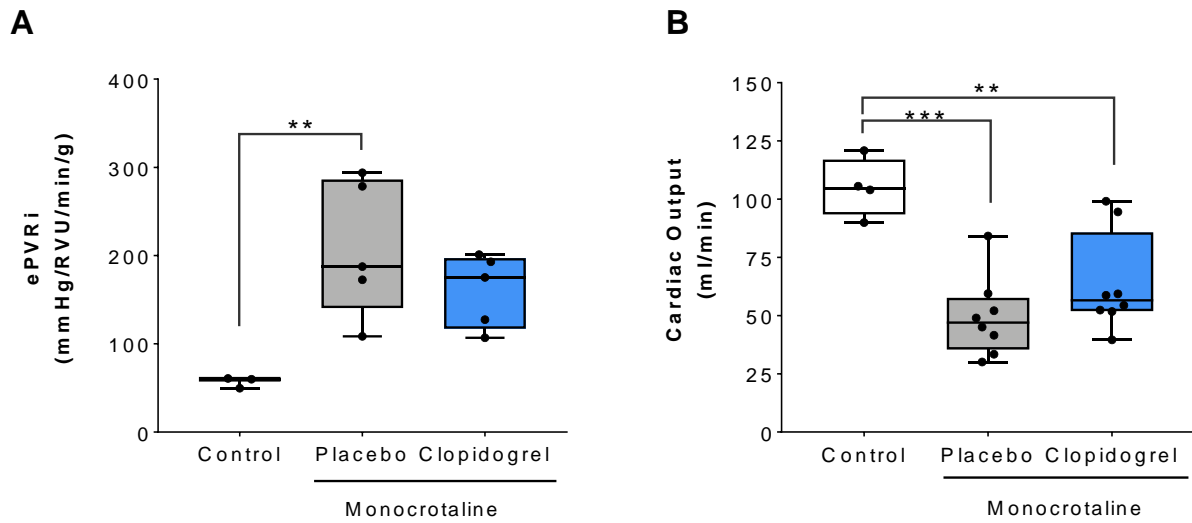
Figure 5-4: Clopidogrel has no effect on estimated pulmonary vascular resistance and cardiac output.

Graphs in Figure 5-4 show the estimated pulmonary vascular resistance (ePVRi, A), and cardiac output (CO, B). Comparison between untreated rats (control), placebo monocrotaline (placebo), monocrotaline clopidogrel (clopidogrel) induced PAH rats. Box plot represents mean ± SEM, 4 saline treated Ctrl rats, and 8 MCT treated rats, and 8 clopidogrel monocrotaline treated rats at d28. * p<0.05, ** p < 0.01, *** p< 0.001 compared to control rats. Box plots show median, IQR and Max-Min data points

5.4.4 Right ventricular hypertrophy

Normal heart shape shows that the left ventricle is bigger than the right ventricle. Normally the right ventricle wall is thin and crescent shaped. In disease, the enlargement of the right ventricle is prominent during electrocardiography test. The results of high pressure in the pulmonary arteries increases the workload of the right ventricle which causes the failure of right ventricle and affects the function of the left ventricle. Right ventricular hypertrophy is a sign of severe pulmonary hypertension as the right ventricle tries to compensate for the sustained raised pressure. This RVH is measured by dividing the weight of the right ventricle by left ventricle and septum.

Right ventricle free wall thickness at diastole Figure 5-5 (A) and right ventricular hypertrophy Figure 5-5 (B) are significantly increased in MCT-treated rats compared to healthy control rats, demonstrating disease development. However, no difference was observed between placebo and monocrotaline clopidogrel treated rats.

A

B
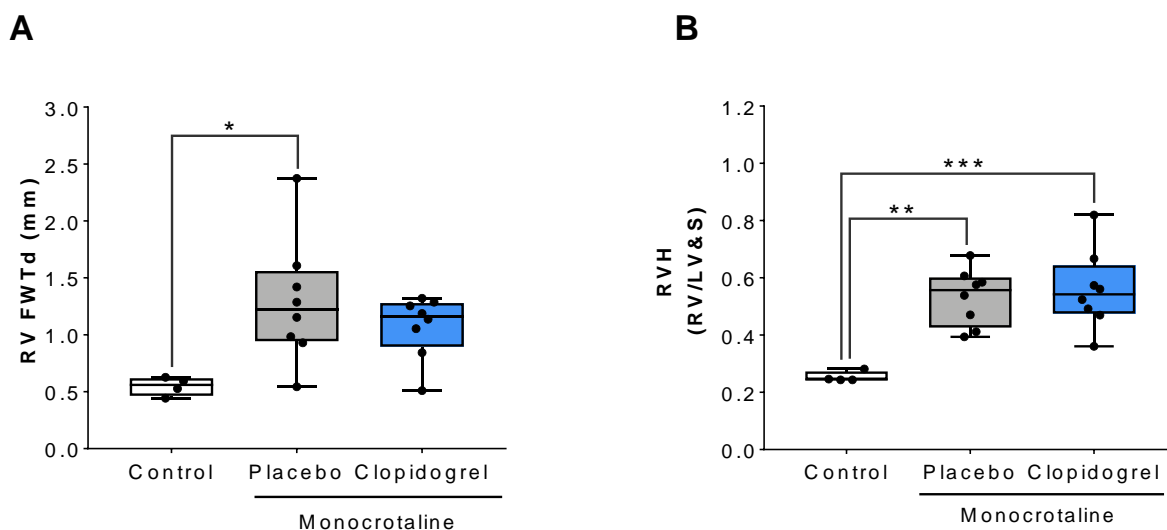
Figure 5-5: Clopidogrel does not affect right ventricular free wall thickness at diastole and right ventricular hypertrophy.

Graphs in Figure 5-5 show the effect of clopidogrel on right ventricular free wall thickness at diastole (RV FWTd, A) and right ventricular hypertrophy (RVH, B). Comparison between untreated rats (control), placebo monocrotaline (placebo), and monocrotaline clopidogrel (clopidogrel) induced PAH rats. Box plot represents mean ± SEM, 4 saline treated Ctrl rats, and 8 monocrotaline treated rats, and 8 clopidogrel monocrotaline treated rats at d28. * = p<0.05, **=p<0.01, ***=p<0.001.

5.4.5 Comparison of non-muscularised and muscularised vessels in clopidogrel treated monocrotaline PAH rats

Histological analysis was performed to assess the effect of clopidogrel treatment on pulmonary arterial remodelling. This was done by measuring both the percentage of vessels muscularised (% muscularisation) and the degree of muscularisation (media/cross-sectional area). Cross-sections of lung stained with alcian blue elastin van gieson (ABEVG) were defined as non-muscularised if they had only one elastic lamina. Muscularised vessels were defined as having two or more elastic lamina. Muscularised vessels show morphological features of coarse elastic lamina as shown in Figure 5-6 and Figure 5-8. The lesions presented in the monocrotaline rats show features of dysregulated elastic lamina which can be found in human disease and thickening of vessels due to disorganised smooth muscle cell proliferation. From the histology analysis, clopidogrel treatment caused a reduction in vessel thickening.

Two sizes of arterioles were selected to analyse the muscularised versus non-muscularised (Figure 5-6) and media/CSA ratio (Figure 5-7); 20 – 70 µM and 71 – 150 µM. Quantitative analysis from muscularisation analysis show a statistically significant increase in the percentage of non-muscularised vessels in the animals treated with clopidogrel at both vessel sizes in comparison to control.

A 20 -70 μm

B 71-150 μm

Non-Muscularised Muscularised

C

Control Monocrotaline Placebo Monocrotaline Clopidogrel
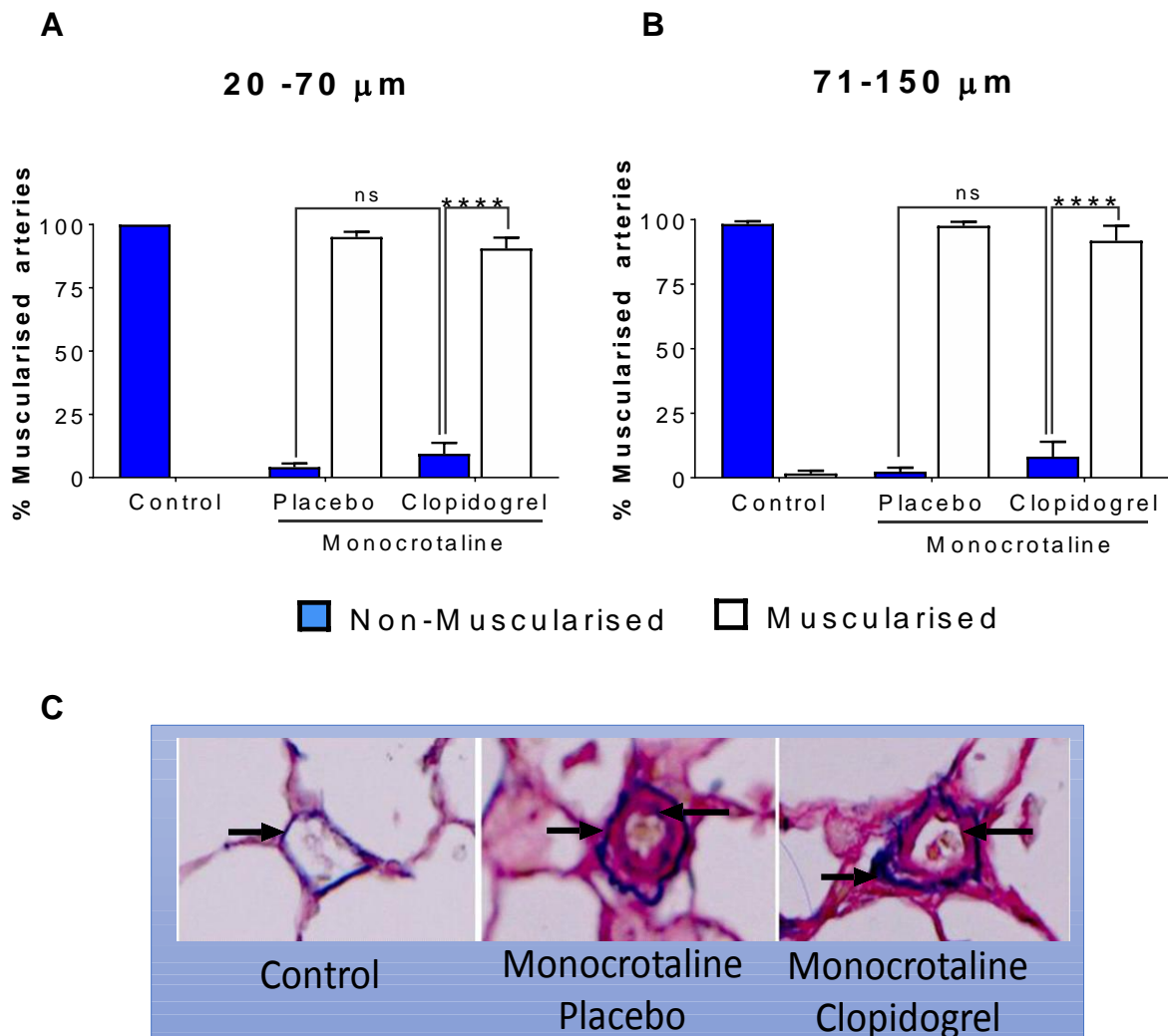
Figure 5-6: The percentage of muscularised vessels versus non-muscularised vessels.

Graphs in Figure 5-6 show the percentage of muscularised vessels versus non-muscularised

vessels in (A) 20 – 70 μM, (B) 71 - 150 μM, and (C) ABEVG stained of pulmonary arteries from

control, monocrotaline placebo and monocrotaline clopidogrel treated rats. Black arrow bars

show internal elastic lamina and external elastic lamina of non-muscularised (control) and

muscularised (monocrotaline treated) rats. Bar represents mean ± SEM, N=4-8 rats per group,

**** p< 0.0001.

174

Assessment of the medial/cross-sectional area (Media/CSA) was subsequently performed. When compared with untreated, placebo monocrotaline and clopidogrel monocrotaline rats, clopidogrel significantly reduced the level of α-SMA positive staining in histological analysis of the lung as shown in Figure 5-8. Vessel muscularisation alterations are more obvious in small size vessels. There was significant increase of vessel muscularisation in vehicle monocrotaline rat compared to untreated rats demonstrating that the model has worked sufficiently. The level of muscularisation was reduced at 28 days by having 14 days treatment with clopidogrel in both vessel size groups.

Assessment of proliferating cell number was made by PCNA staining of the lungs, demonstrating there were positive PCNA cells present in vehicle treated MCT animals (placebo) but there were less present in the lungs of animals treated with clopidogrel.

To further assess cell cycle changes apoptotic cells were visualised using the caspase-3 IHC staining which showed no positive cell staining in clopidogrel treated rats.

5.4.6 Analysis of pulmonary vessel media thickness in clopidogrel monocrotaline treated rats
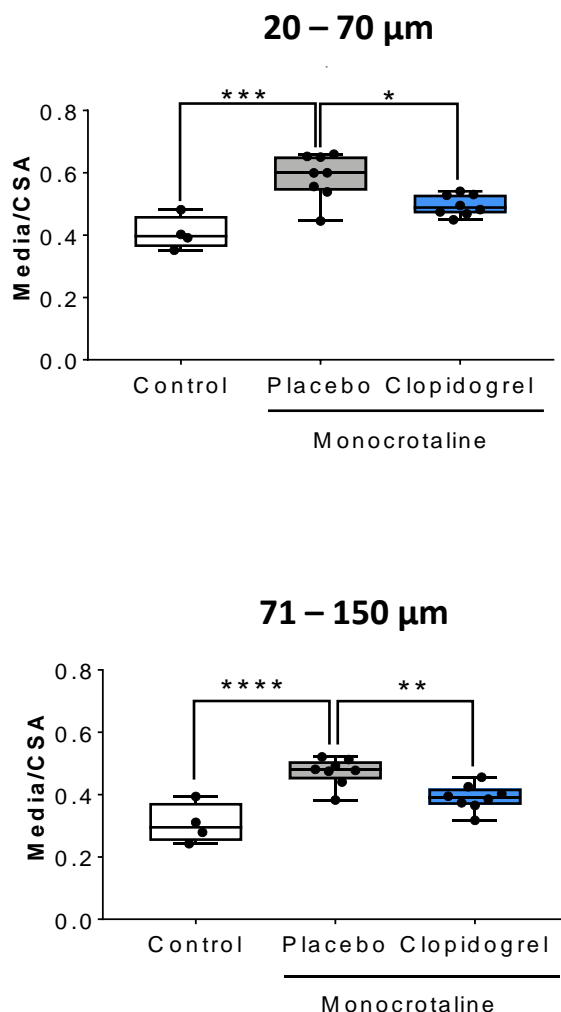
20 – 70 μm

71 – 150 μm

Figure 5-7: The degree of media thickness as a ratio of total vessel size in 20 -70 μM and 71 – 150 μM

*Graphs in Figure 5-7 show the degree of media thickness as a ratio of total vessel size in 20 - 70 and 71 – 150 μM. Muscularisation was calculated as a percentage of medial area divided by total area of vessel. Box plots show median, IQR and Max-Min data points. n= 4- 8 rats per group. Bar represents mean ± SEM., * p<0.05, ** p < 0.01, *** p< 0.001, **** p<0.0001.*
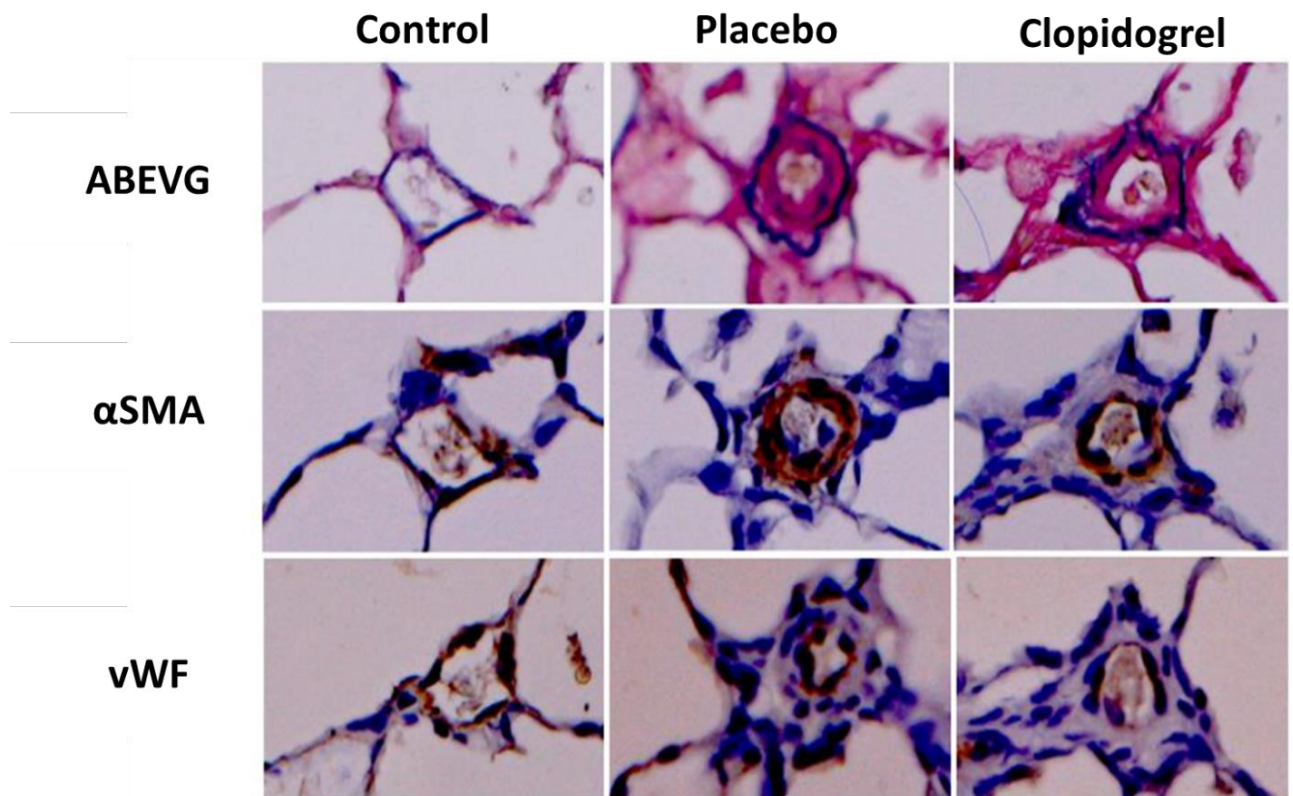
Figure 5-8: Pulmonary artery vascular remodelling under monocrotaline treatment (placebo) and significant reduction of vascular remodelling in rat's treated clopidogrel pulmonary artery.

Figure 5-8 shows representative photomicrograph of lung tissue sections stained with Alcian blue Elastin van Gieson (ABEVG), alpha smooth muscle actin (α-SMA) and von Willebrand factor (vWF) in normal controls, monocrotaline (MCT) (placebo), and MCT-treated clopidogrel rat pulmonary artery. These representative photomicrographs show smooth muscle actin staining the smooth muscle cells (stained in pinked red), vWF staining the intact endothelium (stained in brown) and ABEVG staining the elastin and collagen matrix (stained in dark blue).

Images were scanned and analysed using Zeiss multi slide stage microscope at x20 magnification. Analysis was done using Zen2 software. From the photomicrograph, monocrotaline treated rat shows hypertrophied vessel with accumulation and disorganised of smooth muscle cells characterised by α-smooth muscle actin staining. Elastic lamina stained by ABEVG shows dysregulated and rigid morphology.
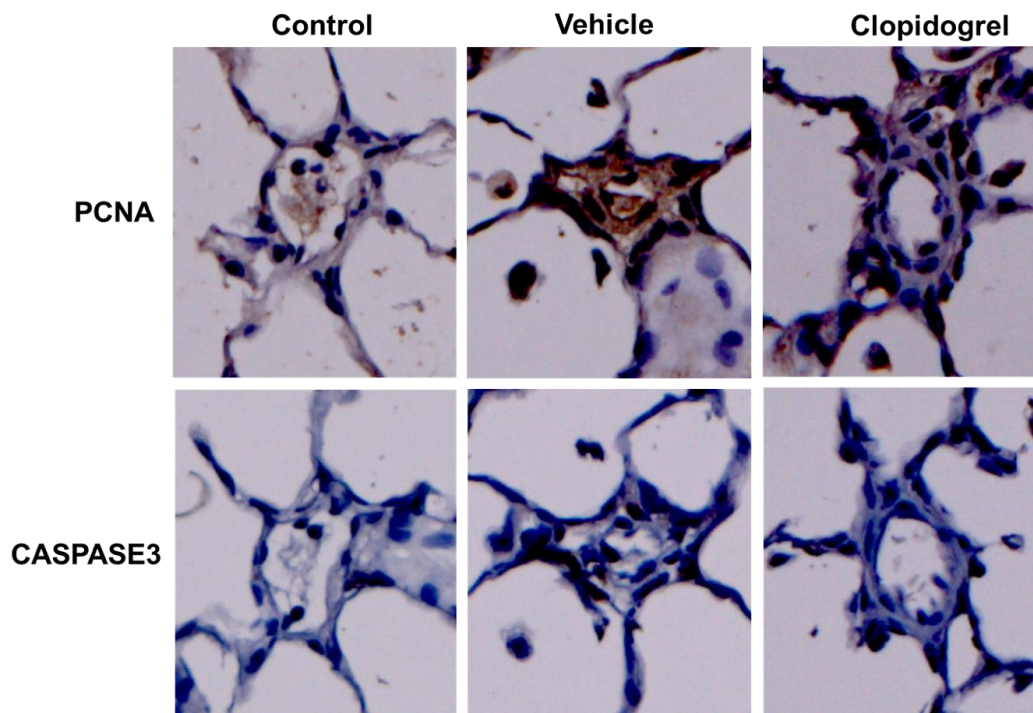
Figure 5-9: PCNA and Caspase-3 Staining

Figure 5-9 shows photomicrographs of lung tissue stained with proliferating nuclear antigen (PCNA) and Caspase-3 in pulmonary artery in all rat groups of monocrotaline clopidogrel treated rats. PCNA is a universal marker for proliferating cells and Caspase-3 detects apoptotic cells. Control shows low level positive of PCNA staining and Caspase-3, while vehicle (placebo) control rat's pulmonary artery is positively stained with PCNA (brown) and Caspase-3 (dark brown). Clopidogrel treated rats shows low level of PCNA staining and markedly no positive Caspase-3 staining. Images were scanned and analysed using Zeiss multi slide stage microscope at x20 magnification. Analysis was done using Zen2 software.

5.4.7 Colocalisation of P2Y$_{12}$ on monocrotaline clopidogrel treated rat pulmonary artery
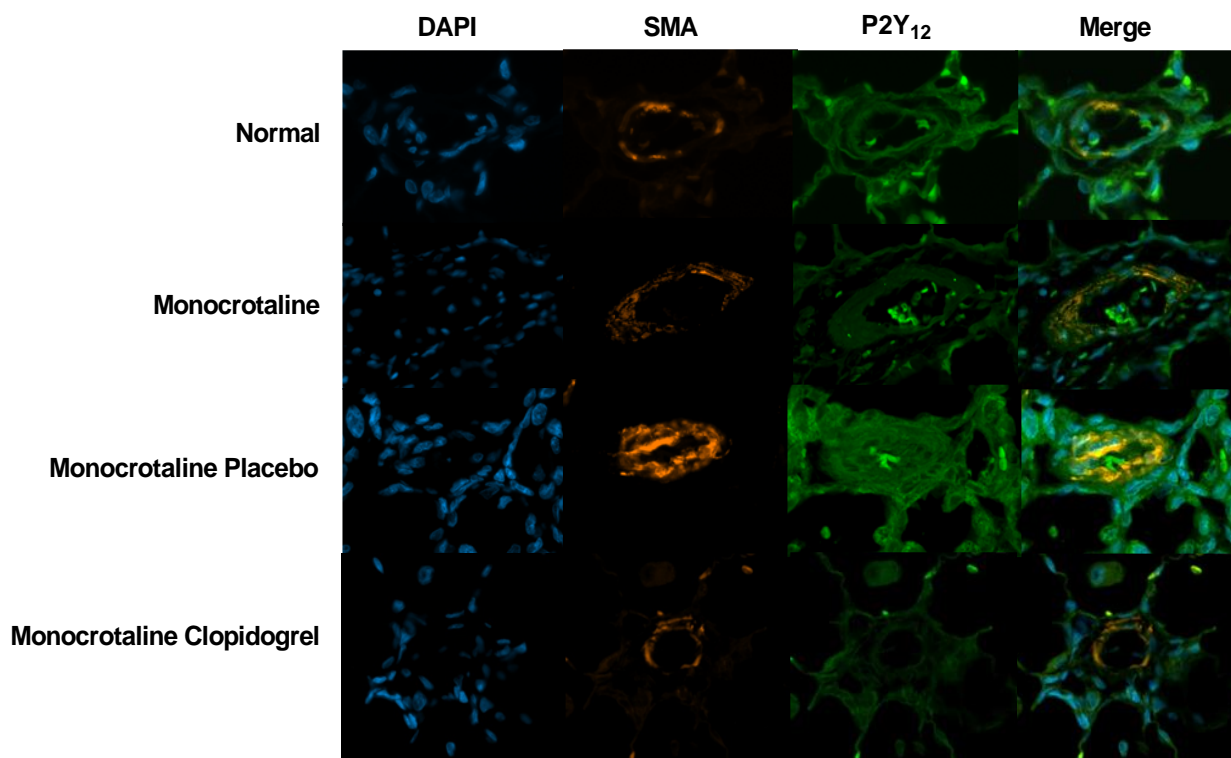
Figure 5-10: P2Y$_{12}$/SMA dual immunofluorescence staining

Figure 5-10 shows representative dual immunofluorescence images of lung sections stained with SMA and P2Y$_{12}$ in controls and clopidogrel monocrotaline treated rats. Nuclei was stained with DAPI. To determine whether I could detect P2Y$_{12}$ expression in PAMSCs, I performed dual immunofluorescence staining for SMA (red) and P2Y$_{12}$ receptor (green).

Figure 5-10 shows there is no obvious co-localisation of P2Y$_{12}$ and SMA in the rat pulmonary artery. A smooth muscle actin expression can be visualised on the pulmonary artery region.

5.5 Summary

This chapter mainly discussed the effect of P2Y$_{12}$ receptor inhibition by a potent P2Y$_{12}$ irreversible inhibitor, clopidogrel and below are the main findings obtained in this chapter:

- Platelet aggregation inhibition assay confirms clopidogrel delivery.

- P2Y$_{12}$ inhibition by clopidogrel significantly reduced pulmonary artery muscularisation in monocrotaline PAH rats.

- Clopidogrel treatment does not affect haemodynamic measurements including RVSP.

- Clopidogrel treatment failed to reduce right ventricular hypertrophy.

- P2Y$_{12}$ protein expression was not seen in the vascular region of MCT rats or in human pulmonary artery.

5.6 Discussion

Having established a role for P2Y$_{12}$ in PASMC migration shown in chapter 4, I next investigated the effect of P2Y$_{12}$ inhibition using clopidogrel in the monocrotaline rat model of PAH. Despite there being no significant effect on right ventricular haemodynamic measurements, there was a reduced PVR by catheter, and significant reduction in pulmonary vascular remodelling by immunohistochemistry.

The first report established 15 years ago (Wihlborg et al., 2004) showed the expression of P2Y$_{12}$ receptor on smooth muscle cells and has since led to other discoveries of vessel P2Y$_{12}$ functions in vascular remodelling and other diseases (Wihlborg et al., 2004; Giachini et al., 2014; West et al., 2014; Sürer et al., 2014; Gündüz et al., 2017). Until now, no research has

shown the effect of P2Y$_{12}$ receptor in PAH. Thus, this has led to my investigation of P2Y$_{12}$ receptor blockade on PAH.

There are several established models that are commonly used in animal studies of PH. In this study, I utilised one of the most common and short-term treatment available to develop severe PH phenotype, which is the monocrotaline rat model. It mimics the disease by having significantly increased right ventricle pressure, pulmonary artery muscularisation and right ventricular hypertrophy (Hill et al., 2017).

In my study, P2Y$_{12}$ receptor is the receptor of interest and there are robust findings showing that targeting the P2Y$_{12}$ receptor and P2Y$_{12}$ antagonist to treat/reverse/reduce disease progression. For instance, study by Sürer et al., (2004) in vascular injury anastomosis model where effective doses of ticagrelor reduced intimal thickness and inhibited the process of intimal hyperplasia in anastomosed right arteries. Besides that, Niu et al., (2017) showed that P2Y$_{12}$ inhibition by clopidogrel in high-fat diet–fed apolipoprotein E–deficient mice model showed reduction in atheroma lesion and patients who consumed clopidogrel showed a decrease in carotid artery plaque lesions (Niu et al., 2017). Other than that, daily administration of clopidogrel monotherapy significantly reduced transplant atherosclerosis (Abele et al., 2009, 2006) and this finding was also further supported by research done in 2009; dual therapy combining clopidogrel and evorolimus (mTOR inhibitor) shown in murine aortic allografts significantly reduced the thickness of the intima (Eckl et al., 2010). All these findings show that targeting P2Y$_{12}$ receptor is promising and clopidogrel is an effective drug modulating vascular disease and further support my choice of drug (clopidogrel) to study the effect of P2Y$_{12}$ inhibition in PAH.

Clopidogrel which is an irreversible P2Y$_{12}$ antagonist, has been used widely preventing thrombosis in cardiovascular disease. It has also been selected to be the choice of treatment due to few reasons. The advantage of clopidogrel is that its inhibitory effect will sustain for few days, as demonstrated. This has been shown in my study, where full inhibition was observed at the final day of the drug treatment, even though the treatment was administered for only 14 days. Other advantages are that it is readily available and clopidogrel activity is naturally eliminated from the body depending on the platelet turnover.

2 weeks of clopidogrel treatment was administered to the rats and platelet aggregometry was used to identify clopidogrel drug treatment efficacy. Platelet aggregation was recorded as final and maximal aggregation. Despite only 14 days of short-term treatment, full inhibition was observed in the monocrotaline rats treated with clopidogrel. Impaired platelet aggregation in clopidogrel treated rat shows that clopidogrel is metabolised and effective in circulation. Platelet aggregation was used in various human clinical study and animal study to identify P2Y$_{12}$ antagonist treatment effectiveness and drug delivery efficacy in treating diseases (Eckl et al., 2010; Judge et al., 2008; Price et al., 2011). These show that the selection of the technique used to verify the efficacy of clopidogrel in monocrotaline rat model in my study is reliable.

Besides that, study by Giachini et al., (2014) shows the effect of clopidogrel on hypertensive rats. They failed to see any effect on systemic pressure but clopidogrel showed an effect on endothelial dysfunction and vascular remodelling. From their results, clopidogrel managed to prevent vascular remodelling in male Sprague Dawley hypertensive rats. These findings support my findings that clopidogrel effectively reduced vascular remodelling, but this was

not reflected haemodynamically. In addition, the selection of rat species they used in their study is the same as in my study which excludes any effect of the animal strain that might cause on the mild reduction in muscularisation (Giachini et al., 2014).

Clopidogrel is an active prodrug which needs metabolic conversion. Since I only observed partial inhibition in vascular remodelling and no inhibition in right heart hypertrophy, it is worth considering that the active metabolite of clopidogrel may not be completely effective as it needs to pass through the endothelium in order to reach the PASMCs. They also produce new $P2Y_{12}$ receptors when they proliferate, therefore complete inhibition may not be achievable, whereas $P2Y_{12}$ antagonism remains stable in platelets until they finished their lifespan, which is approximately 10 days. This might be one of the reasons full inhibition of platelet aggregation was achieved, but only mild muscularisation reduction was observed.

To my knowledge, this is the first study analysing the effect of $P2Y_{12}$ antagonist, clopidogrel on vascular remodelling in chronic pulmonary arterial hypertension. Studies by Giachini et al., (2014), Hogberg et al., (2010), Kylhammar et al., (2014), and Wihlborg et al., (2004) have shown that $P2Y_{12}$ antagonism influences the vasoconstriction pathway. Although I do not see a RVSP response to clopidogrel treatment, this could be due to the relatively modest effect on pulmonary vascular remodelling. It is possible that longer treatment may result in an improved haemodynamic effect, although this is perhaps unlikely, given that there is no evidence of apoptosis, or reduction in proliferation. This study utilised 2 weeks of treatment, 2 weeks after disease was established. It has been shown that clopidogrel in another study using high-fat diet mouse model (Niu et al., 2017), showed that 4 weeks treatment of clopidogrel was insufficient to influence lesion size compared to 12 weeks of clopidogrel

treatment in both aortic arch and whole aorta (Niu et al., 2017). It would be interesting to see whether inhibiting cell migration mediated via P2Y$_{12}$ earlier in the disease time course might have a more pronounced effect, potentially in a prophylactic study design. This most likely reflects the fact that I saw no effect of P2Y$_{12}$ on PASMC proliferation and are therefore only inhibiting the migratory response with clopidogrel. It is possible that the treatment window for preventing migration has been missed in this study.

After I completed my animal study on testing the effect of clopidogrel on PAH, I did a literature search on the effect of clopidogrel in other animal studies and found an interesting finding from Hogberg et al., (2010). They used high dosage of clopidogrel to inhibit vasoconstriction, but it failed. However, an *ex vivo* treatment with another P2Y$_{12}$ inhibitor on the denuded mouse aorta ring, AZD 6140, significantly inhibited vasoconstriction regardless of the clopidogrel oral treatment administered to the mouse (Högberg et al., 2010). This indicates that treatment of P2Y$_{12}$ antagonist shows reduction of vasoconstriction. One possible reason that partial inhibition and no effect in vasoconstriction were seen is that smooth muscle cells are located under the lining of endothelial cells. This may limit the ability of clopidogrel to penetrate the smooth muscle cell region.

Besides, I also speculated that partial reduction of muscularisation might be caused by low expression of the P2Y$_{12}$ receptor as no P2Y$_{12}$ staining was observed by immunofluorescence, however, this is not suitable method for detecting comparatively low expression of proteins.

A study by West et al., (2014) also showed that global P2Y$_{12}$ deficiency has a moderate effect on atheroma lesion and is only present at early atherogenesis (West et al., 2014). Plus, they

184

have found that the P2Y$_{12}$ effect on atheroma lesion was regional and dependent on the vasculature area; P2Y$_{12}$ deficient mice showed a reduction of lesion area in brachiocephalic arteries but not in the aortic sinus. This shows that other factors may contribute to vessel muscularisation such as location in the vasculature – perhaps P2Y$_{12}$ PASMC expression differs between the large and small vessels in the lung but further work is needed to elucidate this.

Next chapter will be on the general discussion, limitations, and future direction for this study.

6. General discussion; PAH and P2Y$_{12}$

P2Y$_{12}$ was first considered to contribute to PAH in studies showing the contribution of P2Y$_{12}$ receptor in vascular remodelling (West et al., 2014). Further studies showed the involvement of P2Y$_{12}$ receptor in acute pulmonary hypertension (Kylhammar et al., 2014). Also, my co supervisors, Prof Rob Storey and Dr Heather Judge have shown that P2Y$_{12}$ antagonism is effective at treating cardiovascular disease (Judge et al., 2008; Storey, 2011; Storey et al., 2010). Thus, it would be wise to investigate the role of P2Y$_{12}$ receptor in pulmonary arterial hypertension.

I demonstrated in chapter 3 that P2Y$_{12}$ is expressed in smooth muscle cells and that this is altered in patients with disease, however, ADP did not manage to inhibit Iloprost induced VASP phosphorylation in these cells. Links to this can be seen in the literature; available treatment focusing on the vasodilation pathway in PH is known to have adverse effect and more to alleviate symptom. In PAH, vasodilator is imbalance and therefore, identifying new treatment that are clinically effective and with a favourable safety profile is crucial. Evidence shows that cAMP levels are lowered in PAH patient (Murray et al., 2007) and therefore, this matches my work demonstrating that the pathway is altered in disease. In this present study, I also showed that, through radioligand binding assays, ADP does bind to functional P2Y$_{12}$ receptor on PASMC. However, this interaction is not inhibited by the P2Y$_{12}$ specific antagonist, cangrelor. Although previously there was a clinical trial on the effect of clopidogrel and aspirin treatment in 19 idiopathic PH patients (Robbins et al., 2006), future step on conducting a clinical trial on the effect of clopidogrel on VASP phosphorylation in PH patients might

elucidate the role of functional $P2Y_{12}$ receptor on vasodilation pathway and its mediators in PAH.

Phenotypic changes seen in chapter 4 showed that ADP did not cause PASMC proliferation, however, there was a significant increase in migration in response to ADP, and this response was inhibited using a $P2Y_{12}$ inhibitor as I expected. Previous findings recapitulated my results in showing that ADP promotes migration in different type of cells; brain cells and smooth muscle cells (Czajkowski et al., 2004; Niu et al., 2009; Harada et al., 2011) and $P2Y_{12}$ inhibitor was proved to inhibit this migration in endothelial cells and proliferation in vascular cells (Korybalska et al., 2018).

In platelet studies, there are several arguments that might be relevant in figuring out the reason behind the failure of $P2Y_{12}$ in causing proliferation. As $P2Y_1$ and $P2Y_{12}$ in platelets work in synergy, and in this study I do not study the effects of $P2Y_1$, and therefore I cannot unravel the cross talk between the two receptors. However, I postulate that there is a pathway regulating migration and preventing $P2Y_{12}$ inhibiting Iloprost-induced VASP phosphorylation. It may be explained by further experiment identifying expression of $P2Y_1$ functional receptor expression.

There are evidence showing $P2Y_{12}$ activation causes the activation or inhibition of certain pathways and modulate phenotypic changes; i.e. p38 mitogen activation (Tatsumi et al., 2015), cofilin (Niu et al., 2017), ERK1/ERK2 (Czajkowski et al., 2004) and etc. As shown in chapter 4, I have examined several potential proteins that might answer the questions as to which pathways are regulating ADP stimulated migration including Akt and PI3K but the mechanism remains unclear.

Modulation of migratory effect of $P2Y_{12}$ activation seen in chapter 4 could be occurring in vascular remodelling in MCT clopidogrel rat model study in chapter 5. There is previous evidence of $P2Y_1$ modulating migration in endothelial cells (Shen & DiCorleto, 2008) but here I have demonstrated this in smooth muscle cells via $P2Y_{12}$.

Previous findings as shown in Table 1-3 shows possible roles of $P2Y_{12}$ receptor at early stages of disease supporting findings from my animal study. Clopidogrel MCT-induced PAH animal model in chapter 5 shows that clopidogrel managed to attenuate vascular remodelling matching results seen *in vitro* using migration assays demonstrating that cangrelor inhibited vascular smooth muscle cell migration. In my opinion, study on expression of $P2Y_{12}$ receptor in different time scale of response to stimulation; early, intermediate and end stage of PAH pathogenesis are crucial.

This study offers new findings on the role of $P2Y_{12}$ receptor in PAH pathogenesis, where increased smooth muscle cell *P2RY12* expression causes pathogenic phenotypic changes. Furthermore, blockade with clopidogrel shows that this receptor may play a role in vascular remodelling in PAH. This suggests that $P2Y_{12}$ inhibition may be beneficial in the treatment of PAH, but this requires further research to elucidate the mechanisms involved.

Limitations

Limitations of this study include the lack of availability of multiple PASMC donors, leading me to perform all my cell culture based experiments on only two primary donors which is too few to draw conclusions due to inconsistencies with such a low n. I tried to counteract this by using multiple commercially available cells to bulk up the numbers and try to negate the effect of using such a low number of primary cell donors.

With regards to the animal studies, a major limitation was the short treatment time and the use of only one model of PAH (the MCT rat model). This model was chosen due to its short experiment time and ease of performance, but this could have been used in conjunction with the Sugen Hypoxia (SuHx) model of PAH as both are considered as standard procedures. However, in the circumstances, there were contributing factors of availability of animals and equipment which lead me to use this model and it is a gold standard model within the field.

The limitation of my radioligand binding assay work was that it needed to be repeated to validate the findings. However, due to the costly nature of this type of experiments and the staffing requirements of trained technical assistance, this could not be done. All these limitations leading into future directions as described next.

Future direction

Data in this thesis shows that 2MeSADP and P2Y$_{12}$ antagonism is involved in PASMC migration and future direction would be to focus on the mechanism of action involved using a non-biased proteomic approach. The cell work would ideally be carried out on using a larger database with cells from patients and healthy volunteers.

I would also like to further investigate the *in vivo* results gained in this study. Prolonged treatment of clopidogrel might increase inhibition of vascular remodelling. Furthermore, we must confirm whether clopidogrel is binding to P2Y$_{12}$ in the vessel and we must also confirm to what extent the penetration of clopidogrel is in the vascular region. Using a cre-lox *P2RY12* mouse, I think, it would have been an ideal way to specifically knock-out expression in EC and SMC allowing me to investigate the effect of a range of vascular cell P2Y$_{12}$ on the background of a PAH model.

7. Appendices

Appendix 1: General solutions

Reagent	Cat.no/Supplier	Preparation
Tris buffered saline	T6664-10PAK, Sigma	1 sachet in 1L of distilled water
Phosphate buffered saline	BR0014G, Oxoid	1 PBS tablet dissolved in 100 ml distilled water
Fixing solution: (3.7% v/v formaldehyde)	101136C, Analar	10 ml of stock solution (37%) in 90 ml of 1X TBS/PBS.
TBS 0.1% Triton X-100	T8787, Sigma Aldrich	5 ml of 10% Triton in 495 ml of 1x TBS/PBS
TBS 0.1% Tween	P1379, Sigma Aldrich	5 ml of 20% of Tween 20 in 995 ml of 1X TBS
Fixative solution: 9% of methanol free formaldehyde in PBS		9 ml of methanol free formaldehyde in 91 ml of PBS

Appendix 2: Stimulants

Material/Reagent	Cat.no/CAS no/concentration	Supplier
2-MesADP	475193-31-8 1000 nmol/l	TOCRIS
ADP	A2754 10 µmol/L	Sigma-Aldrich
Iloprost	10 µmol/L	Ventavis
Cangrelor	AR-C66931 MX 1 µmol/L	AstraZeneca R & D Charnwood (Loughborough, UK)

Appendix 3: Primary antibody

Material/Reagent	Cat.no/CAS no	Dilutions	Supplier
VASP (pSer239)	ALX-804-240-C100	1:50	Enzo Life Sciences
VASP-p (pSer157)	ALX-804-403 C100	1:50	Enzo Life Sciences
Total VASP (942) Rabbit mAb	3132S	1:1000	Cell Signalling Technology
Phospho Akt (Ser 473) (D9E) XP® Rabbit mAb	4060	1:2000	Cell Signalling Technology
Phospho-p38 MAPK (Thr180/Tyr182) (D3F9) XP® Rabbit mAb	4511	1:1000	Cell Signalling Technology
Phospho-p44/42 MAPK (Erk1/2) (Thr202/Tyr204) (D13.14.4E) XP® Rabbit mAb	4370	1:2000	Cell Signalling Technology
PI3K kinase	4249T	1:1000	Cell Signalling Technology
Phospho-Cofilin (Ser3) (77G2) Rabbit mAb.	3313S	1:1000	Cell Signalling Technology

Appendix 4: Materials and reagent for cell culture work

Material/Reagent	Cat.no/CAS no	Supplier
PASMC	CC-2581	LONZA
T75 cm^2 cell culture flask	430641U	Corning®
T75 cm^2 cell culture flask	156267	Nunc, Thermo Fisher scientific
Trypsin-EDTA (1X)	25200-056	Gibco, Life Technologies
Trypsin Neutralising solution	R-002-100	Gibco, Life Technologies
SmGm bullet kits : SmGm-2-singleQuots hEGF hFGF-B FBS GA-1000 Insulin	CC-4149 CC-4230D CC-4068D CC-4102D CC-4081D CC-4021D	LONZA
SmBM growth media	CC-3181	LONZA
Cell culture microplate (96 well), Bottom (chimney well), BLACK, CellStar, TC, lid with condensation rings	655090	Greiner Bio-one
Fibronectin from human plasma	50895-5G	Sigma-Aldrich

Appendix 5: RNA extraction and RT-PCR

Material/Reagent	Cat.no/CAS no	Supplier
TRIzol reagent	15596-029	Invitrogen, Life Technologies
Direct-zol RNA MiniPrep	R250	Zymo, Cambridge Bioscience
Zymo-spin™ IIC column	C1011-50	Zymo, Cambridge Bioscience
Collection tube	C1001-50	Zymo, Cambridge Bioscience
Qiagen Allprep RNA/DNA/Protein tissue kit	80004	Qiagen
Applied Biosystems High Capacity RNA to cDNA™ kit	4368814	Thermo fisher
TaqMan Universal Mastermix	4440038	Thermofisher

Appendix 6: In cell western

Reagent	Cat.no/CAS no	Supplier
Cell culture microplate (96 well), Bottom (chimney well), BLACK, CellStar, TC, lid with condensation rings	655090	Greiner Bio-one
Odyssey Donkey anti-mouse IRDye 800 CW	926-32212	LI-COR
Odyssey Donkey anti-rabbit IRDye 800 CW	926-32213	LI-COR
DRAQ5	409DR50050	Biostatus
Sapphire700	928-40022	LI-COR
Odyssey Blocking buffer	927-40000	LI-COR

Appendix 7: Radioligand binding assay

Reagent	Cat.no/CAS no/ Dilutions	Supplier
^{33}P 2MeSADP	-	Perkin Elmer, Buckinghamshire, UK
Acid citrate dextrose	65 mmol/L citric acid, 80 mmol/L tri-sodium citrate and 110 mmol/L dextrose	
Apyrase	0.01 U/ml	Sigma Aldrich
EDTA	4 mmol/L	Fisher Scientific
PGI2	100 nmol/L	Cambridge Bioscience
MRS 2179	100 µmol/L	Sigma Aldrich

Appendix 8: HT buffer recipe

HEPES-Tyrodes (HT) Buffer	Recipe (Prepared by Dr Heather Judge)
	129 mmol/L NaCl 8.9 mmol/L NaHCO$_3$ 28 mmol/L KCL 0.8 mmol/L KH$_2$PO$_4$ 5.6 mmol/L dextrose 10 mmol/L HEPES

Appendix 9: Flowcytometry

Reagent	Cat.no/CAS no/Dilutions	Supplier
PGE1	10 µmol/L	Cambridge Bioscience
ADP	30 µmol/L	Sigma Aldrich, Gillingham, UK
Permeabilization solution: 0.18% Triton X100 in PBS	T8787 18 µl of Triton X100 in 10 ml of PBS	Sigma Aldrich
anti-CD42a R-PE antibody	1:10 dilution in PBS	Becton Dickinson, San Jose, California, USA
anti-VASP FITC (phosphorylated) (pSer^{239}) (16C2)	1:50 dilution in PBS	Enzo Life Sciences, Exeter, UK
FITC mouse IgG control antibody		Enzo Life Sciences, Exeter, UK

Appendix 10: Transwell migration assay

Reagent	Cat.no/CAS no	Supplier
HTS Multiwell Insert system, 8.0 µm pore size, PET membrane, 24-multiwell format	REF351185	BD Falcon
Diff Quick Stain Kit Solution A = Methyl-alcohol Solution B = Eosin Y Solution C = Azure A + B		

Appendix 11: Antibodies for histology staining

Material/Reagent	Cat.no/CAS no/Dilutions	Supplier
Monoclonal anti-human smooth muscle actin	Cat number: M0851 (1:150 dilution in PBS)	Dako
Rabbit anti-human vWF	cat number A082 1:300 dilution in PBS	Dako
Mouse monoclonal anti human PCNA	M0879 1:125 dilution in PBS	Dako
Rabbit anti-Caspase-3	ab4051 1:100 dilution in PBS	Abcam
Biotinylated goat anti-mouse IgG secondary antibody	1:200 dilution in PBS	Vector Laboratories, Peterborough, UK
Biotinylated goat anti-rabbit IgG secondary antibody	1:200 dilution in PBS	Vector Laboratories, Peterborough, UK

Appendix 12: Immunofluorescence staining

Material/Reagent	Cat.no/CAS no/Dilutions	Supplier
Dako mouse monoclonal anti-human smooth muscle actin α-SMA	M0851 (1:150 dilution) 1% BSA/ 0.5% triton/ PBS	Dako
Rabbit polyclonal anti-P2Y$_{12}$	P4871 (1:100 dilution) 1% BSA/ 0.5% triton/ PBS	Sigma
Alexa Fluor® 488 goat anti-mouse immunoglobulin G (IgG) (H+L), highly adsorbed	cat number A-11034 1% BSA/ PBS (1:200 dilution)	Thermofisher Scientific
Alexa Fluor® 594 goat anti-rabbit immunoglobulin G (IgG) (H+L)	cat number A-11037 1% BSA/ PBS (1:200 dilution)	Thermofisher Scientific
Vectashield mounting medium with DAPI	H-1200 Small drop of volume (approximate 25 µl, sufficient to cover all area)	Vector Laboratories, Peterborough, UK

Appendix 13: Western blot

Material/Reagent	Catno/CASno/Dilutions	Supplier
Mammalian Protein Extraction Reagent (M-PER)	78501	ThermoFisher Scientifc
Halt ™ Protease Inhibitor Cocktail and Halt ™ Phosphatase (100x)	1:100 dilution in MPER	Thermofisher
4X Protein sample loading buffer	928-4000,	LI-COR Biosciences, UK
NuPAGE Sample Reducing agent	NP0009	Invitrogen, UK
NuPAGE 4-12% Bis-Tris Mini gels	NP0321BOX	Invitrogen, UK
Bolt mini tank system	A25977	Invitrogen, UK
Chameleon Duo Pre-stained Protein Ladder	928-60000	LICOR
NuPAGE MOPS SDS Running buffer (20x)	NP0001	Invitrogen, UK
NuPAGE antioxidant	NP0005	Invitrogen, UK
Running buffer preparation: 500 µl of antioxidant added into 25 ml of 20x running buffer		
iBlot™ 2 Dry Blotting System	IB21001	Invitrogen, UK
Nitrocellulose membrane		
30% Odyssey Blocking Buffer: 3 ml of odyssey blocking buffer in 7 ml of PBS	927-40000	LI-COR
Universal antibody detection reagent: Quick Western Kit IRDye 680RD	926-68100	LI-COR
Stripping buffer: Reblot Plus Mild Chemicon solution 1 ml of 10X Reblot Mild Solution in 9 ml of distilled water	2502	Milipore, UK

Appendix 14: Description of healthy control cells used in cell culture experiment

Type of cell	Lot number	Age	Gendre
PASMC	419239	35	Male
PASMC	466718	57	Male
PASMC	559495	64	Male
PASMC	550178	34	Female
PASMC	407340	56	Female

8. References

Abe, K., Toba, M., Alzoubi, A., Ito, M., Fagan, K. A., Cool, C. D., … Oka, M. (2010). Formation of

plexiform lesions in experimental severe pulmonary arterial hypertension. *Circulation*,

121(25), 2747–2754. https://doi.org/10.1161/CIRCULATIONAHA.109.927681

Abele, S., Spriewald, B. M., Ramsperger-Gleixner, M., Wollin, M., Hiemann, N. E., Nieswandt, B.,

… Ensminger, S. M. (2009). Attenuation of transplant arteriosclerosis with clopidogrel is

associated with a reduction of infiltrating dendritic cells and macrophages in murine aortic

allografts. *Transplantation*, *87*(2), 207–216.

https://doi.org/10.1097/TP.0b013e3181938913

Abele, S., Weyand, M., Wollin, M., Hiemann, N. E., Harig, F., Fischlein, T., & Ensminger, S. M.

(2006). Clopidogrel reduces the development of transplant arteriosclerosis. *Journal of*

Thoracic and Cardiovascular Surgery, *131*(5), 1161–1166.

https://doi.org/10.1016/j.jtcvs.2006.01.010

Akagi, S., Nakamura, K., Matsubara, H., Fukushima Kusano, K., Kataoka, N., Oto, T., … Ito, H.

(2013). Prostaglandin I2 induces apoptosis via upregulation of Fas ligand in pulmonary

artery smooth muscle cells from patients with idiopathic pulmonary arterial hypertension.

International Journal of Cardiology, *165*(3), 499–505.

https://doi.org/10.1016/j.ijcard.2011.09.004

Al-Husseini, A., Kraskauskas, D., Mezzaroma, E., Nordio, A., Farkas, D., Drake, J. I., … Voelkel, N.

F. (2015). Vascular endothelial growth factor receptor 3 signaling contributes to

angioobliterative pulmonary hypertension. *Pulmonary Circulation*, *5*(1), 101–116.

https://doi.org/10.1086/679704

Angiolillo, D. J., & Capranzano, P. (2008). Pharmacology of emerging novel platelet inhibitors.

American Heart Journal, *156*(2 SUPPL.), 10–15. https://doi.org/10.1016/j.ahj.2008.06.004

Angiolillo, D. J., Capranzano, P., Goto, S., Aslam, M., Desai, B., Charlton, R. K., … Bass, T. A.

(2008). A randomized study assessing the impact of cilostazol on platelet function profiles

in patients with diabetes mellitus and coronary artery disease on dual antiplatelet therapy:

Results of the OPTIMUS-2 study. *European Heart Journal*, *29*(18), 2202–2211.

https://doi.org/10.1093/eurheartj/ehn287

Angiolillo, D. J., Firstenberg, M. S., Price, M. J., Tummala, P. E., Hutyra, M., Welsby, I. J., … Topol,

E. J. (2012). Bridging antiplatelet therapy with cangrelor in patients undergoing cardiac

surgery: a randomized controlled trial. *Jama*, *307*(3), 265–274.

https://doi.org/10.1001/jama.2011.2002

Arase, T., Uchida, H., Kajitani, T., Ono, M., Tamaki, K., Oda, H., … Maruyama, T. (2009). The UDP-

glucose receptor P2RY14 triggers innate mucosal immunity in the female reproductive

tract by inducing IL-8. *Journal of Immunology (Baltimore, Md. : 1950)*, *182*(11), 7074–7084.

https://doi.org/10.4049/jimmunol.0900001

Archer, S. L., Gomberg-Maitland, M., Maitland, M. L., Rich, S., Garcia, J. G. N., & Weir, E. K.

(2008). Mitochondrial metabolism, redox signaling, and fusion: A mitochondria-ROS-HIF-

1α-Kv1.5 O2-sensing pathway at the intersection of pulmonary hypertension and cancer.

American Journal of Physiology - Heart and Circulatory Physiology, *294*(2), 570–578.

https://doi.org/10.1152/ajpheart.01324.2007

Archer, S. L., Marsboom, G., Kim, G. H., Zhang, H. J., Toth, P. T., Svensson, E. C., … Rehman, J.

(2010). Epigenetic attenuation of mitochondrial superoxide dismutase 2 in pulmonary

arterial hypertension: A basis for excessive cell proliferation and a new therapeutic target.

Circulation, *121*(24), 2661–2671. https://doi.org/10.1161/CIRCULATIONAHA.109.916098

Asaki, T., Kuwano, K., Morrison, K., Gatfield, J., Hamamoto, T., & Clozel, M. (2015). Selexipag: An

Oral and Selective IP Prostacyclin Receptor Agonist for the Treatment of Pulmonary Arterial Hypertension. *Journal of Medicinal Chemistry*, *58*(18), 7128–7137. https://doi.org/10.1021/acs.jmedchem.5b00698

Bagchi, S., Liao, Z., Gonzalez, F. a., Chorna, N. E., Seye, C. I., Weisman, G. a., & Erb, L. (2005). The P2Y2 nucleotide receptor interacts with alphav integrins to activate Go and induce cell migration. *Journal of Biological Chemistry*, *280*(47), 39050–39057. https://doi.org/10.1074/jbc.M504819200

Bar, I., Guns, P., Metallo, J., & Cammarata, D. (2008). Knockout mice reveal a role for P2Y6 receptor in macrophages, endothelial cells, and vascular smooth muscle cells. *Molecular Pharmacology*, *74*(3), 777–784. https://doi.org/10.1124/mol.108.046904.their

Bassil, A. K., Bourdu, S., Townson, K. a, Wheeldon, A., Jarvie, E. M., Zebda, N., … Moore, G. B. T. (2009). UDP-glucose modulates gastric function through P2Y 14 receptor-dependent and -independent mechanisms. *American Journal of Physiology - Gastrointestinal and Liver Physiology*, *296*, 923–930. https://doi.org/10.1152/ajpgi.90363.2008.

Ben Addi, A., Cammarata, D., Conley, P. B., Boeynaems, J.-M., & Robaye, B. (2010). Role of the P2Y12 receptor in the modulation of murine dendritic cell function by ADP. *The Journal of Immunology*, *185*(10), 5900–5906. https://doi.org/10.4049/jimmunol.0901799

Benza, R. L., Miller, D. P., & Barst, R. J. (2012). An Evaluation of Long-term Survival From Time of Diagnosis in Pulmonary Arterial Hypertension From the REVEAL Registry. *CHEST*, *142*(2), 448–456. https://doi.org/10.1378/chest.11-1460

Bhatt, D. L., Stone, G. W., Mahaffey, K. W., Gibson, C. M., Steg, P. G., Hamm, C. W., … Harrington, R. A. (2013). Effect of Platelet Inhibition with Cangrelor during PCI on Ischemic Events. *New England Journal of Medicine*, *368*(14), 1303–1313. https://doi.org/10.1056/NEJMoa1300815

Biver, G., Wang, N., Gartland, a, Orriss, I., Arnett, T. R., Boeynaems, J. M., & Robaye, B. (2013).

    Role of the P2Y receptor in the differentiation of bone marrow stromal cells into

    osteoblasts and adipocytes. *Stem Cells*, 2747–2758. https://doi.org/10.1002/stem.1411

Bonnet, S., Michelakis, E. D., Porter, C. J., Andrade-Navarro, M. A., Thébaud, B., Bonnet, S., …

    Archer, S. L. (2006). An Abnormal mitochondrial-hypoxia inducible factor-1α-Kv channel

    pathway disrupts oxygen sensing and triggers pulmonary arterial hypertension in fawn

    hooded rats: Similarities to human pulmonary arterial hypertension. *Circulation*, *113*(22),

    2630–2641. https://doi.org/10.1161/CIRCULATIONAHA.105.609008

Bouallegue, A., Bou Daou, G., & Srivastava, A. (2007). Endothelin-1-Induced Signaling Pathways

    in Vascular Smooth Muscle Cells. *Current Vascular Pharmacology*, *5*(1), 45–52.

    https://doi.org/10.2174/157016107779317161

Britain, G. (2019). NAPH 10 th Annual Report National Audit of Pulmonary Hypertension Tenth

    Annual Report Introduction : Foreword, (October).

Butt, E., Abel, K., Krieger, M., Palm, D., Hoppe, V., Hoppe, J., & Walter, U. (1994). cAMP- and

    cGMP-dependent protein kinase phosphorylation sites of the focal adhesion vasodilator-

    stimulated phosphoprotein (VASP) in vitro and in intact human platelets. *Journal of*

    Biological Chemistry, *269*(20), 14509–14517.

Campo, G., Sega, F. V. D., Pavasini, R., Aquila, G., Gallo, F., Fortini, F., … Ferrari, R. (2017).

    Biological effects of ticagrelor over clopidogrel in patients with stable coronary artery

    disease and chronic obstructive pulmonary disease. *Thrombosis and Haemostasis*, *117*(6),

    1–10. https://doi.org/10.1160/TH16-12-0973

Cattaneo, M. (2015). P2Y $_{12}$ receptors: structure and function. *Journal of Thrombosis and*

    Haemostasis, *13*, S10–S16. https://doi.org/10.1111/jth.12952

Cattaneo, M, Lecchi, a, Randi, a M., McGregor, J. L., & Mannucci, P. M. (1992). Identification of

a new congenital defect of platelet function characterized by severe impairment of platelet responses to adenosine diphosphate. *Blood*, *80*(11), 2787–2796. Retrieved from http://www.ncbi.nlm.nih.gov/pubmed/1333302

Cattaneo, Marco. (2011). The platelet P2Y$_{12}$ receptor for adenosine diphosphate: congenital and drug-induced defects. *Blood*, *117*(7), 2102–2112. https://doi.org/10.1182/blood-2010-08-263111

Chazova, I., Loyd, J. E., Zhdanov, V. S., Newman, J. H., Belenkov, Y., & Meyrick, B. (1995). Pulmonary artery adventitial changes and venous involvement in primary pulmonary hypertension. *The American Journal of Pathology*, *146*(2), 389–397. Retrieved from http://www.pubmedcentral.nih.gov/articlerender.fcgi?artid=1869854&tool=pmcentrez&rendertype=abstract

Clapp, L. H., Finney, P., Turcato, S., Tran, S., Rubin, L. J., & Tinker, A. (2001). Differential effects of stable prostacyclin analogues on smooth muscle cell proliferation and cyclic AMP generation in human pulmonary artery. *American Journal of Respiratory Cell and Molecular Biology*, *In Press*(.).

Czajkowski, R., Banachewicz, W., Ilnytska, O., Drobot, L. B., & Baranska, J. (2004). Differential effects of P2Y1 and P2Y12 nucleotide receptors on ERK1/ERK2 and phosphatidylinositol 3-kinase signalling and cell proliferation in serum-deprived and nonstarved glioma C6 cells. *British Journal of Pharmacology*, *141*(3), 497–507. https://doi.org/10.1038/sj.bjp.0705639

Dangelmaier, C., Jin, J., Smith, J. B., & Kunapuli, S. P. (2001). Potentiation of thromboxane A2-induced platelet secretion by Gi signaling through the phosphoinositide-3 kinase pathway. *Thrombosis and Haemostasis*, *85*(2), 341–348. https://doi.org/01020341 [pii]

Daniel, J. L., Dangelmaier, C., Jin, J., Ashby, B., Smith, J. B., & Kunapuli, S. (1998). Molecular basis for ADP-induced platelet activation. I. Evidence for three distinct receptors on human

platelets. *J Biol.Chem.*, *273*(4), 2024–2029.

Das, M., Burns, N., Wilson, S. J., Zawada, W. M., & Stenmark, K. R. (2008). Hypoxia exposure

induces the emergence of fibroblasts lacking replication repressor signals of PKCζ in the

pulmonary artery adventitia. *Cardiovascular Research*, *78*(3), 440–448.

https://doi.org/10.1093/cvr/cvn014

Defawe, O. D., Kim, S., Chen, L., Huang, D., Kenagy, R. D., Renné, T., … Clowes, A. W. (2010).

VASP phosphorylation at serine239 regulates the effects of NO on smooth muscle cell

invasion and contraction of collagen. *Journal of Cellular Physiology*, *222*(1), 230–237.

https://doi.org/10.1002/jcp.21942

Denslow, A., Świtalska, M., Jarosz, J., Papiernik, D., Porshneva, K., Nowak, M., & Wietrzyk, J.

(2017). *Clopidogrel in a combined therapy with anticancer drugs—effect on tumor growth,*

metastasis, and treatment toxicity: Studies in animal models. *PLoS ONE* (Vol. 12).

https://doi.org/10.1371/journal.pone.0188740

Diehl, P., Olivier, C., Haischeid, C., Helbing, T., Bode, C., & Moser, M. (2010). Clopidogrel affects

leukocyte dependent platelet aggregation by P2Y 12 expressing leukocytes. *Basic Research*

in Cardiology, *105*(3), 379–387. https://doi.org/10.1007/s00395-009-0073-8

Eckl, S., Heim, C., Abele-Ohl, S., Hoffmann, J., Ramsperger-Gleixner, M., Weyand, M., &

Ensminger, S. M. (2010). Combination of clopidogrel and everolimus dramatically reduced

the development of transplant arteriosclerosis in murine aortic allografts. *Transplant*

International, *23*(9), 959–966. https://doi.org/10.1111/j.1432-2277.2010.01072.x

El Kasmi, K. C., Pugliese, S. C., Riddle, S. R., Poth, J. M., Anderson, A. L., Frid, M. G., … Stenmark,

K. R. (2014). Adventitial Fibroblasts Induce a Distinct Proinflammatory/Profibrotic

Macrophage Phenotype in Pulmonary Hypertension. *The Journal of Immunology*, *193*(2),

597–609. https://doi.org/10.4049/jimmunol.1303048

Evans, D. J. W., Jackman, L. E., Chamberlain, J., Crosdale, D. J., Judge, H. M., Jetha, K., … Storey, R. F. (2009). Platelet P2Y12 Receptor Influences the Vessel Wall Response to Arterial Injury and Thrombosis. *Circulation*, *119*(1), 116–122. https://doi.org/10.1161/CIRCULATIONAHA.107.762690

Fan, Z., Chen, Y., & Liu, H. (2015). Calcium channel blockers for pulmonary arterial hypertension. *Cochrane Database of Systematic Reviews*, *2015*(9). https://doi.org/10.1002/14651858.CD010066.pub2

Fernandez, R. A., Wan, J., Song, S., Smith, K. A., Gu, Y., Tauseef, M., … Yuan, J. X. J. (2015). Upregulated expression of STIM2, TRPC6, and orai2 contributes to the transition of pulmonary arterial smooth muscle cells from a contractile to proliferative phenotype. *American Journal of Physiology - Cell Physiology*, *308*(8), C581–C593. https://doi.org/10.1152/ajpcell.00202.2014

Fessel, J. P., Hamid, R., Wittmann, B. M., Robinson, L. J., Blackwell, T., Tada, Y., … West, J. D. (2012). Metabolomic analysis of bone morphogenetic protein receptor type 2 mutations in human pulmonary endothelium reveals widespread metabolic reprogramming. *Pulmonary Circulation*, *2*(2), 201–213. https://doi.org/10.4103/2045-8932.97606

Fijalkowska, I., Xu, W., Comhair, S. A. A., Janocha, A. J., Mavrakis, L. A., Krishnamachary, B., … Tuder, R. M. (2010). Hypoxia inducible-factor1alpha regulates the metabolic shift of pulmonary hypertensive endothelial cells. *The American Journal of Pathology*, *176*(3), 1130–1138. https://doi.org/10.2353/ajpath.2010.090832

Foster, C. J., Prosser, D. M., Agans, J. M., Zhai, Y., Smith, M. D., Lachowicz, J. E., … Chintala, M. S. (2001). Molecular identification and characterization of the platelet ADP receptor targeted by thienopyridine antithrombotic drugs. *Journal of Clinical Investigation*, *107*(12), 1591–1598. https://doi.org/10.1172/JCI12242

Geiger, J., Brich, J., Hönig-Liedl, P., Eigenthaler, M., Schanzenbächer, P., Herbert, J. M., & Walter, U. (1999). Specific impairment of human platelet P2Y(AC) ADP receptor-mediated signaling by the antiplatelet drug clopidogrel. *Arteriosclerosis, Thrombosis, and Vascular Biology*, *19*(8), 2007–2011. https://doi.org/10.1161/01.ATV.19.8.2007

Ghofrani, H. A., Pepke-Zaba, J., Barbera, J. A., Channick, R., Keogh, A. M., Gomez-Sanchez, M. A., … Grimminger, F. (2004). Nitric oxide pathway and phosphodiesterase inhibitors in pulmonary arterial hypertension. *Journal of the American College of Cardiology*, *43*(12 SUPPL.). https://doi.org/10.1016/j.jacc.2004.02.031

Giachini, F. R., Leite, R., Osmond, D. A., Lima, V. V., Inscho, E. W., Webb, R. C., & Tostes, R. C. (2014). Anti-platelet therapy with clopidogrel prevents endothelial dysfunction and vascular remodeling in aortas from hypertensive rats. *PLoS ONE*, *9*(3), 1–8. https://doi.org/10.1371/journal.pone.0091890

Glenn, J. R., Dovlatova, N., White, A. E., Dhillon, K., Heptinstall, S., & Fox, S. C. (2013). "VASPFix" for measurement of VASP phosphorylation in platelets and for monitoring effects of P2Y12 antagonists. *Thrombosis and Haemostasis*, *111*(3), 539–548. https://doi.org/10.1160/TH13-07-0581

Gomberg-Maitland, M., Dufton, C., Oudiz, R. J., & Benza, R. L. (2011). Compelling evidence of long-term outcomes in pulmonary arterial hypertension?: A clinical perspective. *Journal of the American College of Cardiology*, *57*(9), 1053–1061. https://doi.org/10.1016/j.jacc.2010.11.020

Gräf, S., Haimel, M., Bleda, M., Hadinnapola, C., Southgate, L., Li, W., … Morrell, N. W. (2018). Identification of rare sequence variation underlying heritable pulmonary arterial hypertension. *Nature Communications*, *9*(1). https://doi.org/10.1038/s41467-018-03672-4

Grignola, J. C. (2011). Hemodynamic assessment of pulmonary hypertension. *World Journal of*

Cardiology, *3*(1), 10–17. https://doi.org/10.4330/wjc.v3.i1.10

Grobben, B., Claes, P., Van Kolen, K., Roymans, D., Fransen, P., Sys, S. U., & Slegers, H. (2001).
Agonists of the P2Y(AC)-receptor activate MAP kinase by a ras-independent pathway in rat
C6 glioma. *Journal of Neurochemistry*, *78*(6), 1325–1338. Retrieved from
http://www.ncbi.nlm.nih.gov/pubmed/11579141

Grzesk, G., Kozinski, M., Tantry, U. S., Wicinski, M., Fabiszak, T., Navarese, E. P., … Kubica, J.
(2013). High-Dose, but Not Low-Dose, Aspirin Impairs Anticontractile Effect of Ticagrelor
following ADP Stimulation in Rat Tail Artery Smooth Muscle Cells. *BioMed Research
International*, *2013*, 928271. https://doi.org/10.1155/2013/928271

Gündüz, D., Tanislav, C., Schlute, K. D., Schulz, R., Hamm, C., & Aslam, M. (2017). Effect of
ticagrelor on endothelial calcium signalling and barrier function. *Thrombosis and
Haemostasis*, *117*(2), 371–381. https://doi.org/10.1160/TH16-04-0273

Hagen, M., Fagan, K., Steudel, W., Carr, M., Lane, K., Rodman, D. M., & West, J. (2007).
Interaction of interleukin-6 and the BMP pathway in pulmonary smooth muscle. *American
Journal of Physiology. Lung Cellular and Molecular Physiology*, *292*(6), L1473–L1479.
https://doi.org/10.1152/ajplung.00197.2006

Harada, K., Matsumoto, Y., & Umemura, K. (2011). Adenosine diphosphate receptor P2Y 12-
mediated migration of host smooth muscle-like cells and leukocytes in the development of
transplant arteriosclerosis. *Transplantation*, *92*(2), 148–154.
https://doi.org/10.1097/TP.0b013e318221d407

Hardy, A. R., Jones, M. L., Mundell, S. J., & Poole, A. W. (2004). Reciprocal cross-talk between
P2Y 1 and P2Y 12 receptors at the level of calcium signaling in human platelets. *Blood*,
104(6), 1745–1752. https://doi.org/10.1182/blood-2004-02-0534.Supported

Haynes, S. E., Hollopeter, G., Yang, G., Kurpius, D., Dailey, M. E., Gan, W.-B., & Julius, D. (2006).

The P2Y12 receptor regulates microglial activation by extracellular nucleotides. *Nature Neuroscience*, *9*(12), 1512–1519. https://doi.org/10.1038/nn1805

Hill, N. S., Gillespie, M. N., & McMurtry, I. F. (2017). Fifty Years of Monocrotaline-Induced Pulmonary Hypertension: What Has It Meant to the Field? *Chest*, *152*(6), 1106–1108. https://doi.org/10.1016/j.chest.2017.10.007

Högberg, C., Svensson, H., Gustafsson, R., Eyjolfsson, A., & Erlinge, D. (2010). The reversible oral P2Y 12 antagonist AZD6140 inhibits ADP-induced contractions in murine and human vasculature. *International Journal of Cardiology*, *142*(2), 187–192. https://doi.org/10.1016/j.ijcard.2008.12.091

Hollopeter, G., Jantzen, H. M., Vincent, D., Li, G., England, L., Ramakrishnan, V., … Conley, P. B. (2001). Identification of the platelet ADP receptor targeted by antithrombotic drugs. *Nature*, *409*(6817), 202-7. https://doi.org/10.1038/35051599

Honda, S., Sasaki, Y., Ohsawa, K., Imai, Y., Nakamura, Y., Inoue, K., & Kohsaka, S. (2001). Extracellular ATP or ADP induce chemotaxis of cultured microglia through Gi/o-coupled P2Y receptors. *Journal of Neuroscience*, *21*(6), 1975–1982. https://doi.org/10.1523/jneurosci.21-06-01975.2001

Humbert, M., Morrell, N. W., Archer, S. L., Stenmark, K. R., MacLean, M. R., Lang, I. M., … Rabinovitch, M. (2004). Cellular and molecular pathobiology of pulmonary arterial hypertension. *Journal of the American College of Cardiology*, *43*(12 SUPPL.), S13–S24. https://doi.org/10.1016/j.jacc.2004.02.029

Humbert, M., Sitbon, O., Chaouat, A., Bertocchi, M., Habib, G., Gressin, V., … Simonneau, G. (2006). Pulmonary Arterial Hypertension in France. *American Journal of Respiratory and Critical Care Medicine*, *173*(9), 1023–1030. https://doi.org/10.1164/rccm.200510-1668OC

Humbert, M., Sitbon, O., & Simonneau, G. (2004). Treatment of pulmonary arterial

hypertension. *The New England Journal of Medicine*, *351*, 1425–1436.

https://doi.org/10.1056/NEJMra040291

Itoh, T., Nagaya, N., Ishibashi-Ueda, H., Kyotani, S., Oya, H., Sakamaki, F., … Nakanishi, N.

(2006). Increased plasma monocyte chemoattractant protein-1 level in idiopathic

pulmonary arterial hypertension. *Respirology (Carlton, Vic.)*, *11*, 158–163.

https://doi.org/10.1111/j.1440-1843.2006.00821.x

Izikki, M., Guignabert, C., Fadel, E., Humbert, M., Tu, L., Zadigue, P., … Eddahibi, S. (2009).

Endothelial-derived FGF2 contributes to the progression of pulmonary hypertension in

humans and rodents. *Journal of Clinical Investigation*, *119*(3), 512–523.

https://doi.org/10.1172/JCI35070

Jonigk, D., Golpon, H., Bockmeyer, C. L., Maegel, L., Hoeper, M. M., Gottlieb, J., … Laenger, F.

(2011). Plexiform lesions in pulmonary arterial hypertension: Composition, architecture,

and microenvironment. *American Journal of Pathology*, *179*(1), 167–179.

https://doi.org/10.1016/j.ajpath.2011.03.040

Judge, H. M., Buckland, R. J., Sugidachi, A., Jakubowski, J. A., & Storey, R. F. (2008). The active

metabolite of prasugrel effectively blocks the platelet P2Y12 receptor and inhibits

procoagulant and pro-inflammatory platelet responses. *Platelets.*, *19*(2), 125–133.

https://doi.org/10.1080/09537100701694144

Kauffenstein, G., Bergmeier, W., Eckly, a, Ohlmann, P., Léon, C., Cazenave, J. P., … Gachet, C.

(2001). The P2Y(12) receptor induces platelet aggregation through weak activation of the

alpha(IIb)beta(3) integrin--a phosphoinositide 3-kinase-dependent mechanism. *FEBS

Letters*, *505*(2), 281–290. https://doi.org/S0014-5793(01)02824-1 [pii]

Kaufmann, A., Musset, B., Limberg, S. H., Renigunta, V., Sus, R., Dalpke, A. H., … Hanley, P. J.

(2005). "Host tissue damage" signal ATP promotes non-directional migration and

negatively regulates toll-like receptor signaling in human monocytes. *The Journal of Biological Chemistry*, *280*(37), 32459–32467. https://doi.org/10.1074/jbc.M505301200

Kim, J. W., Tchernyshyov, I., Semenza, G. L., & Dang, C. V. (2006). HIF-1-mediated expression of pyruvate dehydrogenase kinase: A metabolic switch required for cellular adaptation to hypoxia. *Cell Metabolism*, *3*(3), 177–185. https://doi.org/10.1016/j.cmet.2006.02.002

Kolen, K., & Slegers, H. (2006). Integration of P2Y receptor-activated signal transduction pathways in G protein-dependent signalling networks. *Purinergic Signalling*, *2*(3), 451–469. https://doi.org/10.1007/s11302-006-9008-0

Korybalska, K., Rutkowski, R., Luczak, J., Czepulis, N., Karpinski, K., & Witowski, J. (2018). The role of purinergic P2Y 12 receptor blockers on the angiogenic properties of endothelial cells: An in vitro study. *Journal of Physiology and Pharmacology*, *69*(4), 1–14. https://doi.org/10.26402/jpp.2018.4.06

Kylhammar, D., Bune, L. T., & Rådegran, G. (2014). P2Y1 and P2Y12 receptors in hypoxia- and adenosine diphosphate-induced pulmonary vasoconstriction in vivo in the pig. *European Journal of Applied Physiology*, 1995–2006. https://doi.org/10.1007/s00421-014-2921-y

Lawrie, A., Hameed, A. G., Chamberlain, J., Arnold, N., Kennerley, A., Hopkinson, K., … Francis, S. E. (2011). Paigen diet-fed apolipoprotein E knockout mice develop severe pulmonary hypertension in an interleukin-1-dependent manner. *The American Journal of Pathology*, *179*(4), 1693–1705. https://doi.org/10.1016/j.ajpath.2011.06.037

Léon, C., Hechler, B., Freund, M., Eckly, A., Vial, C., Ohlmann, P., … Gachet, C. (1999). Defective platelet aggregation and increased resistance to thrombosis in purinergic P2Y1 receptor-null mice. *Journal of Clinical Investigation*, *104*(12), 1731–1737. https://doi.org/10.1172/JCI8399

Li, B. B., Jiang, Z., Sheng, J. Y., & Yao, K. (2011). Sildenafil potentiates the proliferative effect of

porcine pulmonary artery smooth muscle cells induced by serotonin in vitro. *Chinese Medical Journal*, *124*(17), 2733–2740. https://doi.org/10.3760/cma.j.issn.0366-6999.2011.17.030

Li, M., Riddle, S. R., Frid, M. G., Kasmi, K. C. El, Mckinsey, T. A., Sokol, R. J., … Anwar, A. (2012). Emergence of Fibroblasts With a Proinflammatory, *187*(5), 2711–2722. https://doi.org/10.4049/jimmunol.1100479.EMERGENCE

Liao, Z., Seye, C. I., Weisman, G. a, & Erb, L. (2007). The P2Y2 nucleotide receptor requires interaction with alpha v integrins to access and activate G12. *Journal of Cell Science*, *120*(Pt 9), 1654–1662. https://doi.org/10.1242/jcs.03441

Lichtenstein, L., Serhan, N., Espinosa-Delgado, S., Fabre, A., Annema, W., Tietge, U. J. F., … Martinez, L. O. (2015). Increased atherosclerosis in P2Y13/apolipoprotein E double-knockout mice: contribution of P2Y13 to reverse cholesterol transport. *Cardiovascular Research*, *106*(2), 314–323. https://doi.org/10.1093/cvr/cvv109

Liu, Y., Gao, X. M., Fang, L., Jennings, N. L., Su, Y., Xu, Q., … Du, X. J. (2011). Novel role of platelets in mediating inflammatory responses and ventricular rupture or remodeling following myocardial infarction. *Arteriosclerosis, Thrombosis, and Vascular Biology*, *31*(4), 834–841. https://doi.org/10.1161/ATVBAHA.110.220467

Luna, R. C. P., De Oliveira, Y., Lisboa, J. V. C., Chaves, T. R., De Araújo, T. A. M., De Sousa, E. E., … De Brito Alves, J. L. (2018). Insights on the epigenetic mechanisms underlying pulmonary arterial hypertension. *Brazilian Journal of Medical and Biological Research*, *51*(12), 1–12. https://doi.org/10.1590/1414-431X20187437

Ma, L., Roman-Campos, D., Austin, E. D., Eyries, M., Sampson, K. S., Soubrier, F., … Chung, W. K. (2013). A Novel Channelopathy in Pulmonary Arterial Hypertension. *New England Journal of Medicine*, *369*(4), 351–361. https://doi.org/10.1056/NEJMoa1211097

Marcus, D. C., Liu, J., Lee, J. H., Scherer, E. Q., Scofield, M. a, & Wangemann, P. (2005). Apical

   membrane P2Y4 purinergic receptor controls K+ secretion by strial marginal cell

   epithelium. *Cell Communication and Signaling : CCS*, *3*, 13. https://doi.org/10.1186/1478-

   811X-3-13

Masyuk, A. I., Gradilone, S. a, Banales, J. M., Huang, B. Q., Masyuk, T. V, Lee, S.-O., … Larusso, N.

   F. (2008). Cholangiocyte primary cilia are chemosensory organelles that detect biliary

   nucleotides via P2Y12 purinergic receptors. *American Journal of Physiology.*

   Gastrointestinal and Liver Physiology, *295*(507), G725–G734.

   https://doi.org/10.1152/ajpgi.90265.2008

Meister, J., Le Duc, D., Ricken, A., Burkhardt, R., Thiery, J., Pfannkuche, H., … Schulz, A. (2014).

   The G Protein-coupled Receptor P2Y14 Influences Insulin Release and Smooth Muscle

   Function in Mice. *The Journal of Biological Chemistry*, *289*(34), 0–27.

   https://doi.org/10.1074/jbc.M114.580803

Mitchell, C., Syed, N. -i.-H., Tengah, A., Gurney, A. M., & Kennedy, C. (2012). Identification of

   Contractile P2Y1, P2Y6, and P2Y12 Receptors in Rat Intrapulmonary Artery Using Selective

   Ligands. *Journal of Pharmacology and Experimental Therapeutics*, *343*(3), 755–762.

   https://doi.org/10.1124/jpet.112.198051

Montani, D., Günther, S., Dorfmüller, P., Perros, F., Girerd, B., Garcia, G., … Sitbon, O. (2013).

   Pulmonary arterial hypertension. *Orphanet Journal of Rare Diseases*, *8*(1), 97.

   https://doi.org/10.1186/1750-1172-8-97

Mülsch, A., Oelze, M., Klöss, S., Mollnau, H., Töpfer, A., Smolenski, A., … Münzel, T. (2001).

   Effects of in vivo nitroglycerin treatment on activity and expression of the guanylyl cyclase

   and cGMP-dependent protein kinase and their downstream target vasodilator-stimulated

   phosphoprotein in aorta. *Circulation*, *103*(17), 2188–2194.

https://doi.org/10.1161/01.CIR.103.17.2188

Murray, F., Patel, H. H., Suda, R. Y. S., Zhang, S., Thistlethwaite, P. A., Yuan, J. X. J., & Insel, P. A. (2007). Expression and activity of cAMP phosphodiesterase isoforms in pulmonary artery smooth muscle cells from patients with pulmonary hypertension: Role for PDE1. *American Journal of Physiology - Lung Cellular and Molecular Physiology*, *292*(1), 294–303. https://doi.org/10.1152/ajplung.00190.2006

Naeije, R. (2013). Physiology of the pulmonary circulation and the right heart. *Current Hypertension Reports*, *15*(6), 623–631. https://doi.org/10.1007/s11906-013-0396-6

Nickel, N. P., Spiekerkoetter, E., Gu, M., Li, C. G., Li, H., Kaschwich, M., … Rabinovitch, M. (2015). Elafin reverses pulmonary hypertension via caveolin-1-dependent bone morphogenetic protein signaling. *American Journal of Respiratory and Critical Care Medicine*, *191*(11), 1273–1286. https://doi.org/10.1164/rccm.201412-2291OC

Niu, Xiaomei, Nouraie, M., Campbell, A., Rana, S., Minniti, C. P., Sable, C., … Gordeuk, V. R. (2009). Angiogenic and inflammatory markers of cardiopulmonary changes in children and adolescents with sickle cell disease. *PloS One*, *4*(11), e7956. https://doi.org/10.1371/journal.pone.0007956

Niu, Xuan, Pi, S. L., Baral, S., Xia, Y. P., He, Q. W., Li, Y. N., … Hu, B. (2017). P2Y12 Promotes Migration of Vascular Smooth Muscle Cells Through Cofilin Dephosphorylation during Atherogenesis. *Arteriosclerosis, Thrombosis, and Vascular Biology*, *37*(3), 515–524. https://doi.org/10.1161/ATVBAHA.116.308725

Nozik-Grayck, E., Woods, C., Stearman, R. S., Venkataraman, S., Ferguson, B. S., Swain, K., … Domann, F. E. (2016). Histone deacetylation contributes to low extracellular superoxide dismutase expression in human idiopathic pulmonary arterial hypertension. *American Journal of Physiology - Lung Cellular and Molecular Physiology*, *311*(1), L124–L134.

https://doi.org/10.1152/ajplung.00263.2015

Ntelis, K., Gkizas, V., Filippopoulou, A., Davlouros, P., Alexopoulos, D., Andonopoulos, A. P., & Daoussis, D. (2016). Clopidogrel treatment may associate with worsening of endothelial function and development of new digital ulcers in patients with systemic sclerosis : results from an open label , proof of concept study. *BMC Musculoskeletal Disorders*, 1–8. https://doi.org/10.1186/s12891-016-1072-1

O'Brien, K. A., Gartner, T. K., Hay, N., & Du, X. (2012). ADP-Stimulated Activation of Akt During Integrin Outside-In Signaling Promotes Platelet Spreading by Inhibiting Glycogen Synthase Kinase-3 . *Arteriosclerosis, Thrombosis, and Vascular Biology*, *32*(9), 2232–2240. https://doi.org/10.1161/ATVBAHA.112.254680

Oelze, M., Mollnau, H., Hoffmann, N., Warnholtz, A., Bodenschatz, M., Smolenski, A., … Münzel, T. (2000). Vasodilator-stimulated phosphoprotein serine 239 phosphorylation as a sensitive monitor of defective nitric oxide/cGMP signaling and endothelial dysfunction. *Circulation Research*, *87*(11), 999–1005. https://doi.org/10.1161/01.RES.87.11.999

Ohsawa, K., Irino, Y., Sanagi, T., Nakamura, Y., Suzuki, E., Inoue, K., & Kohsaka, S. (2010). P2Y $_{12}$ receptor-mediated integrin-β1 activation regulates microglial process extension induced by ATP. *Glia*, *801*(December 2009), NA-NA. https://doi.org/10.1002/glia.20963

Orriss, I. R., Wang, N., Burnstock, G., Arnett, T. R., Gartland, A., Robaye, B., & Boeynaems, J.-M. (2011). The P2Y(6) receptor stimulates bone resorption by osteoclasts. *Endocrinology*, *152*(10), 3706–3716. https://doi.org/10.1210/en.2011-1073

Patti, G., Colonna, G., Pasceri, V., Pepe, L. L., Montinaro, A., & Di Sciascio, G. (2005). Randomized trial of high loading dose of clopidogrel for reduction of periprocedural myocardial infarction in patients undergoing coronary intervention: Results from the ARMYDA-2 (Antiplatelet therapy for Reduction of MYocardial Damage during Angioplasty).

Circulation, *111*(16), 2099–2106. https://doi.org/10.1161/01.CIR.0000161383.06692.D4

Paul, B. Z. S., Jin, J., & Kunapuli, S. P. (1999). Molecular Mechanism of Thromboxane A 2 induced Platelet Aggregation. *Journal of Biological Chemistry*, *274*(41), 29108–29114.

Paulin, R., Courboulin, A., Meloche, J., Mainguy, V., Dumas De La Roque, E., Saksouk, N., … Bonnet, S. (2011). Signal transducers and activators of transcription-3/Pim1 Axis plays a critical role in the pathogenesis of human pulmonary arterial hypertension. *Circulation*, *123*(11), 1205–1215. https://doi.org/10.1161/CIRCULATIONAHA.110.963314

Perros, F., Montani, D., Dorfmüller, P., Durand-Gasselin, I., Tcherakian, C., Le Pavec, J., … Humbert, M. (2008). Platelet-derived growth factor expression and function in idiopathic pulmonary arterial hypertension. *American Journal of Respiratory and Critical Care Medicine*, *178*(1), 81–88. https://doi.org/10.1164/rccm.200707-1037OC

Pfarr, N., Fischer, C., Ehlken, N., Becker-Grünig, T., López-González, V., Gorenflo, M., … Grünig, E. (2013). Hemodynamic and genetic analysis in children with idiopathic, heritable, and congenital heart disease associated pulmonary arterial hypertension. *Respiratory Research*, *14*(1). https://doi.org/10.1186/1465-9921-14-3

Pickworth, J., Rothman, A., Iremonger, J., Casbolt, H., Hopkinson, K., Hickey, P. M., … Lawrie, A. (2017). Differential IL-1 signaling induced by BMPR2 deficiency drives pulmonary vascular remodeling. *Pulmonary Circulation*, *7*(4), 768–776. https://doi.org/10.1177/2045893217729096

Pokreisz, P., Marsboom, G., & Janssens, S. (2007). Pressure overload-induced right ventricular dysfunction and remodelling in experimental pulmonary hypertension: The right heart revisited. *European Heart Journal, Supplement*, *9*(H). https://doi.org/10.1093/eurheartj/sum021

Pozios, K. C., Ding, J., Degger, B., Upton, Z., & Duan, C. (2001). IGFs stimulate zebrafish cell

proliferation by activating MAP kinase and PI3-kinase-signaling pathways. *American Journal of Physiology Regulatory, Integrative and Comparative Physiology*, *280*(4), R1230-9. Retrieved from http://ajpregu.physiology.org/content/ajpregu/280/4/R1230.full.pdf

Price, M. J., Berger, P. B., Teirstein, P. S., Tanguay, J. F., Angiolillo, D. J., Spriggs, D., … Topol, E. J. (2011). Standard- vs high-dose clopidogrel based on platelet function testing after percutaneous coronary intervention: The GRAVITAS randomized trial. *JAMA - Journal of the American Medical Association*, *305*(11), 1097–1105. https://doi.org/10.1001/jama.2011.290

Qian, J., Tian, W., Jiang, X., Tamosiuniene, R., Sung, Y. K., Shuffle, E. M., … Nicolls, M. R. (2015). Leukotriene B4 Activates Pulmonary Artery Adventitial Fibroblasts in Pulmonary Hypertension. *Hypertension*, *66*(6), 1227–1239. https://doi.org/10.1161/HYPERTENSIONAHA.115.06370

Qiao, F., Zou, Z., Liu, C., Zhu, X., Wang, X., Yang, C., … Chen, Y. (2016). ROCK2 mediates the proliferation of pulmonary arterial endothelial cells induced by hypoxia in the development of pulmonary arterial hypertension. *Experimental and Therapeutic Medicine*, *11*(6), 2567–2572. https://doi.org/10.3892/etm.2016.3214

Quinton, T M, Murugappan, S., Kim, S., Jin, J., & Kunapuli, S. P. (2004). Different G protein-coupled signaling pathways are involved in alpha granule release from human platelets. *Journal of Thrombosis and Haemostasis : JTH*, *2*(6), 978–984. https://doi.org/10.1111/j.1538-7836.2004.00741.x

Quinton, Todd M, Kim, S., Dangelmaier, C., Dorsam, R. T., Jin, J., Daniel, J. L., & Kunapuli, S. P. (2002). Protein kinase C- and calcium-regulated pathways independently synergize with Gi pathways in agonist-induced fibrinogen receptor activation. *The Biochemical Journal*, *368*(Pt 2), 535–543. https://doi.org/10.1042/BJ20020226

Rabinovitch, M. (2008). Molecular pathogenesis of pulmonary arterial hypertension. *Journal of Clinical Investigation*, *118*(7), 2372–2379. https://doi.org/10.1172/JCI33452.2372

Ranchoux, B., Antigny, F., Rucker-Martin, C., Hautefort, A., Péchoux, C., Bogaard, H. J., … Perros, F. (2015). Endothelial-to-mesenchymal transition in pulmonary hypertension. *Circulation*, *131*(11), 1006–1018. https://doi.org/10.1161/CIRCULATIONAHA.114.008750

Rauch, B. H., Rosenkranz, A. C., Ermler, S., Böhm, A., Driessen, J., Fischer, J. W., … Schrör, K. (2010). Regulation of functionally active P2Y12 ADP receptors by thrombin in human smooth muscle cells and the presence of P2Y12 in carotid artery lesions. *Arteriosclerosis, Thrombosis, and Vascular Biology*, *30*, 2434–2442. https://doi.org/10.1161/ATVBAHA.110.213702

Remijn, J. A., Wu, Y. P., Jeninga, E. H., IJsseldijk, M. J. W., Van Willigen, G., De Groot, P. G., … Nurden, P. (2002). Role of ADP receptor P2Y12 in platelet adhesion and thrombus formation in flowing blood. *Arteriosclerosis, Thrombosis, and Vascular Biology*, *22*(4), 686–691. https://doi.org/10.1161/01.ATV.0000012805.49079.23

Ren, W., Watts, S. W., & Fanburg, B. L. (2011). Serotonin transporter interacts with the PDGFβ receptor in PDGF-BB-induced signaling and mitogenesis in pulmonary artery smooth muscle cells. *American Journal of Physiology. Lung Cellular and Molecular Physiology*, *300*(3), L486-97. https://doi.org/10.1152/ajplung.00237.2010

Rendu, F., & Brohard-Bohn, B. (2001). The platelet release reaction: Granules' constituents, secretion and functions. *Platelets*, *12*(5), 261–273. https://doi.org/10.1080/09537100120068170

Robbins, I. M., Kawut, S. M., Yung, D., Reilly, M. P., Lloyd, W., Cunningham, G., … Barst, R. J. (2006). A study of aspirin and clopidogrel in idiopathic pulmonary arterial hypertesion. *European Respiratory Journal*, *27*(3), 578–584.

https://doi.org/10.1183/09031936.06.00095705

Rothman, A. M. K., Arnold, N. D., Pickworth, J. A., Iremonger, J., Ciuclan, L., Allen, R. M. H., …
Lawrie, A. (2016). W(1)=0.0947, *126*(1), 947.
https://doi.org/10.1172/JCI83361.suppression

Sanchez, O., Marcos, E., Perros, F., Fadel, E., Tu, L., Humbert, M., … Eddahibi, S. (2007). Role of
endothelium-derived CC chemokine ligand 2 in idiopathic pulmonary arterial hypertension.
American Journal of Respiratory and Critical Care Medicine, *176*(10), 1041–1047.
https://doi.org/10.1164/rccm.200610-1559OC

Sapey, E., Greenwood, H., Walton, G., Mann, E., Love, A., Aaronson, N., … Lord, J. M. (2014).
Phosphoinositide 3-kinase inhibition restores neutrophil accuracy in the elderly: Toward
targeted treatments for immunosenescence. *Blood*, *123*(2), 239–248.
https://doi.org/10.1182/blood-2013-08-519520

Sarkar, J., Gou, D., Turaka, P., Viktorova, E., Ramchandran, R., & Raj, J. U. (2010). MicroRNA-21
plays a role in hypoxia-mediated pulmonary artery smooth muscle cell proliferation and
migration. *American Journal of Physiology - Lung Cellular and Molecular Physiology*,
299(6), 861–871. https://doi.org/10.1152/ajplung.00201.2010

Sarkar, S., Engler-Chiurazzi, E. B., Cavendish, J. Z., Povroznik, J. M., Russell, A. E., Quintana, D. D.,
… Simpkins, J. W. (2019). Over-expression of miR-34a induces rapid cognitive impairment
and Alzheimer's disease-like pathology. *Brain Research*, *1721*(March), 146327.
https://doi.org/10.1016/j.brainres.2019.146327

Satonaka, H., Nagata, D., Takahashi, M., Kiyosue, A., Myojo, M., Fujita, D., … Hirata, Y. (2015).
Involvement of P2Y12 receptor in vascular smooth muscle inflammatory changes via MCP-
1 upregulation and monocyte adhesion. *American Journal of Physiology - Heart and
Circulatory Physiology*, *308*(8), H853–H861. https://doi.org/10.1152/ajpheart.00862.2013

Savai, R., Pullamsetti, S. S., Kolbe, J., Bieniek, E., Voswinckel, R., Fink, L., … Schermuly, R. T. (2012). Immune and inflammatory cell involvement in the pathology of idiopathic pulmonary arterial hypertension. *American Journal of Respiratory and Critical Care Medicine*, *186*(9), 897–908. https://doi.org/10.1164/rccm.201202-0335OC

Savale, L., Tu, L., Rideau, D., Izziki, M., Maitre, B., Adnot, S., & Eddahibi, S. (2009). Impact of interleukin-6 on hypoxia-induced pulmonary hypertension and lung inflammation in mice. *Respiratory Research*, *10*, 6. https://doi.org/10.1186/1465-9921-10-6

Schäfer, A., Burkhardt, M., Vollkommer, T., Bauersachs, J., Münzel, T., Walter, U., & Smolenski, A. (2003). Endothelium-dependent and -independent relaxation and VASP serines 157/239 phosphorylation by cyclic nucleotide-elevating vasodilators in rat aorta. *Biochemical Pharmacology*, *65*(3), 397–405. https://doi.org/10.1016/S0006-2952(02)01523-X

Schermuly, R. T., Dony, E., Ghofrani, H. A., Pullamsetti, S., Savai, R., Roth, M., … Grimminger, F. (2005). Reversal of experimental pulmonary hypertension by PDGF inhibition. *Journal of Clinical Investigation*, *115*(10), 2811–2821. https://doi.org/10.1172/JCI24838

Schulz, E., Tsilimingas, N., Rinze, R., Reiter, B., Wendt, M., Oelze, M., … Münzel, T. (2002). Functional and biochemical analysis of endothelial (Dys)function and NO/cGMP signaling in human blood vessels with and without nitroglycerin pretreatment. *Circulation*, *105*(10), 1170–1175. https://doi.org/10.1161/hc1002.105186

Shanker, G., Kontos, J. L., Eckman, D. M., Wesley-Farrington, D., & Sane, D. C. (2006). Nicotine upregulates the expression of P2Y12 on vascular cells and megakaryoblasts. *Journal of Thrombosis and Thrombolysis*, *22*(3), 213–220. https://doi.org/10.1007/s11239-006-9033-4

Shatos, M. a., Gu, J., Hodges, R. R., Lashkari, K., & Dartt, D. a. (2008). ERK/p44p42 mitogen-activated protein kinase mediates EGF-stimulated proliferation of conjunctival goblet cells

in culture. *Investigative Ophthalmology and Visual Science*, *49*(8), 3351–3359.

https://doi.org/10.1167/iovs.08-1677

Shen, J., & DiCorleto, P. E. (2008). ADP stimulates human endothelial cell migration via P2Y1

nucleotide receptor-mediated mitogen-activated protein kinase pathways. *Circulation*

Research, *102*(4), 448–456. https://doi.org/10.1161/CIRCRESAHA.107.165795

Simonneau, Gerald, Gatzoulis, M. A., Adatia, I., Celermajer, D., Denton, C., Ghofrani, A., …

Souza, R. (2013). Updated Clinical Classification of Pulmonary Hypertension. *Journal of the*

American College of Cardiology, *62*(25), D34–D41.

https://doi.org/10.1016/j.jacc.2013.10.029

Simonneau, Gérald, Montani, D., Celermajer, D. S., Denton, C. P., Gatzoulis, M. A., Krowka, M.,

… Souza, R. (2019). Haemodynamic definitions and updated clinical classification of

pulmonary hypertension. *The European Respiratory Journal*, *53*(1).

https://doi.org/10.1183/13993003.01913-2018

Smolenski, A., Bachmann, C., Reinhard, K., Hönig-Liedl, P., Jarchau, T., Hoschuetzky, H., &

Walter, U. (1998). Analysis and regulation of vasodilator-stimulated phosphoprotein serine

239 phosphorylation in vitro and in intact cells using a phosphospecific monoclonal

antibody. *Journal of Biological Chemistry*, *273*(32), 20029–20035.

https://doi.org/10.1074/jbc.273.32.20029

Soon, E., Holmes, A. M., Treacy, C. M., Doughty, N. J., Southgate, L., MacHado, R. D., … Morrell,

N. W. (2010). Elevated levels of inflammatory cytokines predict survival in idiopathic and

familial pulmonary arterial hypertension. *Circulation*, *122*(9), 920–927.

https://doi.org/10.1161/CIRCULATIONAHA.109.933762

Stacher, E., Graham, B. B., Hunt, J. M., Gandjeva, A., Groshong, S. D., McLaughlin, V. V., …

Tuder, R. M. (2012). Modern age pathology of pulmonary arterial hypertension. *American*

Journal of Respiratory and Critical Care Medicine, *186*(3), 261–272.

https://doi.org/10.1164/rccm.201201-0164OC

Steiner, M. K., Syrkina, O. L., Kolliputi, N., Mark, E. J., Hales, C. A., & Waxman, A. B. (2009).

Interleukin-6 overexpression induces pulmonary hypertension. *Circulation Research*,

104(2), 236–244. https://doi.org/10.1161/CIRCRESAHA.108.182014

Steinhubl, S. R., Badimon, J. J., Bhatt, D. L., Herbert, J. M., & Luscher, T. F. (2007). Clinical

evidence for anti-inflammatory effects of antiplatelet therapy in patients with

atherothrombotic disease. *Vasc.Med*, *12*(2), 113–122.

https://doi.org/10.1177/1358863X07077462

Stenmark, K. R., Frid, M. G., Yeager, M., Li, M., Riddle, S., McKinsey, T., & El Kasmi, K. C. (2012).

Targeting the adventitial microenvironment in pulmonary hypertension: A potential

approach to therapy that considers epigenetic change. *Pulmonary Circulation*, *2*(1), 3–14.

https://doi.org/10.4103/2045-8932.94817

Storey, R. F. (2011). New P2Y12 inhibitors. *Heart*, *97*(15), 1262–1267.

https://doi.org/10.1136/hrt.2009.184242

Storey, R F. (2006). Biology and pharmacology of the platelet P2Y12 receptor. *Curr.Pharm.Des*,

12(10), 1255–1259. https://doi.org/10.2174/138161206776361318

Storey, Robert F, Angiolillo, D. J., Patil, S. B., Desai, B., Ecob, R., Husted, S., … Wallentin, L.

(2010). Inhibitory effects of ticagrelor compared with clopidogrel on platelet function in

patients with acute coronary syndromes: the PLATO (PLATelet inhibition and patient

Outcomes) PLATELET substudy. *Journal of the American College of Cardiology*, *56*(18),

1456–1462. https://doi.org/10.1016/j.jacc.2010.03.100

Strange, G., Gabbay, E., Kermeen, F., Williams, T., Carrington, M., Stewart, S., & Keogh, A.

(2013). Time from symptoms to definitive diagnosis of idiopathic pulmonary arterial

hypertension: The delay study. *Pulmonary Circulation*, *3*(1), 89–94.

https://doi.org/10.4103/2045-8932.109919

Su, X., Floyd, D. H., Hughes, A., Xiang, J., Schneider, J. G., Uluckan, O., … Weilbaecher, K. N.

(2012). The ADP receptor P2RY12 regulates osteoclast function and pathologic bone

remodeling. *The Journal of Clinical Investigation*, *122*(10), 3579–3592.

https://doi.org/10.1172/JCI38576

Sürer, S., Toktas, F., Ay, D., Eris, C., Yavuz, S., Turk, T., … YalcInkaya, U. (2014). Effect of the

P2Y12 antagonist ticagrelor on neointimal hyperplasia in a rabbit carotid anastomosis

model. *Interactive Cardiovascular and Thoracic Surgery*, *19*(2), 198–204.

https://doi.org/10.1093/icvts/ivu087

Syberg, S., Brandao-Burch, A., Patel, J. J., Hajjawi, M., Arnett, T. R., Schwarz, P., … Orriss, I. R.

(2012). Clopidogrel (Plavix), a P2Y12 receptor antagonist, inhibits bone cell function in vitro

and decreases trabecular bone in vivo. *Journal of Bone and Mineral Research : The Official

Journal of the American Society for Bone and Mineral Research*, *27*(11), 2373–2386.

https://doi.org/10.1002/jbmr.1690

Takahashi, K., Kogaki, S., Matsushita, T., Nasuno, S., Kurotobi, S., & Ozono, K. (2007). Hypoxia

induces alteration of bone morphogenetic protein receptor signaling in pulmonary artery

endothelial cell. *Pediatric Research*, *61*(4), 392–397.

https://doi.org/10.1203/pdr.0b013e3180332cba

Tantry, U. S., Bliden, K. P., Wei, C., Storey, R. F., Armstrong, M., Butler, K., & Gurbel, P. a. (2010).

First analysis of the relation between CYP2C19 genotype and pharmacodynamics in

patients treated with ticagrelor versus clopidogrel: The ONSET/OFFSET and RESPOND

genotype studies. *Circulation: Cardiovascular Genetics*, *3*(6), 556–566.

https://doi.org/10.1161/CIRCGENETICS.110.958561

Taraseviciene-Stewart, L., Kasahara, Y., Alger, L., Hirth, P., Mc, M., Waltenberger, J., … Tuder, R. M. (2001). Inhibition of the VEGF receptor 2 combined with chronic hypoxia causes cell death-dependent pulmonary endothelial cell proliferation and severe pulmonary hypertension. *The FASEB Journal : Official Publication of the Federation of American Societies for Experimental Biology*, *15*(2), 427–438. https://doi.org/10.1096/fj.00-0343com

Tatsumi, E., Yamanaka, H., Kobayashi, K., Yagi, H., Sakagami, M., & Noguchi, K. (2015). RhoA/ROCK pathway mediates p38 MAPK activation and morphological changes downstream of P2Y12/13 receptors in spinal microglia in neuropathic pain. *Glia*, *63*(2), 216–228. https://doi.org/10.1002/glia.22745

Teichert-Kuliszewska, K., Kutryk, M. J. B., Kuliszewski, M. A., Karoubi, G., Courtman, D. W., Zucco, L., … Stewart, D. J. (2006). Bone morphogenetic protein receptor-2 signaling promotes pulmonary arterial endothelial cell survival: Implications for loss-of-function mutations in the pathogenesis of pulmonary hypertension. *Circulation Research*, *98*(2), 209–217. https://doi.org/10.1161/01.RES.0000200180.01710.e6

Thenappan, T., Shah, S. J., Rich, S., & Gomberg-Maitland, M. (2007). A USA-based registry for pulmonary arterial hypertension: 1982-2006. *European Respiratory Journal*, *30*(6), 1103–1110. https://doi.org/10.1183/09031936.00042107

Thenappan, Thenappan, Ormiston, M. L., Ryan, J. J., & Archer, S. L. (2018). Pulmonary arterial hypertension: Pathogenesis and clinical management. *BMJ (Online)*, *360*(fig 1). https://doi.org/10.1136/bmj.j5492

Thomson, J. R., Machado, R. D., Pauciulo, M. W., Morgan, N. V, Humbert, M., Elliott, G. C., … Nichols, W. C. (2000). Sporadic primary pulmonary hypertension is associated with germline mutations of the gene encoding BMPR-II, a receptor member of the TGF-beta family. *Journal of Medical Genetics*, *37*(10), 741–745.

https://doi.org/10.1136/jmg.37.10.741

Toshner, M., Voswinckel, R., Southwood, M., Al-Lamki, R., Howard, L. S. G., Marchesan, D., … Morrell, N. W. (2009). Evidence of dysfunction of endothelial progenitors in pulmonary arterial hypertension. *American Journal of Respiratory and Critical Care Medicine*, *180*(8), 780–787. https://doi.org/10.1164/rccm.200810-1662OC

Trumel, C., Payrastre, B., Plantavid, M., Hechler, B., Viala, C., Presek, P., … Gachet, C. (1999). A key role of adenosine diphosphate in the irreversible platelet aggregation induced by the PAR1-activating peptide through the late activation of phosphoinositide 3-kinase. *Blood*, *94*(12), 4156–4165. Retrieved from http://www.ncbi.nlm.nih.gov/pubmed/10590060

Tuder, R., & Graham, B. (2010). The diseased endothelium: Would it explain it all? *PVRI Review*, *2*(1), 5. https://doi.org/10.4103/0974-6013.58622

Tuder, R. M., Cool, C. D., Geraci, M. W., Wang, J., Abman, S. H., Wright, L., … Voelkel, N. F. (1999). Prostacyclin synthase expression is decreased in lungs from patients with severe pulmonary hypertension. *American Journal of Respiratory and Critical Care Medicine*, *159*(6), 1925–1932. https://doi.org/10.1164/ajrccm.159.6.9804054

Uehara, K., & Uehara, A. (2014). Integrin αvβ5 in endothelial cells of rat splenic sinus: An immunohistochemical and ultrastructural study. *Cell and Tissue Research*, *356*, 183–193. https://doi.org/10.1007/s00441-014-1796-x

Van Kolen, K., Gilany, K., Moens, L., Esmans, E. L., & Slegers, H. (2006). P2Y12 receptor signalling towards PKB proceeds through IGF-I receptor cross-talk and requires activation of Src, Pyk2 and Rap1. *Cellular Signalling*, *18*(8), 1169–1181. https://doi.org/10.1016/j.cellsig.2005.09.005

Vaughan, K. R., Stokes, L., Prince, L. R., Marriott, H. M., Meis, S., Kassack, M. U., … Whyte, M. K. B. (2007). Inhibition of neutrophil apoptosis by ATP is mediated by the P2Y11 receptor.

Journal of Immunology (Baltimore, Md. : 1950), 179(12), 8544–8553.

https://doi.org/10.4049/jimmunol.179.12.8544

Visovatti, S. H., Hyman, M. C., Bouis, D., Neubig, R., McLaughlin, V. V, & Pinsky, D. J. (2012).

Increased CD39 nucleotidase activity on microparticles from patients with idiopathic

pulmonary arterial hypertension. PloS One, 7(7), e40829.

https://doi.org/10.1371/journal.pone.0040829

Voelkel, N. F., Gomez-Arroyo, J., Abbate, A., Bogaard, H. J., & Nicolls, M. R. (2014). Pathobiology

of pulmonary arterial hypertension and right ventricular failure. European Respiratory

Journal, 40(6), 1555–1565. https://doi.org/10.1183/09031936.00046612.Pathobiology

Wang, L., Ostberg, O., Wihlborg, A.-K., Brogren, H., Jern, S., & Erlinge, D. (2003). Quantification

of ADP and ATP receptor expression in human platelets. Journal of Thrombosis and

Haemostasis : JTH, 1(2), 330–336.

Wang, Y.-F., Tian, H., Tang, C.-S., Jin, H.-F., & Du, J.-B. (2007). Nitric oxide modulates hypoxic

pulmonary smooth muscle cell proliferation and apoptosis by regulating carbon monoxide

pathway. Acta Pharmacologica Sinica, 28(1), 28–35. https://doi.org/10.1111/j.1745-

7254.2007.00483.x

Ward, M. M., Puthussery, T., & Fletcher, E. L. (2008). Localization and possible function of P2Y4

receptors in the rodent retina. Neuroscience, 155, 1262–1274.

https://doi.org/10.1016/j.neuroscience.2008.06.035

West, L E, Steiner, T., Judge, H. M., Francis, S. E., & Storey, R. F. (2014). Vessel wall, not platelet,

P2Y12 potentiates early atherogenesis. Cardiovascular Research, 102(3), 429–435.

https://doi.org/10.1093/cvr/cvu028

West, Laura E., Steiner, T., Judge, H. M., Francis, S. E., & Storey, R. F. (2014). Vessel wall, not

platelet, P2Y12 potentiates early atherogenesis. Cardiovascular Research, 102(3), 429–435.

224

https://doi.org/10.1093/cvr/cvu028

Wihlborg, A.-K. (2004). ADP Receptor P2Y12 Is Expressed in Vascular Smooth Muscle Cells and

Stimulates Contraction in Human Blood Vessels. *Arteriosclerosis, Thrombosis, and Vascular*

Biology, *24*(10), 1810–1815. https://doi.org/10.1161/01.ATV.0000142376.30582.ed

Wihlborg, A. K., Wang, L., Braun, O. Ö., Eyjolfsson, A., Gustafsson, R., Gudbjartsson, T., &

Erlinge, D. (2004). ADP receptor P2Y12 is expressed in vascular smooth muscle cells and

stimulates contraction in human blood vessels. *Arteriosclerosis, Thrombosis, and Vascular*

Biology, *24*(10), 1810–1815. https://doi.org/10.1161/01.ATV.0000142376.30582.ed

Wilkin, F., Duhant, X., Bruyns, C., Suarez-Huerta, N., Boeynaems, J. M., & Robaye, B. (2001). The

P2Y11 receptor mediates the ATP-induced maturation of human monocyte-derived

dendritic cells. *Journal of Immunology (Baltimore, Md. : 1950)*, *166*(12), 7172–7177.

https://doi.org/10.4049/jimmunol.166.12.7172

Wilkins, M. R. (2012). Pulmonary hypertension: the science behind the disease spectrum.

European Respiratory Review : An Official Journal of the European Respiratory Society,

21(123), 19–26. https://doi.org/10.1183/09059180.00008411

Woulfe, D., Jiang, H., Mortensen, R., Yang, J., & Brass, L. F. (2002). Activation of Rap1B by Gi

family members in platelets. *Journal of Biological Chemistry*, *277*(26), 23382–23390.

https://doi.org/10.1074/jbc.M202212200

Xiao, Y., Peng, H., Hong, C., Chen, Z., Deng, X., Wang, A., … Qin, X. (2017). PDGF Promotes the

Warburg Effect in Pulmonary Arterial Smooth Muscle Cells via Activation of the

PI3K/AKT/mTOR/HIF-1α Signaling Pathway. *Cellular Physiology and Biochemistry*, *42*(4),

1603–1613. https://doi.org/10.1159/000479401

Yang, X., Long, L., Southwood, M., Rudarakanchana, N., Upton, P. D., Jeffery, T. K., … Morrell, N.

W. (2005). Dysfunctional Smad signaling contributes to abnormal smooth muscle cell

proliferation in familial pulmonary arterial hypertension. *Circulation Research*, *96*(10), 1053–1063. https://doi.org/10.1161/01.RES.0000166926.54293.68

Yu, X., Li, T., Liu, X., Yu, H., Hao, Z., Chen, Y., … Zhu, D. (2015). Modulation of pulmonary vascular remodeling in hypoxia: Role of 15-LOX-2/15-HETE-MAPKs pathway. *Cellular Physiology and Biochemistry*, *35*(6), 2079–2097. https://doi.org/10.1159/000374015

Yusuf, S., Mehta, S., Anand, S., Avezum, A., Awan, N., Bertrand, M., … Sosa Liprandi, A. (2000). The Clopidogrel in Unstable angina to prevent Recurrent Events (CURE) trial programme: Rationale, design and baseline characteristics including a meta-analysis of the effects of thienopyridines in vascular disease. *European Heart Journal*, *21*(24), 2033–2041. https://doi.org/10.1053/euhj.2000.2474

Zambahari, R., Kwok, O. H., Javier, S., Mak, K. H., Piyamitr, S., Tri Ho, H. Q., … Chow, W. H. (2007). Clinical use of clopidogrel in acute coronary syndrome. *International Journal of Clinical Practice*, *61*(3), 473–481. https://doi.org/10.1111/j.1742-1241.2007.01315.x

Zhang, H., Xu, M., Xia, J., & Qin, R.-Y. (2013). Association between serotonin transporter (SERT) gene polymorphism and idiopathic pulmonary arterial hypertension: a meta-analysis and review of the literature. *Metabolism: Clinical and Experimental*, *62*(12), 1867–1875. https://doi.org/10.1016/j.metabol.2013.08.012